Cellular Targets of Propranolol in Infantile Hemangioma

Cellular Targets of Propranolol in Infantile Hemangioma

A dissertation presented

by

Daniel K Lee

to

The Divison of Medical Sciences

in partial fulfillment of the requirements

for the degree of

Doctor of Philosophy

in the subject of

Human Biology and Translational Medicine

Harvard University

Cambridge, Massachusetts

September 2013

Dissertation Advisor: Dr. Joyce Bischoff Daniel K Lee

Cellular Targets of Propranolol in Infantile Hemangioma

Abstract

Infantile hemangioma (IH) is a vascular neoplasm that affects 4-10 percent of infants. Propranolol, a non-selective β-adrenergic receptor (AR) antagonist, was serendipitously discovered to accelerate regression of IH in 2008; however, its mechanism in IH is unclear.

A number of approaches were used to investigate the mechanism(s) by which propranolol accelerates the involution of IH. Two of the likely targets of propranolol, β_1 and β_2-ARs, were found expressed in IH tissues by quantitative real time polymerase chain reaction (qRT-PCR). *In vitro* contractility assays were developed to examine effects of propranolol on cellular activities, and they showed that wrinkles formed by hemangioma-derived pericytes (Hem-Pericytes) relaxed in response to epinephrine, but this was strongly inhibited if propranolol was added 5 minutes before epinephrine. These responses were blunted by silencing β_2-AR with siRNA. Propranolol had no effect on the contractility of placental or retinal pericytes in this assay. Propranolol also blocked proliferation of Hem-Pericytes and hemangioma-derived endothelial cells (HemECs), but not stem cells (HemSCs).

In order to reproduce the clinical effect of propranolol on IH patients, a murine model of IH was utilized. HemECs and Hem-Pericytes suspended in Matrigel were implanted in mice and allowed to form blood vessels. At 7 days, vascular perfusion of

the cell/Matrigel implants was verified; mice were divided into two groups and treated with vehicle or propranolol for 7 days. Contrast-enhanced micro-ultrasonography of the implants showed a significantly decreased vascular volume in propranolol-treated mice, but no reduction in those treated with vehicle. These experiments indicated that propranolol may affect contractility of Hem-Pericytes to reduce vascular volume of IH, to accomplish quick improvement seen in patients, and they identified HemECs, Hem-Pericytes and β_2-AR as likely targets of propranolol.

Table of Contents

Chapter I

Characteristics of infantile hemangioma

1.1 An introduction to vascular anomalies

Vascular anomalies are divided into tumors and malformations. Tumors, or abnormally enlarged lesions, include pyogenic granuloma, Kaposiform hemangioendothelioma, congenital hemangioma and infantile hemangioma (IH). Pyogenic granuloma usually appears on superficial skin and bleeds easily. Kaposiform hemangioendothelioma is associated with a low number of platelets, which predisposes patients to frequent bleeding. Congenital hemangioma is notable at birth; it regresses on its own (rapidly involuting) or does not (non-involuting). Malformations can occur at various sites including arteries, arteriovenous connections, veins, lymphatic vessels and capillaries. Malformations with arterial component exhibit fast blood flow, whereas those with venous component exhibit slow blood flow. Depending on sites of occurrence, malformations can lead to symptoms such as color change from normal skin, swelling and pain (Figure 1; Mulliken, Fishman et al. 2000; Hammill, Wentzel et al. 2011).

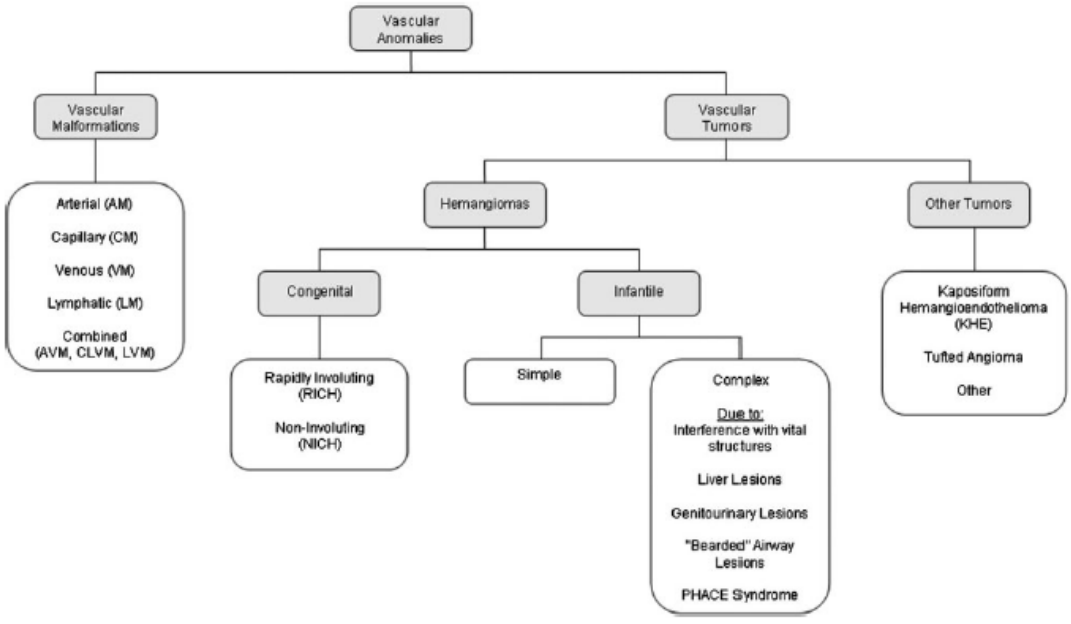

Figure 1. Vascular anomalies classification.
Pediatric Blood Cancer. **57**(6): 1018-24, 2011, Copyright Wiley Periodicals Inc. This material is reproduced with permission of John Wiley & Sons, Inc.

An introduction to IH

IH is the most common and best-studied vascular tumor. IH is a pediatric vascular tumor that appears as red, raised flesh a few weeks after birth in 5-10 % of neonates, and it is more common in the prematurely-born and in females. Approximately two-thirds of lesions occur in head and neck region, with the rest appearing elsewhere on the skin or deep inside the body- e.g., liver, trachea and parotid glands, etc. IH is characterized by three phases, proliferating, involuting and involuted. The vascular lesion grows the fastest during proliferating phase, stops growing during involuting phase and shrinks in involuted phase. In terms of vascular architecture, proliferating phase is characterized by dense, disorganized vessels consisting of plump endothelial cells and lasts until age 9-12 months. Involuting phase is characterized by enlarged, well-organized vessels consisting of flattened endothelial cells and follows the proliferating phase for 3-5 years. In both proliferating and involuting phases, numerous pericytes have been noted to surround IH vessels. Finally, involuted phase is characterized by few vessels with an abundance of adipocytes and lasts until age 5-8 years (Mulliken, Fishman et al. 2000).

Deciphering the origin of IH

Several hypotheses have been proposed about the origin of IH. A group of researchers examined methylation patterns in HemECs. The cells displayed a non-random pattern of X-chromosomal inactivation, indicating clonality and lending credence to a genetic basis for IH (Boye, Yu et al. 2001; Walter, North et al. 2002).

Others believe that the tumor microenvironment contributes to the genesis of IH. A group of researchers examined formalin-fixed, paraffin-embedded hemangioma tissues from the 3 phases. They noted that the epidermis overlying proliferative phase hemangiomas expressed higher levels of pro-angiogenic factors, such as basic fibroblast growth factor (bFGF) and vascular endothelial growth factor (VEGF), but lower levels of an inhibitor of angiogenesis, such as interferon-β (IFN-β), compared to the epidermis overlying involuted phase. Therefore, they reasoned that the interaction and imbalance of angiogenic signals between IH and adjacent epidermis are key factors in the origin and pathogenesis of IH (Bielenberg, Bucana et al. 1999).

Others have postulated that IH arises from fetal placental cells based on shared immunophenotypes. They noted that IH and placenta share markers such as glucose transporter-1 (GLUT1), Lewis Y antigen and merosin, which are not expressed by the normal vasculature of skin. If pregnant mothers were to receive chorionic villus sampling to diagnose potential genetic abnormalities, placental cells might be dislodged and embolize to fetus through right-to-left shunts, normal for fetal circulation. These dislodged and embolized placental cells may give rise to IH in the fetus (North, Waner et al. 2002). Although some have reported an increased incidence of IH in those whose mothers underwent chorionic villus sampling (Kaplan, Normandin et al. 1990; Burton, Schulz et al. 1995), a positive correlation with the procedure was not verified in a multi-center study of 1058 children with hemangioma (Haggstrom, Drolet et al. 2007). Overall, researchers have made strides, but more work needs to be done to clarify the origin of IH.

1.2 Molecular pathways implicated in IH

Vascular endothelial growth factor (VEGF)

VEGF is a central regulator of normal developmental and pathological angiogenesis, and several studies have implicated VEGF and its receptors in IH. A summary of the key players and mechanisms of the VEGF pathway in angiogenesis are provided here.

The mammalian VEGF family consists of VEGF-A, -B, -C and -D. Among them, VEGF-A has been the most well-characterized, with roles including endothelial cell survival and morphogenesis, cellular migration to form vessel lumen and stimulation of vessel dilation and permeability. Alternative splicing of the 8 exons of VEGF-A gives rise to isoforms of different lengths, which include VEGF-A_{121}, -A_{145}, -A_{165}, -A_{189} and -A_{206}. These isoforms differ in their inclusion of exons 6 and/or 7, which encode domains for binding heparan sulfate proteoglycans (HSPGs) and neuropilins (NRPs), co-receptors of VEGF, in the extracellular matrix. As a result, VEGF-A_{121} is very diffusible, VEGF-A_{165} less diffusible and VEGF-A_{206} even less diffusible but with strong interactions via binding HSPGs and NRPs in the matrix. Relative proportions of these isoforms affect VEGF-A gradients and its levels. VEGF-B, -C and –D were discovered after VEGF-A, and their lengths range 167-400 amino acids. While VEGF-B has not been as prominently featured in angiogenesis as VEGF-A, it has been reported to be important in embryonic cardiac angiogenesis, and its expression was detected IH (Boscolo, Mulliken et al. 2011). VEGF-C and –D have been reported to be involved in lymphangiogenesis. Although not studied as extensively as VEGFs, placental growth factor (PlGF) has been reported to be involved in angiogenesis, too (Bautch 2012; Olsson, Dimberg et al. 2006).

VEGF dimers bind vascular endothelial growth factor receptors (VEGFRs), which are referred as VEGFR-1, -2 and -3. Alternative names for VEGFRs are Flt-1 for VEGFR-1, Flk-1/KDR for VEGFR-2 and Flt-4 for VEGFR-3. VEGF-A binds VEGFR-1 and -2, VEGF-B binds VEGFR-1 and VEGF-C and-D each binds VEGFR-2 and -3. VEGF-E, a non-human form, binds VEGFR-2, and PlGFs bind VEGFR-1. Interaction of VEGFs with VEGFRs and co-receptors HSPGs and NRPs influences parameters such as VEGF gradient and its duration of signaling. VEGFRs are tyrosine kinase receptors that have an extracellular region with 7 immunoglobulin-like domains for binding VEGF, a single transmembrane region and a split intracellular tyrosine kinase region. Upon binding of dimerized ligands, VEGFRs dimerize and trans-autophosphorylate at specific tyrosines in the cytoplasmic domains, such as tyrosines 951, 1175 and 1214 for VEGFR-2. Creation of phosphorylated tyrosines (phosphotyrosines) within the kinase domain increases the kinase activity of the receptor, while phosphotyrosines outside the kinase domain create high-affinity docking sites for binding of signaling proteins, such as phosphoinositide 3-kinase (PI 3-kinase), phospholipase C-γ (PLC-γ) and adaptors, which have SH2 or PTB domains for binding phosphotyrosines.

Signaling through the three VEGFRs serves diverse functions. For instance, VEGFR-1 is involved in recruitment of hematopoietic progenitors, migration of monocytes and macrophages, and it has been noted as a decoy receptor for VEGFR-2 by reducing the availability of VEGF-A that can bind VEGFR-2. VEGFR-2 is involved in activities such as endothelial cell survival and dilation, growth and permeability of vessels. VEGFR-3 is noted to be important in lymphangiogenesis (Bautch 2012; Olsson, Dimberg et al. 2006; Figure 2).

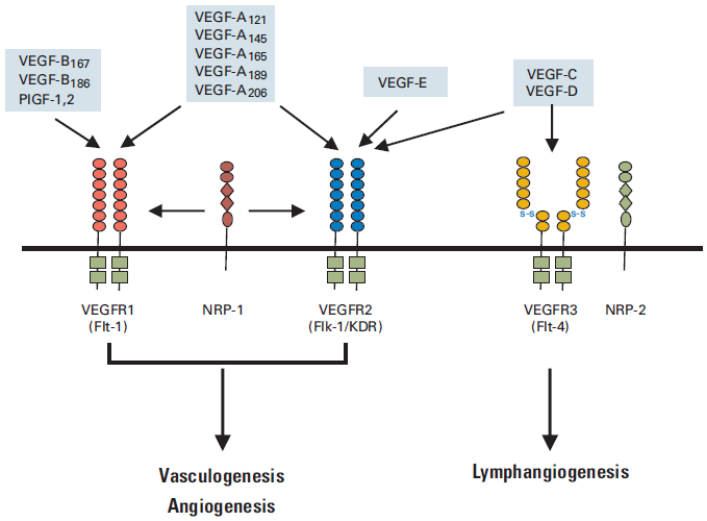

Figure 2. Ligands, VEGFRs and downstream effects . Alternative names for VEGFRs are indicated in parentheses. Co-receptors HSPGs (not shown) and NRPs increase binding affinity of ligands to VEGFRs.
Reproduced with permission from J Clin Oncol. **23**(5): 1011-27, 2005, Copyright American Society of Clinical Oncology.

An example of angiogenesis driven by VEGF-A occurs in hypoxia, which is an important physiologic and pathologic regulator of VEGF-A. Low oxygen levels induce an intracellular accumulation of a gene regulatory protein, hypoxia-inducible factor 1α (HIF1α), which dimerizes with HIF1β. HIF1α/β complex translocates to the nucleus, binds VEGF promoter to stimulate its transcription. VEGF-A in turn stimulates neighboring endothelial cells to proliferate, to produce proteases to digest basal lamina of existing vessels and to form vessel sprouts, which consist of a tip cell and stalk cells behind it. The tip cells respond to VEGF-A gradient by moving towards it using their filopodia, while stalk cells respond to VEGF-A levels by proliferating and forming vessel lumens. The newly-formed vessels transport blood to the hypoxic tissue, so more oxygen is delivered. As a result, HIF1α is hydroxylated at proline residues, allowing their recognition for ubiquitination and subsequent targeting for degradation, eventually decreasing VEGF-A production. Thus, VEGF-A production is controlled by negative

feedback, and it plays a key role during angiogenesis in response to hypoxia (Gerhardt, Golding et al. 2003).

Researchers have been interested in clinical applications of angiogenesis. For instance, promotion of vessel growth is desired if healthy tissue has died due to decreased oxygen supply, in conditions such as heart attack and stroke. On the other hand, inhibition of vessel growth is preferred if angiogenesis is pathologic in select areas, in conditions such as diabetes-related vision changes and cancer. A well-known anti-VEGF therapeutic is Bevacizumab, also known as Avastin. It is a VEGF-A-neutralizing antibody, and if combined with chemotherapy, it prolongs survival of patients with cancer in brain, colon, kidneys and lungs (Olsson, Dimberg et al. 2006).

Thus, VEGF and its signaling through VEGFRs present wide areas of research, which may encompass IH pathogenesis. Indeed, a group of researchers found that cells cultured from surgically resected hemangiomas released VEGF and VEGFR-2. Anti-VEGF IgG and antisense oligonucleotides directed against the translation initiation codon of VEGFR-2 reduced proliferation of these cells. Therefore, VEGF was postulated to be a key molecule in the pathogenesis of IH (Berard, Sordello et al. 1997). In addition, VEGF-A levels were elevated in serum of patients with proliferating phase IH compared to age-matched controls (Zhang, Lin et al. 2005; Kleinman, Greives et al. 2007); in terms of location, VEGF-A expression was noted in stroma of IH from proliferating phase (Greenberger, Boscolo et al. 2010). On the other hand, VEGFR-1 expression was noted to be low in hemangioma tissues from both proliferating and involuting phases compared to a non-pathologic tissue like placenta (Picard, Boscolo et al. 2008). Regardless of its low expression, signaling through

VEGFR-1 has been noted to important in formation of hemangioma vessels in a murine model of IH (Boscolo, Mulliken et al. 2011).

A group of researchers published data showing hyperphosphorylated VEGFR-2 in hemangioma-derived endothelial cells compared to human dermal microvascular endothelial cells (HDMECs). In hemangioma-derived endothelial cells from some patients, they found mutations in the genes encoding VEGFR-2 and tumor endothelial marker-8 (TEM8). They hypothesized that the mutated VEGFR-2 and TEM8 help downregulate nuclear factor of activated T cells (NFAT), a transcription factor required for VEGFR-1 activity regulation. Expression of VEGFR-1 in hemangioma-derived endothelial cells was reduced compared to non-hemangioma-derived cells like HDMECs and human umbilical vein endothelial cells (HUVECs). With decreased numbers of VEGFR-1, VEGF more likely binds VEGFR-2 to trigger hyper-proliferation of hemangioma-derived endothelial cells (Jinnin, Medici et al. 2008). Traits of hemangioma-derived cells will be explained further in Section 1.3.

Notch signaling pathway

Notch pathway plays important roles in controlling cell fates in development of various organs in mammals, which possess 4 different receptors, Notch1-4. Notch receptors consist of 36 epidermal growth factor (EGF)-like domains in the extracellular region, a single-pass transmembrane region and an intracellular region. Their ligands include Jagged and Delta proteins.

As noted above, Notch receptor plays important roles in controlling cell fates, and a well-known example involves neural cells in *Drosophila*. Among progenitor cells, one

may become a neural cell, and this cell inhibits its neighbors from also becoming neural cells. This process, called lateral inhibition, is accomplished by Notch receptor signaling activated by Delta, a single-pass transmembrane signal protein with 9 EGF-like domains. On its surface, a future neural cell displays Delta, which is bound by Notch receptors on its neighboring cells that are inhibited from becoming neural cells.

Notch receptor signaling by Delta is facilitated by 3 proteolytic cleavages, the last 2 of which occur after binding by Delta. First, Notch receptor is cleaved in the Golgi apparatus by Furin-like protease to generate a heterodimer and transported to cell surface. Delta ligand on the future neural cell and Notch receptor on a neighboring cell bind through their EGF-like domains, which is followed by a second cleavage with ADAM family protease 10 or 17 in the extracellular region of Notch receptor. While the bound Delta-Notch is endocytosed by the future neural cell, a third cleavage occurs on the transmembrane region of Notch receptor by γ-secretase. Notch intracellular domain (NICD) migrates to nucleus of a neighboring cell to bind responsive elements in target genes and activates their transcription with regulatory proteins. Notch signaling leads to inhibition of neural cell differentiation and maintenance of a neighboring cell as a progenitor, while neural cell differentiation occurs in the Delta-expressing cell (Figure 3; Bray 2006; Musse, Meloty-Kapella et al. 2012).

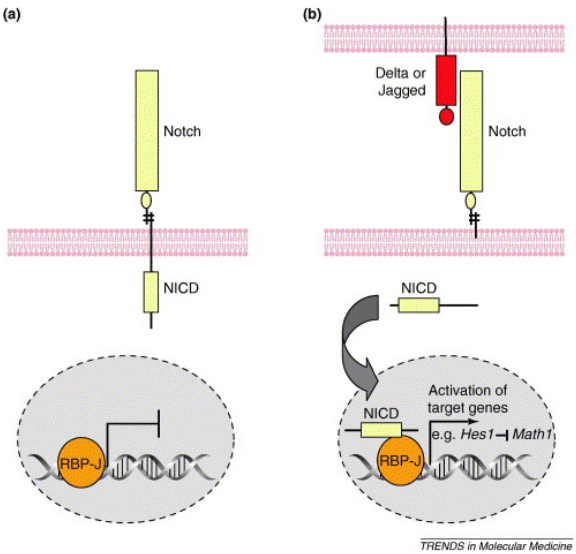

Figure 3. Notch receptor signaling overview.
(a) In the absence of Notch signaling, RBP-J, a regulatory protein, is a transcriptional repressor. The first proteolytic cleavage creates a heterodimeric receptor, with extracellular Notch and Notch intracellular domain (NICD). (b) Ligand (Delta or Jagged) binding induces 2 additional proteolytic cleavages. NICD migrates to nucleus to bind RBP-J and activate transcription of target genes. Reproduced with permission from Trends Mol Med. **11**(11): 496-502, 2005, Copyright Elsevier.

Notch signaling and lateral inhibition is directly relevant to angiogenesis. As noted above, vessel sprouts form in response to VEGF-A, and sprouts consist of a tip cell and stalk cells. VEGF-A binds VEGFR-2 to induce Delta-like 4 expression in a future tip cell; Delta-like 4 then binds Notch receptors in its neighbors, which become stalk cells. Selection of tip and stalk cells is aided by the Fringe family of glycosyltransferases; they are abundantly expressed in sprouts and glycosylate Notch at EGF-like domains. This modification enhances Notch signaling by Delta-like 4, but reduces Notch signaling upon binding of Jagged1, another Notch ligand. Therefore, Jagged1, highly expressed in stalk cells, acts as an antagonist of Delta-like 4, so that stalk cells do not activate Notch signaling in adjacent tip cells. Jagged1 also interferes

with signaling of Delta-like 4 through Notch in stalk cells to help maintain VEGFRs, so that stalk cells proliferate in response to VEGF-A. Thus, in the sprouts responding to VEGF-A, Notch signaling is low in tip cells, but high in stalk cells. In support of this hypothesis, inhibition of Notch signaling increased numbers of tip cells, but activation of Notch signaling reduced numbers of tip cells (Hellström, Phng et al. 2007; Benedito, Roca et al. 2009).

In addition to its role in angiogenesis, Notch signaling was found to be potentially relevant in IH. Laser capture microdissection and genome-wide transcriptional profiling of vessels from proliferating IHs showed that RNA levels of Jagged1 and Notch4 were upregulated 6- and 3-fold, respectively, compared to placental vessels (Calicchio, Collins et al. 2009). In support of these findings, Jagged1 was found important in differentiation of hemangioma-derived cells and hemangioma vessel formation in a murine model of IH (Boscolo, Stewart et al. 2011). In addition, researchers noted that while RNA levels of Notch4 and Jagged1 were elevated in involuting IHs compared to normal skin and placenta, immunostaining for Notch3 showed change in location by phases- in interstitial cells outside hemangioma vessels in proliferating phase, but in pericytes in involuting phase (Wu, Adepoju et al. 2010). In a follow-up study, expression of Notch target genes, including Hes1, was detected in hemangioma-derived cells (Adepoju, Wong et al. 2011). Thus, similar to its roles in neural cell determination and vessel sprouting, Notch may play a role in intercellular communications of IH. Laser capture microdissection and genome-wide transcriptional profiling of vessels from proliferating IHs also showed that RNA levels of another molecule, angiopoietin-2, was

upregulated 33-fold compared to placental vessels. The potential relevance of this finding in IH will be discussed in the following section.

Angiopoietins and Tie receptors

Angiopoietins are divided into angiopoietins-1-4, and they bind Tie receptor tyrosine kinases. Tie1 and 2 are expressed in endothelial cells, and the binding of angiopoietin-1 or -2 on Tie2 has been well-characterized. In contrast, effects of angiopoietins-3 and -4 binding on Tie receptors and Tie1 receptor signaling have not been as well-characterized. Hence, this section will focus on angiopoietins-1, -2 and Tie2 receptor.

Tyrosine kinase receptors such as Tie2 have an extracellular region for binding ligands, a single transmembrane region and an intracellular tyrosine kinase region. Upon binding of angiopoietin-1 ligands, Tie2 receptors multimerize, trans-autophosphorylate and create phosphotyrosine docking sites. PI 3-kinase is recruited to activated Tie2 receptors and docked on such phosphotyrosines. PI 3-kinase creates phosphoinositides such as $PI(3,4,5)P_3$, upon which Akt is docked with its pleckstrin homology domain for phosphorylation and activation by entities such as phosphoinositol-dependent kinase and mammalian target of rapamycin (mTOR). Activated Akt phosphorylates numerous targets on serines and threonines including Bad, a pro-apoptotic protein. Unphophorylated Bad binds Bcl2, an anti-apoptotic protein, to keep it inactive; upon phophorylation, Bad is bound by cytosolic protein 14-3-3, and Bcl2 is released from its inactive state, so apoptosis is inhibited (Downward 2004). Another effect of angiopoietin-1 signaling through Tie2 receptors is inhibition of nuclear factor-kB (NF-kB), which is involved in inflammation. Thus, endothelial cell

survival is promoted, and vessels are stabilized by diminishment of inflammatory responses. Researchers have postulated that angiopoietin-1 signaling induces trans-association of Tie2 at cell-cell junctions, promoting endothelial cell survival and anti-inflammation. On the other hand, extracellular cellular matrix-bound Tie2 signaling, in the absence of cell-cell junctions, promotes endothelial cell proliferation and migration (Figure 4; Fiedler and Augustin 2006; Huang, Bhat et al. 2010; Eklund and Saharinen 2013).

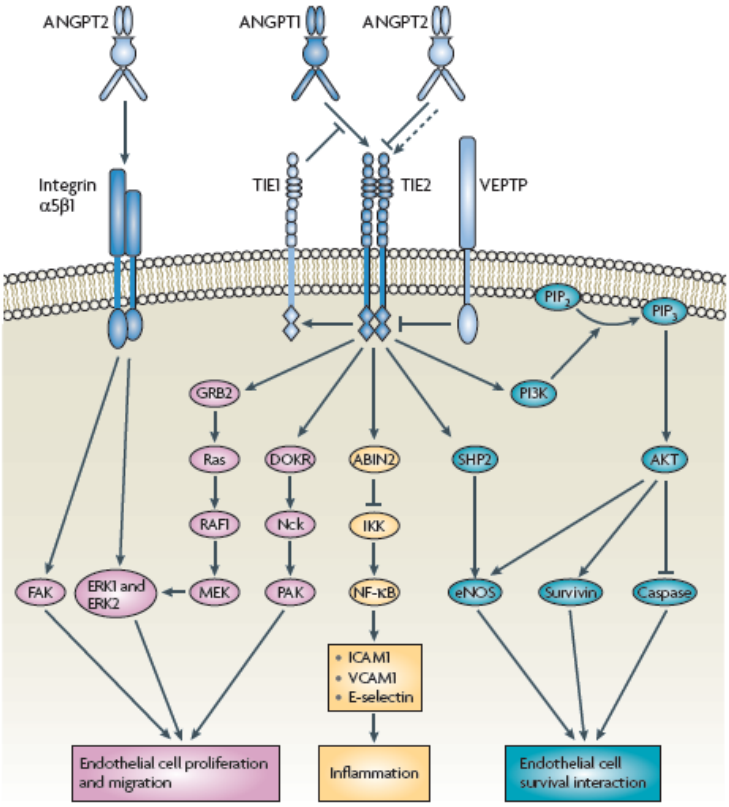

Figure 4. Angiopoietins signaling through Tie receptors. Angiopoietin-1 multimers bind to Tie2, which multimerize and trans-autophosphorylate to activate targets. Angiopoietin-2 exerts antagonistic actions but can act as a partial Tie2 agonist in some contexts (dashed arrow). Activated Tie2 stimulates Tie1, which interferes with Tie2 signaling by angiopoietin-1. Purple shapes indicate action through matrix-bound Tie2, whereas gold and blue shapes indicate action through trans-associated Tie2. Reproduced with permission from Nat Rev Cancer. **10**(8): 575-85, 2010, Copyright Nature Publishing Group.

Interestingly, angiopoietin-1 signaling through Tie2 receptors leads to inhibition of angiopoietin-2 expression and secretion, which indicates potentially antagonistic actions of angiopoietins-1 and -2. In affirmation of this possibility, angiopoietin-2 binding to Tie2 receptors does not lead to rapid autophosphorylation of Tie2 receptor; therefore, in contrast to angiopoietin-1 signaling, endothelial cell apoptosis is promoted, and vessels are destabilized and become more receptive to inflammatory responses (Figure 4; Fiedler and Augustin 2006; Huang, Bhat et al. 2010).

To add complexity to angiopoietins-1 and -2 signaling, these responses were found to be influenced by VEGF. Large amounts of angiopoietin-2 mRNA were noted near degenerated vessels of unfertilized rat ovarian follicles with low VEGF mRNA levels. However, in the presence of high levels of angiopoietin-2 and VEGF mRNAs, numerous vessel sprouts were detected. Researchers hypothesized that in the presence of VEGF, angiopoietin-2 promotes vessel sprouting by blocking the vessel stabilization effect of angiopoietin-1. In the absence of VEGF, antagonism of angiopoietin-1 by angiopoietin-2 leads to vessel destabilization and regression (Koh 2013; Maisonpierre, Suri et al. 1997).

Besides the antagonistic actions of angiopoietins-1 and -2 on the common receptor Tie2, another point of interest is different locations of expression of angiopoietins-1 and -2. Angiopoietin-1 is mostly expressed in non-endothelial cells such as fibroblasts, smooth muscle cells and pericytes. On the other hand, angiopoietin-2 is synthesized in endothelial cells, stored and released from storage granules called Weibel-Palade bodies. The significance of these differences is unclear, but it may be tied to the contrasting effects that angiopoietin-1 or -2 accomplishes

through Tie2 signaling. For instance, angiopoietin-1 expressed by a pericyte precursor binds Tie2 receptor on endothelial cells. This leads to endothelial cell survival, pericyte precursor attachment and stabilization of vessels, which are expected in normal, physiologic processes of angiogenesis such as wound healing (Gaengel, Genové et al. 2008).

In contrast, actions of angiopoietin-2 in animal studies provide clues on pathologic angiogenesis. Endogenous angiopoietin-2 is upregulated in retinas of animals with diabetes. The vessels in retinas show pericyte loss and degeneration. Similarly, exogenous angiopoietin-2, either by injection of recombinant protein into retinas or transgenic overexpression selectively in retinas, leads to a similar phenotype (Hammes, Lin et al. 2004; Feng, vom Hagen et al. 2007). As noted above, in the presence of VEGF, angiopoietin-2 signaling promotes formation of vessel sprouts, whereas in the absence of VEGF, angiopoietin-2 signaling promotes endothelial cell apoptosis and vessel destabilization. These findings may have relevance in IH because low availability of VEGFR-1 in hemangioma-derived endothelial cells directs VEGF-A to VEGFR-2, leading to cellular hyperproliferation (Jinnin, Medici et al. 2008). Vessel sprouting is induced by upregulated angiopoietin-2 in the presence of VEGF, so the combination of angiopoietin-2 and VEGF may lead to pathological angiogenesis as in IH.

Researchers have confirmed the importance of angiopoietin signaling through Tie2 receptor in IH. For instance, hemangioma-derived endothelial cells expressed higher levels of Tie2 compared to HDMECs (Yu, Varughese et al. 2001). As described above, RNA levels of angiopoietin-2 was upregulated 33-fold in endothelium of

proliferating IHs compared to placental vessels (Calicchio, Collins et al. 2009). On the other hand, angiopoietin-1 levels were low in hemangioma-derived pericytes compared to non-hemangioma pericytes (Boscolo, Mulliken et al. 2013). An in-depth discussion of hemangioma-derived cells will follow in Section 1.3.

Tie2 and VEGFR are both receptors with tyrosine kinase domains in the intracellular region. Multimer ligand binding induces proximity of receptors, and trans-autophosphorylation occurs by kinase domains to initiate downstream signaling. In addition, signaling with angiopoietins-1 and -2 through Tie2 receptor influences cellular interactions in angiogenesis, somewhat similar to effects brought on by Delta signaling through Notch receptors. Thus, signaling through VEGFR, Notch and Tie receptors converge in IH.

Other characteristics of IH

GLUT1, an erythrocyte-type glucose transporter protein, was found to be a useful diagnostic marker for IH in all 3 phases. In a retrospective study, 97% of IHs had endothelial GLUT1 immunoreactivity by immunohistochemistry (IHC), whereas normal skin or other vascular anomalies such as arteriovenous and venous malformations and port-wine stain had not expressed GLUT1. GLUT1 is expressed in placenta, which led researchers to speculate on a placental origin for IH (North, Waner et al. 2000). It should be noted that even though most vessels in IH express GLUT1, some endothelial cells are $GLUT1^{+}$, whereas others are $GLUT1^{-}$. This dichotomy may indicate different origins for cells in IH and underscores the need to clarify the origin of IH.

As noted above, IH occurs more frequently in females, so high levels of serum estrogen in IH patients were suspected by some to be correlated with IH (Zhou, Wang et al. 1991). Researchers detected that hemangioma-derived endothelial cells grew more rapidly in the presence of estrogen, but this was suppressed by tamoxifen, an antagonist of the estrogen receptor (Xiao, Hong et al. 1999). The same group of researchers noted that estrogen increased proliferation of hemangioma-derived endothelial cells, but not as highly as VEGF. They also detected that estrogen and VEGF synergistically increased proliferation (Xiao, Liu et al. 2004). Although these findings were intriguing, hormonal effects in IH have not been studied actively.

E-selectin, an endothelial-cell-specific leukocyte adhesion molecule, was highly expressed in proliferating phase IH tissues and co-localized with dividing endothelial cells, as determined by $Ki67^{+}$ immunoreactivity. E-selectin immunoreactivity was also high in placenta and neonatal foreskin, tissues with ongoing angiogenesis, but low in involuting phase IH tissues and adult skin. These findings indicated E-selectin as a diagnostic marker for proliferating endothelium and its possible role in angiogenesis (Kräling, Razon et al. 1996). Indeed, recombinant E-selectin and $E\text{-selectin}^{+}$ hemangioma-derived endothelial cells enhanced migration and adhesion of hemangioma-derived stem cells *in vitro*. Blocking mAb against E-selectin did not affect proliferation of hemangioma-derived stem cells, but the same antibody inhibited formation of blood vessels when hemangioma-derived endothelial cells and hemangioma-derived stem cells were implanted in Matrigel. These findings identified E-selectin as an important modulator of interactions between hemangioma-derived endothelial cells and hemangioma-derived stem cells (Smadja, Mulliken et al. 2012).

As noted above, like E-selectin, angiopoietin-2 was highly expressed in endothelium of proliferating phase IH tissues. This commonality could indicate their shared roles in regulating pathogenesis of IH.

1.3 Hemangioma-derived cells and their characteristics

Endothelial cells, pericytes and stem cells have been isolated from hemagioma tumor specimens. The Bischoff Laboratory has developed the following terminologies for these cells: hemangioma-derived endothelial cell (HemEC), hemangioma-derived pericyte (Hem-Pericyte) and hemangioma-derived stem cell (HemSC). Each cell type has distinct characteristics.

HemECs

HemECs display endothelial markers such as CD31, CD146, E-selectin and VE-cadherin. As noted above, HemECs displayed a non-random pattern of X-chromosomal inactivation, indicating clonality. They proliferated faster than mature human ECs, such as HDMECs with or without exogenous VEGF. They showed increased migration upon treatment with an angiogenesis inhibitor endostatin, which was the opposite of HDMECs (Boye, Yu et al. 2001).

The Bischoff Laboratory researchers also found that HemECs expressed higher levels of Tie2 compared to normal ECs such as HDMECs. Higher numbers of HemECs than HDMECs migrated in response to angiopoietin-1. HemECs also proliferated faster than HDMECs in response to angiopoietin-1. On the other hand, both HemECs and HDMECs had undetectable levels of VEGF and angiopoietin-1 but similar levels of

CD31, VE-cadherin, Tie1, VEGFR-1 and VEGFR-2. As was noted in endothelium of hemangiomas from proliferating phase, angiopoietin-2 was expressed in HemECs (Yu, Varughese et al. 2001).

Notch signaling pathway plays important roles in neural cell determination and vessel sprouting, and a group of researchers noted that RNA levels of Jagged1, a Notch ligand, were higher in HemECs compared to HDMECs. On the other hand, RNA levels of Delta-like 4, another Notch ligand, were lower in HemECs compared to HDMECs (Wu, Adepoju et al. 2010). While the significance of these findings wasn't clear, they hinted that Notch signaling was present and active in IH.

Hem-Pericytes

Hem-Pericytes display markers of pericytes like alpha smooth muscle actin (αSMA), calponin, neural glial antigen-2 (NG2), platelet-derived growth factor receptor β (PDGFR-β) and smooth muscle myosin heavy chain (smMHC). These markers are expressed by perivascular cells in proliferating phase of IH, so cultured Hem-Pericytes match expression pattern of pericytes in IH tissue. Hem-Pericytes isolated from proliferating phase of IH displayed lower levels of baseline contractility *in vitro*, compared to those from involuting phase of IH and human retinal pericytes. Also, compared to human retinal pericytes, they express lower angiopoietin-1 levels. In co-culture assays, Hem-Pericytes were unable to reduce proliferation or migration of endothelial cells. Thus, Hem-Pericytes surround vessels, but they are unable to stabilize endothelial cell growth and migration. In other words, Hem-Pericytes display reduced ability to support mature, stable vessels (Boscolo, Mulliken et al. 2013).

Compared to HemECs and HemSCs, less is known about Hem-Pericytes because they were discovered relatively recently.

HemSCs

HemSCs display stem cell markers such as CD133 and Oct-4, express mesenchymal marker CD90, but do not express endothelial, hematopoietic or pericytic cell markers. The Bischoff Laboratory researchers found that the $CD133^{+}$ cells (HemSCs) generated human, $GLUT1^{+}$ blood vessels in immunodeficient mice after 7 days. After two months, the number of blood vessels decreased, while the number of adipocytes increased. GFP-tagged lentivirus was used to label HemSCs, so they could be tracked *in vivo.* This allowed confirmation that the HemSCs formed the blood vessels and then adipocytes in immunodeficient mice. Thus, HemSCs recapitulated certain aspects of the phases of IH, blood vessels followed by fatty tissue, in an expedited time frame. HemSCs can self-renew, and they can differentiate to adipocytes, endothelial cells, pericyte/smooth muscle cells and also neuroglial cells (Khan, Boscolo et al. 2008). Although they comprise fewer than 1% of cells from hemangioma tissue, in tissue culture they grow the fastest and express the highest levels of VEGF-A among the 3 hemangioma-derived cell types.

The Bischoff Laboratory researchers also noted that VEGF-A or VEGF-B can bind VEGFR-1 on HemSCs. This leads to phosphorylation of extracellular signal-regulated kinases 1/2 (ERK 1/2) and promotes differentiation of HemSCs to HemECs. Suppression of VEGFR-1 with shRNA prevented this differentiation and decreased

formation of blood vessels *in vivo*. Therefore, VEGFR-1 was determined critical for differentiation of HemSCs to HemECs (Boscolo, Mulliken et al. 2011).

More discoveries were made concerning differentiation of HemSCs to other cell types. The Bischoff Laboratory researchers used GFP-labeled HemSCs to find that HemSCs differentiate to Hem-Pericytes when injected on immunodeficient mice. This differentiation was dependent on direct contact of HemSCs with cord blood endothelial colony-forming cells (cbECFCs) or HemECs. Differentiation of HemSCs to Hem-Pericytes was reduced *in vivo* with recombinant Jagged1 or silencing of Jagged1 in the cbECFCs with shRNA. As noted above, Jagged1 binds Notch receptors. Thus, Jagged1 and Notch signaling were found critical for differentiation of HemSCs to Hem-Pericytes (Boscolo, Stewart et al. 2011).

Chapter II

Treatments of infantile hemangioma

2.1 Therapeutic options for IH

As noted above, IH regresses on its own over time, so some pediatricians, in consultation with the parents, choose not to treat it. On the other hand, locations of IH in areas like eyelids and cheeks have directed some to seek treatments because of possible detriment to vision and likely disfigurement, respectively.

Until recently, standard treatments of IH included laser therapy, surgical resection and corticosteroids. Interferon had been reported be effective when patients with vision-threatening hemangiomas were treated daily for 3 months (Hastings, Milot et al. 1997). However, some patients suffered from spastic diplegia, in which lower extremity muscles are stiffened and ambulation is reduced. Such a severe side effect discouraged its adoption (Barlow, Priebe et al. 1998).

Among the treatments for IH, surgical resection and corticosteroids have been utilized for decades. As described above, location of IH in conspicuous areas like cheeks may motivate patients to seek consultation for removal. Clinicians typically opt for surgical resection when IH is felt to have started involuting, in order to reduce the size of scar as much as possible. Corticosteroids are either injected into IH and/or given orally, with a taper beginning after a few weeks, based on patients' weight. Corticosteroids suppress VEGF-A expressed and secreted by HemSCs, which may be the underlying mechanism for their efficacy (Greenberger, Boscolo et al. 2010). Although corticosteroids have a myriad of side effects including insulin resistance and growth retardation, they have been widely used for a variety of conditions, in addition to IH, for many years. Therefore, they had been the main non-surgical treatment option for IH until the adoption of propranolol.

Recently, rapamycin, a mTOR inhibitor, was shown to reduce proliferation and differentiation capability of HemSCs. In addition, vascular volume of hemangioma vessels, in a murine model of IH, was reduced as a result of rapamycin treatment. These findings provide an intriguing possibility that it might become a treatment option of IH, like surgical resection, corticosteroids and propranolol (Greenberger, Yuan et al. 2011).

Propranolol is a non-selective β-adrenergic receptor (AR) antagonist developed by the British scientist James Black in the 1960s (Figure 5). It is metabolized by liver, and it has been effective for treating high blood pressure and irregular heart rhythm because of its antagonism at β_1-AR (Black, Crowther et al. 1964). Propranolol also binds 5-hydroxytryptamine 1B (5-HT_{1B}) receptors in the brain, which are involved in various neurological processes such as memory and learning. In addition to its use for cardiac indications as listed above, propranolol has been prescribed for migraine prophylaxis because its activity at 5-HT_{1B} receptors leads to vasoconstriction for relief of symptoms (Diener, Kaube et al. 1998; Zhelyazkova-Savova and Zhelyazkov 2003).

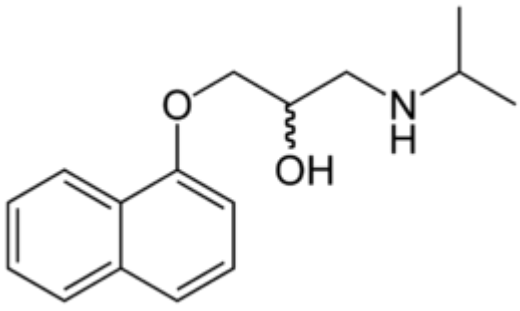

Figure 5. Molecular structure of propranolol.

2.2 β-ARs- an overview

As noted above, propranolol binds β-ARs and 5-HT_{1B} receptors. β-ARs are more prevalent throughout the body than 5-HT_{1B} receptors that are traditionally associated with regulatory functions in the brain. Thus, based on their prevalence and locations, β-ARs are likely candidates to be involved in reduction of IH by propranolol.

β-ARs are further subdivided into β_1-, β_2- and β_3-ARs. β_1-AR is well-characterized in the heart, where stimulation of the receptor by agonists such as epinephrine and norepinephrine leads to increases of heart rate and contractility, thereby increasing volume of output from the heart. Stimulation of the receptor in kidneys increases secretion of renin, which is tied to vascular volume regulation and hence blood pressure control. β_2-AR is widely distributed throughout the body, and its function depends on location of the receptor. Some effects of its stimulation by agonists such as epinephrine and albuterol include relaxation of airway, dilation of vessels, increase of glucose via glycogenolysis and gluconeogenesis and relaxation of non-pregnant uterus. β_3-AR is well-characterized in adipose tissue and bladder, and its stimulation by an agonist such as Solabegron increases lipolysis and heat production in adipose tissue and relaxation of bladder detrusor muscle. All β-ARs are coupled to G stimulatory (G_s) protein, except β_2-AR, which can also be coupled to G inhibitory (G_i) protein (Mersmann 1998; Wallukat 2002). The downstream effects of $\beta_{1,\,2}$-ARs stimulation will be described further.

An agonist such as epinephrine will bind $\beta_{1,\,2}$-ARs, allowing G_s proteins to bind and activate adenylyl cyclase to increase cyclic adenosine monophosphate (cAMP). Four molecules of cAMP will bind regulatory subunits of protein kinase A (PKA), a

serine/threonine kinase, to induce a conformational change. As a result, catalytic subunits of PKA are dissociated and activated, and they phosphorylate various targets to mediate intracellular events. If G_i protein were to be stimulated as in the case of β_2-AR, adenylyl cyclase will be inactivated and cAMP decreased; therefore, PKA will not be activated. Thus, G_s and G_i proteins mediate opposite effects.

One action of PKA is phosphorylation and activation of phosphodiesterase, which converts cAMP to 5'-AMP. By doing so, further activation of PKA by cAMP is reduced. Thus, PKA is downregulated by negative feedback, and its downstream effects are reduced.

Receptor desensitization

Pathways exist to prevent over-stimulation of β-ARs, and these have been shown in β_2-AR. As noted above, agonist binding of β_2-AR allows the coupled G_s protein to bind and activate adenylyl cyclase; subsequently, cAMP increases, and four molecules of cAMP activate PKA. In turn, PKA phosphorylates intracellular regions of β_2-AR adjacent to where G_s protein is coupled and change their conformation. As a result, further activation of adenylyl cyclase by G_s protein is inhibited (Hausdorff, Caron et al. 1990). β-AR kinase, another serine/threonine kinase, has been noted to play a role in β_2-AR desensitization, too. It phosphorylates agonist-occupied β_2-AR on its intracellular C-terminal regions. This allows receptor binding by β-arrestin, which in turn uncouples G protein from β_2-AR to prevent further signaling, similar to effects of PKA phosphorylation noted above. Thus, PKA, β-AR kinase and β-arrestin desensitize β_2-AR to prevent its over-stimulation (Pippig, Andexinger et al. 1993; Wallukat 2002). PKA phosphorylation

of β_2-AR has also been reported to switch its coupled protein from G_s to G_i (Daaka, Luttrell et al. 1997). Interestingly, β-arrestin has been reported to recruit phosphodiesterase to decrease cAMP, which augments its desensitization of the receptor, and it also participates in β-AR signaling independently of G proteins (Figure 6; Patel, Tilley et al. 2009).

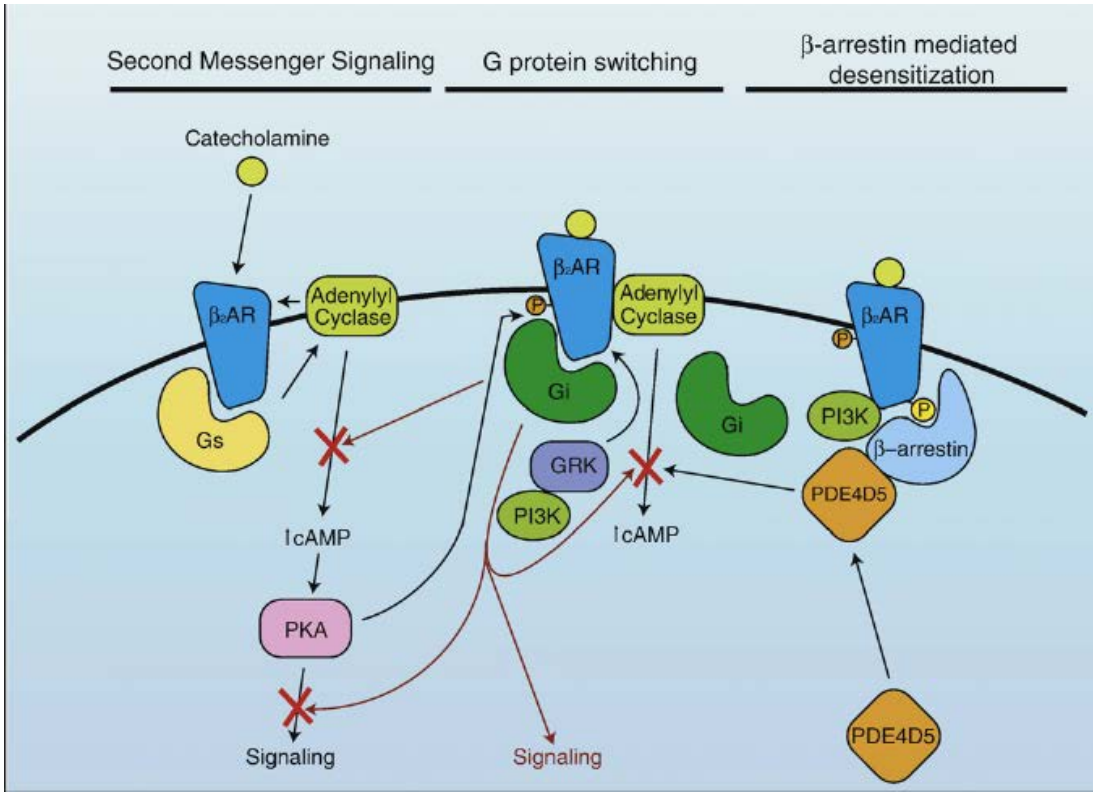

Figure 6. β_2-AR signaling, desensitization and purported players.
Adenylyl cyclase and PKA are activated as a result of catecholamine (e.g., epinephrine) stimulation. PKA and G-protein receptor kinase (GRK or β-AR kinase in text) phosphorylate β_2-AR to desensitize the receptor. G_s switches to G_i upon phosphorylation by PKA. β-arrestin uncouples G_i from β_2-AR and recruits phosphodiesterase-4D5 (PDE4D5).
Reproduced with permission from J Mol Cell Cardiol. **46**(3): 300-8, 2009, Copyright Elsevier.

β-ARs- potential relevance in IH

As described above, β-ARs are involved in various functions throughout the body, so researchers have wondered about their possible involvement in regulations of disease states. Indeed, a group of researchers noted that $\beta_{1,2}$-ARs were expressed in pancreatic cancer cells. They detected that migration of the cells was increased by treatment with norepinephrine, another agonist at the receptors, but propranolol treatment reduced such increase. In addition, norepinephrine treatment increased VEGF levels of pancreatic cancer cells, but propranolol inhibited such increase, as detected by enzyme-linked immunosorbent assay (ELISA) and qRT-PCR (Guo, Ma et al. 2009). Such an example of relationship between β-AR signaling and VEGF may be relevant in IH pathogenesis.

Propranolol is a non-selective β-AR antagonist, so it will oppose actions of agonist at the receptors. Therefore, in the absence of agonist, propranolol may not exert effects at β-ARs. If propranolol were to exert effects at β-ARs without agonist, it would also be classified as an inverse agonist that, by definition, will decrease activity of a constitutively active receptor. Interestingly, researchers found that propranolol could act as an inverse agonist at β_2-AR. They first verified β_2-AR expression in rat hearts by Western blot and then depleted catecholamines such as epinephrine by treating rats with reserpine, which blocks transport of catecholamines from cytoplasm to extracellular membrane. Propranolol decreased contractile force of rat heart muscles, which indicated its inverse agonism at β_2-AR (Varma, Shen et al. 1999). Such intriguing findings may have relevance in IH.

Another group of researchers noted that in Chinese Hamster Ovary cells expressing β_2-AR, 10 μM of propranolol reduced basal cAMP production to 54% of value without stimulation by an agonist; this confirmed that propranolol is an inverse agonist at the receptor. Unexpectedly, propranolol increased mitogen-activated protein kinase (MAPK) phosphorylation, which occurs downstream of cAMP increase and PKA activation, comparable to the level achieved by an agonist, isoproterenol. These findings indicated that not only can propranolol act as an inverse agonist at β_2-AR, but it can stimulate MAPK pathway independently of G proteins (Baker, Hall et al. 2003). As noted above, β-arrestin could participate in β-AR signaling independently of G proteins; researchers found that propranolol increased MAPK phosphorylation in Human Embryonic Kidney 293 cells expressing β_2-AR, and it promoted β-arrestin recruitment to β_2-AR in the cells transfected with β-arrestin and β_2-AR (Azzi, Charest et al. 2003). Therefore, activation of MAPK by propranolol could occur through β-arrestin. In summary, these studies demonstrated that β-AR signaling could occur through multiple paths, including agonism, antagonism, inverse agonism and β-arrestin.

2.3 Propranolol as an effective therapeutic for IH

In 2008, propranolol was serendipitously discovered to be effective for treating IH. A patient responded minimally to corticosteroids and developed cardiomyopathy during treatment. The patient likely developed cardiomyopathy either because IH was a high-volume lesion, causing strain to the heart, or as a side effect of corticosteroids. The patient was prescribed a β-AR antagonist, propranolol, to decrease cardiac workload, and soon after redness and firmness of lesion decreased. These effects were maintained after corticosteroids were tapered off, with continuation of propranolol only

(Figure 7; Léauté-Labrèze, Dumas de la Roque et al. 2008). Although patients varied by gender, age, location and severity of IH, propranolol has been effective with minor side effects, such as nausea, diarrhea and agitation while sleeping. Effects were seen as early as 24 hours after initial treatment (Sans, de la Roque et al. 2009; Lv, Fan et al. 2012). Clinicians noted that some patients experienced rebound in size and color after cessation of treatment, which prompted many to keep patients on propranolol until the lesion reached involuting phase (Zaher, Rasheed et al. 2011).

Figure 7. Treatment with propranolol.
A- 9 weeks of age after 4 weeks of steroids. B- 10 weeks of age, 1 week after propranolol treatment with steroids. C- 6 months of age on propranolol monotherapy. D- 9 months of age.
Reproduced with permission from the N Engl J Med. **358**(24): 2649-51, 2008, Copyright Massachusetts Medical Society.

Researchers have been interested in finding explanations behind efficacy of propranolol in IH, which also became my goal. Although it is effective, patients are maintained on it for months, while some do not respond. Finding how and why propranolol works in IH will help tailor therapies for individual patients, likely expediting

recovery and improving quality of their lives. Therefore, several groups studied this topic and published their findings in literature. Initial studies were carried out with non-pathologic human endothelial cells. For example, propranolol was reported to decrease proliferation of HUVECs through a cell cycle arrest at G_0/G_1, with corresponding decreases in cyclins D1, D3 and cyclin-dependent kinase 6. In addition, formation of capillary-like tubes by HDMECs was reduced, with 50% reduction of tube lengths occurring at ~ 37 μM (Lamy, Lachambre et al. 2010). These findings were detected in the absence of agonist such as epinephrine.

Researchers from the same group found that tube formation capability of another endothelial cell type, human brain microvascular endothelial cells (HBMECs), was also reduced, with a noticeable decrease starting at 10 μM. However, migration and apoptosis of HBMECs were unaffected by propranolol concentrations up to 100 μM. They also noted that propranolol reduced secretion of matrix metalloproteinase 9 (MMP-9), an enzyme involved in matrix degradation and cell migration, after treatment with a tumor-promoting agent phorbol 12-myristate 13-acetate (Annabi, Lachambre et al. 2009). As above, propranolol exerted such effects in the absence of agonist, so findings by this group highlighted the possible inverse agonism of propranolol at β-ARs.

Another group assessed the effect of propranolol on HemECs and HemSCs. Proliferation of HemECs and HemSCs was reduced by propranolol at 50 μM. Propranolol treatment of HemSCs stimulated transcription of adipogenic genes, such as *PPARδ* and *RXRα*, and this was verified by Oil Red O staining (Wong, Hardy et al. 2012). Others showed that propranolol inhibits proliferation of HemECs at 300 μM and also increases their apoptosis (Chim, Armijo et al. 2012; Ji, Li et al. 2012). In

summary, researchers from different groups found various effects of propranolol on hemangioma-derived and non-hemangioma-derived cells, with and without agonist. Therefore, propranolol may affect a variety of cell types, in addition to hemangioma-derived cells, by mechanisms including antagonism and inverse agonism at β-ARs.

Some have hypothesized that propranolol exerts multiple effects to reduce IH. First, as a β-AR antagonist, propranolol reduces levels of cAMP, subsequently affecting PKA, endothelial nitric oxide synthase (eNOS) and decreasing production and release of nitric oxide (NO); eventually vasoconstriction occurs. Second, as β-AR agonists increase pro-angiogenic factors such as VEGF and MMP-9, propranolol likely decreases them to oppose angiogenesis. Third, β-AR agonists signal through G_s protein to increase cAMP and activate PKA; one molecule activated by PKA is Src, a tyrosine kinase. Src, in turn, phosphorylates caspase-8 and inactivates it to inhibit apoptosis. Therefore, authors reasoned that as a β-AR antagonist, propranolol induces apoptosis (Storch and Hoeger 2010). In support of the first possibility, hemangioma tissues were surgically resected from patients treated or not treated with propranolol, and eNOS levels were shown to be decreased in tissues from patients treated with propranolol compared to the untreated group. In addition, eNOS levels decreased as hemangiomas progressed through their 3 phases (Dai, Hou et al. 2012).

In summary, researchers have gained leads on how and why propranolol could reduce IH since the initial report in 2008, but finding its mechanism remains a work in progress. In the experiments described in this dissertation, HemECs and Hem-Pericytes were affected by propranolol both *in vitro* and *in vivo*. Therefore, they may be the key players, through which propranolol reduces IH.

2.4 Abbreviations

5-hydroxytryptamine 1B	$5\text{-}HT_{1B}$
adrenergic receptor	AR
alpha smooth muscle actin	αSMA
basic fibroblast growth factor	bFGF
bone marrow mesenchymal progenitor cells	bmMPCs
cyclic adenosine monophosphate	cAMP
cord blood endothelial colony-forming cells	cbECFCs
diaminobenzidine	DAB
diacylglycerol	DAG
4', 6-diamidino-2-phenylindole	DAPI
Dulbecco's Modified Eagle Medium	DMEM
Endothelial Basal Medium-2	EBM-2
epidermal growth factor	EGF
Endothelial Growth Medium-2	EGM-2
enzyme-linked immunosorbent assay	ELISA
endothelial nitric oxide synthase	eNOS
extracellular signal-regulated kinases 1/2	ERK 1/2
fetal bovine serum	FBS
glyceraldehyde 3-phosphate dehydrogenase	GAPDH
glucose transporter-1	GLUT1
human brain microvascular endothelial cells	HBMECs
human dermal microvascular endothelial cells	HDMECs
hematoxylin & eosin	H & E
hemangioma-derived endothelial cells	HemECs
hemangioma-derived pericytes	Hem-Pericytes
hemangioma-derived stem cells	HemSCs
hypoxia-inducible factor 1α	HIF1α
heparan sulfate proteoglycan	HSPG
human umbilical vein endothelial cells	HUVECs
hypoxanthine phosphoribosyltransferase 1	HPRT1
immunofluorescence	IF
infantile hemangioma	IH
immunohistochemistry	IHC
interferon-β	IFN-β
inositol 1, 4, 5-trisphosphate	IP_3
mitogen-activated protein kinases	MAPK
mammalian target of rapamycin	mTOR
matrix metalloproteinase 9	MMP-9
microvessel density	MVD
nuclear factor of activated T cells	NFAT
nuclear factor-kB	NF-kB
neural glial antigen-2	NG2
Notch intracellular domain	NICD

2.4 Abbreviations (continued)

nitric oxide	NO
neuropilin	NRP
phosphate buffered saline	PBS
platelet-derived growth factor receptor β	PDGFR-β
polydimethylsiloxane	PDMS
phosphoinositide 3-kinase	PI 3-kinase
phosphatidylinositol 4,5-bisphosphate	PIP_2
protein kinase A	PKA
protein kinase C	PKC
phospholipase C	PLC
placental growth factor	PlGF
quantitative real time polymerase chain reaction	qRT-PCR
red blood cell	RBC
smooth muscle cells	SMCs
smooth muscle myosin heavy chain	smMHC
tumor endothelial marker-8	TEM8
urokinase plasminogen activator receptor	uPAR
vascular endothelial growth factor A	VEGF-A
vascular endothelial growth factor B	VEGF-B
vascular endothelial growth factor receptor-1	VEGFR1
vascular endothelial growth factor receptor-2	VEGFR2
vascular endothelial growth factor receptor-3	VEGFR3

Chapter III

Confirming the presence of known targets of propranolol in IH

3.1 Preliminary studies

Since its discovery as an effective therapeutic for IH in 2008, propranolol has been widely adopted in medical centers around the world (Sans, de la Roque et al. 2009). Patients respond differently to various medications, so clinicians need to tailor appropriate therapies for patients. In order to design individualized therapies for patients, it will be important to clarify mechanism of propranolol in IH.

As described above, several experimental results have been reported. Some showed that propranolol inhibits proliferation of HemECs at 300 μM and also increases their apoptosis (Chim, Armijo et al. 2012; Ji, Li et al. 2012). Another group showed that propranolol inhibits tube formation of brain endothelial cells (Annabi, Lachambre et al. 2009). These results suggested that propranolol might block angiogenic activities of endothelial cells.

Shoshana Greenberger, a former Bischoff Laboratory member, was interested in finding out the effects of propranolol on hemangioma-derived cells. She observed that propranolol treatment did not affect RNA or protein levels of VEGF-A in HemSCs, part of which I confirmed by qRT-PCR in other HemSCs. She also treated HemECs and HemSCs with propranolol for 48 hours. She took the conditioned media and tested them for simultaneous detection of 43 proteins commonly associated with angiogenesis, obtained from protein array kits. However, no significant changes were detected with propranolol treatment (not shown).

In her studies, proliferation of HemSCs and differentiation of HemSCs to ECs or HemSCs to smooth muscle cells were not affected by propranolol treatment (not shown).

A note on the molarity of propranolol chosen for *in vitro* studies

As described above, effects of propranolol on hemangioma- and non-hemangioma-derived cells have been noted by other researchers at 10-300 μM. Its half life is 3-5 hours, and the binding affinities of propranolol for β_1- and β_2-ARs are 2.8 nM and 0.62 nM (K_i), respectively (Pauwels, Gommeren et al. 1988). Clinicians prescribe 1-5 mg/kg per day for patients, and its plasma concentrations after 1 mg/kg treatments were reported to range from 0 to 1.4 μM (Sans, de la Roque et al. 2009; Lv, Fan et al. 2012; Zhang, Mai et al. 2013). A concentration of 10 μM was chosen for *in vitro* experiments based on literature reports and to avoid adding vastly excessive amounts of drug. Propranolol was also added twice daily for *in vitro* assays lasting days because of its half life.

3.2 Tube formation of HemECs and HemSCs not affected by propranolol

As noted above, researchers found that tube formation capability of normal endothelial cells such as HDMECs was reduced, with 50% reduction of tube lengths occurring at ~ 37 μM of propranolol (Lamy, Lachambre et al. 2010). They found that tube formation capability of HBMECs was also reduced, with a noticeable decrease starting at 10 μM of propranolol (Annabi, Lachambre et al. 2009). Consequently, it was of interest to find out whether tube formation capability of hemangioma-derived cells would be affected by propranolol treatment.

In addition to HemECs, HemSCs have been noted to form tubes on a thin layer of Matrigel. This indicated their possession of endothelial-cell-like properties, on top of their stem cell traits, even before their differentiation to HemECs (Boscolo, Mulliken et

al. 2011). Therefore, HemECs and HemSCs were tested in tube formation assays. Hem-Pericytes were not assayed.

HemECs, HemSCs and HDMECs were tested in tube formation assay, with HDMECs as a positive control cell type (Figure 8). For each type, cells were either treated with vehicle or propranolol once. As shown in Figure 8, no noticeable differences were detected in the tubes formed by vehicle- and propranolol-treated HemECs, HemSCs and HDMECs after 18 hours. Pictures are representative of multiple experiments on 2 different HemECs (133 and I-69) and 5 different HemSCs (125, 129, 133, 140 and I-54).

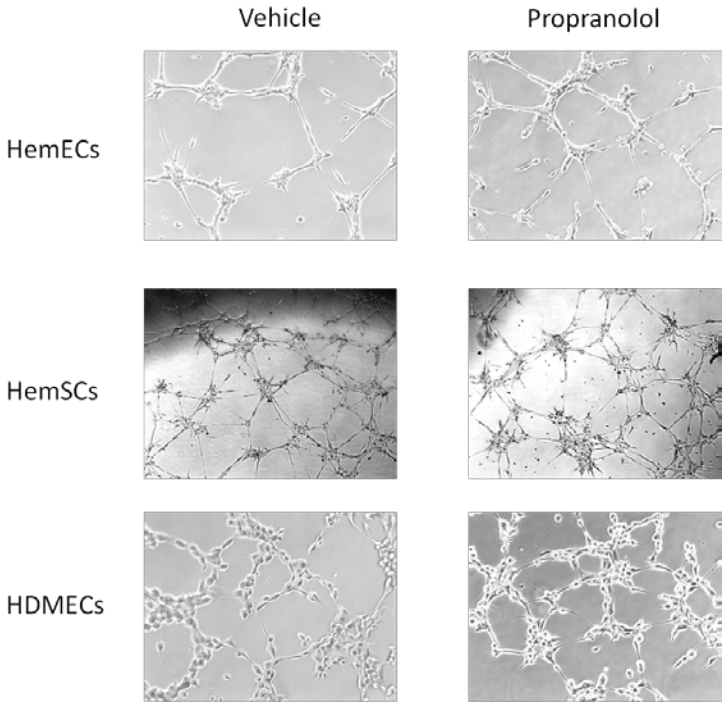

Figure 8. Tube formation assays of HemECs, HemSCs and HDMECs. Cells were treated once with vehicle or propranolol. Pictures are representative of images from 4 wells and multiple experiments.

As noted above, researchers reported that propranolol decreased tube formation of HBMECs and HDMECs. Their experiments were conducted without an agonist such

as epinephrine. Therefore, propranolol might have acted on targets other than β-ARs or as inverse agonists to decrease tube formation. Tube formation assays in Figure 8 could have been performed more comprehensively, for example by taking measurements of tube lengths, adding epinephrine on top of propranolol or adding an inhibitor (e.g., Avastin) and assessing whether or not propranolol duplicates the effects of the inhibitor. Given the negative results from Figure 8 and high degrees of variability and subjectivity of tube formation assays, such steps were not taken.

3.3 Assessing for presence of 5-HT_{1B} receptors in IH

After such negative results, it was decided that confirming the presence of known receptors of propranolol, 5-HT_{1B} and β-ARs, in IH might be a good starting point. They are known targets of the drug, so their presence may indicate drug binding to lead to further actions. Presence of 5-HT_{1B} receptor in IH tissue was assessed by immunofluorescence (IF), and human brain tissue used as a positive control (Figure 9).

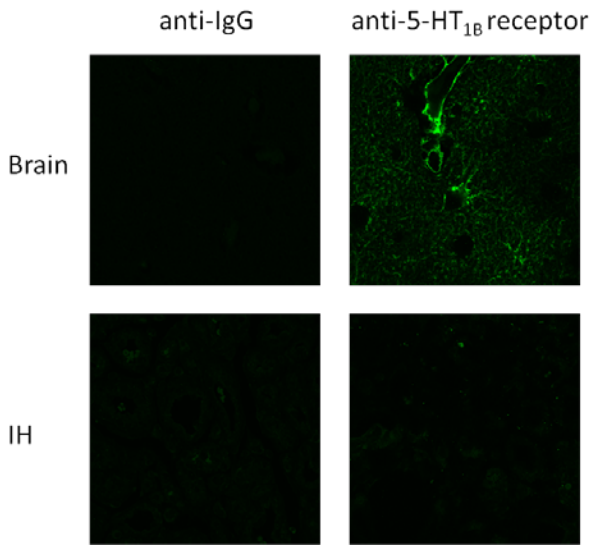

Figure 9. Immunostaining for 5-HT_{1B} receptor in brain and IH tissue. The receptor was visualized by utilizing Alexa Fluor 488 as the secondary.

RNA levels of 5-HT_{1B} receptor in HemECs and Hem-Pericytes were assessed, with bone marrow mesenchymal progenitor cells (bmMPCs) as a positive control (Figure 10).

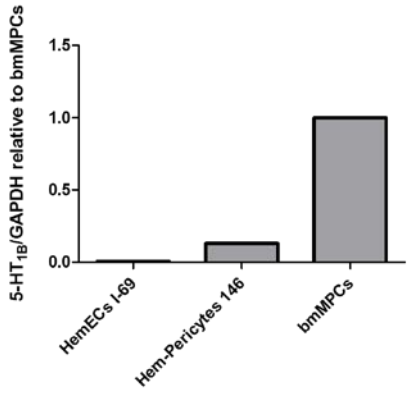

Figure 10. RNA levels of 5-HT_{1B} receptor.
Ratios of 5-HT_{1B}/GAPDH in hemangioma-derived cells were re-normalized to that of bmMPCs, set to 1.

5-HT_{1B} receptor was not detected in IH by IHC (Figure 9), but low levels of the receptor were detected in Hem-Pericytes 146 by qRT-PCR (Figure 10). However, only few samples of hemangioma-derived cells, one each of HemECs and Hem-Pericytes, were used in qRT-PCR, and bmMPCs might not be a good positive control for 5-HT_{1B} receptor. Rather, a better control might be brain cells known to be involved in serotonergic neurotransmission. Although cDNA samples of cells were loaded into triplicate wells for qRT-PCR, these provided technical replicates for pipetting accuracy; cells were grown and harvested from single plates, from which RNA extracted and cDNA reverse-transcribed. As they were not grown in multiple wells or plates, no error bars could be added to the graph in Figure 10.

In summary, 5-HT_{1B} receptor was not detected by IHC with a good positive control, and very little was detected in two hemangioma-derived cell types by qRT-PCR. Therefore, receptor expression was low in IH, and from this point on, the focus shifted to

confirming presence of adrenergic receptors in IH. Adrenergic receptors are widely expressed throughout the body, whereas 5-HT_{1B} receptors are more highly-associated with the nervous system. Based on this fact, adrenergic receptors are more likely to be expressed than 5-HT_{1B} receptors in IH.

3.4 IHC studies of α_{1b}- and β_2-ARs in IH

Propranolol binds β-ARs, so presence of adrenergic receptors was assessed in IH tissues by IHC. Human brain tissue expresses both 5-HT_{1B} and adrenergic receptors, so it was used as a positive control again. Presence of α_{1b}-AR was assessed in addition to β_2-AR because epinephrine, agonist at β-ARs, may exert effects at α_{1b}-AR if β-ARs are bound by propranolol. Immunostaining for α_{1b}-AR hinted at expression by endothelial cells in one IH tissue (IH #1; Figure 11), whereas expression was more difficult to detect in another (IH #2; Figure 11).

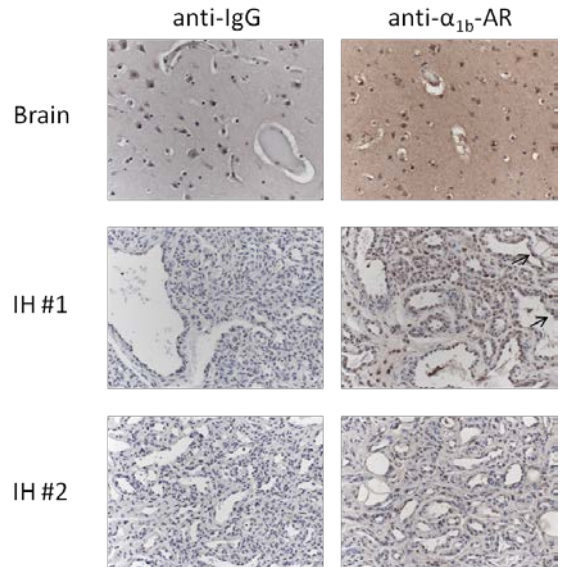

Figure 11. Immunostaining for α_{1b}-AR in brain and IH tissues. The receptor was visualized by utilizing horse radish peroxidase as the secondary. IH #1 showed potential expression by endothelial cells, but expression was more difficult to detect in IH #2.

Immunostaining for β_2-AR hinted at expression by endothelial and some stromal cells in two tissues (IH #1, Ab #1; IH #2, Ab #1; Figure 12). However, immunostaining in the same tissues with another commercially available antibody showed expression not by hemangioma vessels or stroma but by sweat glands and mast cells, respectively (IH #1, Ab #2; IH #2, Ab #2; Figure 12). These findings were confirmed by a review with Dr. Harry Kozakewich, a pathologist at Boston Children's Hospital.

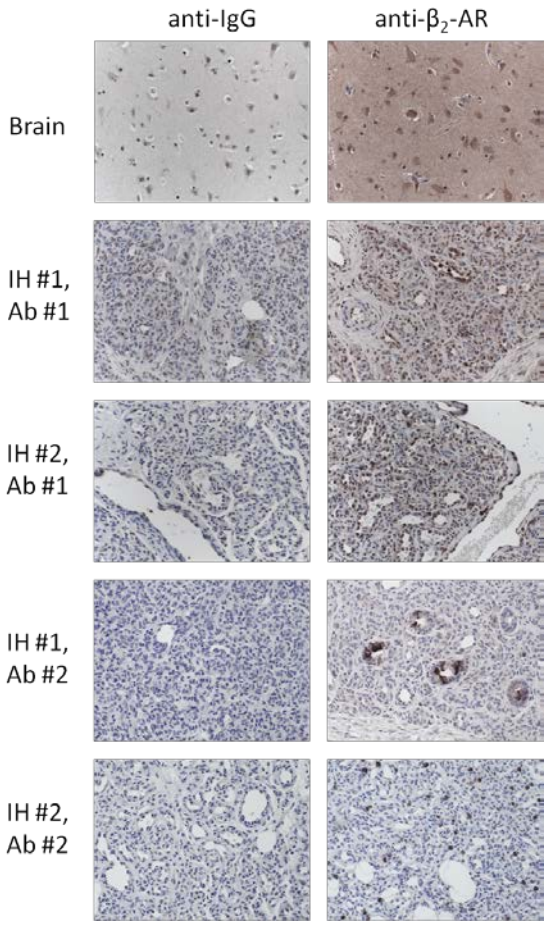

Figure 12. Immunostaining for β_2-AR in brain and IH tissues. The receptor was visualized by utilizing horse radish peroxidase as the secondary. Ab #1 in IHs #1 & #2 hinted at expression by endothelial and some stromal cells, but Ab #2 in IH #1 showed expression by sweat glands. Ab #2 in IH #2 showed expression by mast cells.

In summary, even though immunohistochemistry (IHC) with adrenergic receptor antibodies was performed on select hemangioma tissues, patterns of staining were inconsistent from tissue to tissue for both α_{1b}- and β_2-ARs. This might have been reflective of variability of ARs expression levels from tissue to tissue, and mast cells have been described in literature to express β_2-AR (Johnson 2002). However, the different results from 2 antibodies for β_2-AR on the same tissues were concerning (IH #1, Ab #1 vs. IH #1, Ab #2; IH #2, Ab #1 vs. IH #2, Ab #2; Figure 12). These phenomena might be attributed to factors such as quality of the antibodies and the difficulty of antibody-labeling adrenergic receptors that are highly embedded in the plasma membrane with 7-transmembrane spanning domains.

On the other hand, a group of researchers used a tissue microarray that contained various vascular anomalies, including IH, and immunostained for $\beta_{2,3}$-ARs and phosphorylated form of β_2-AR. They found that all 3 phases of IH expressed all 3 receptors tested, except that the proliferating phase expressed phosphorylated form of β_2-AR weakly. Although no isotype-matched or positive controls were shown, a variety of vascular anomalies were tested for comparison (Chisholm, Chang et al. 2012). Even though the reasons behind their success may be multifactorial, they used different antibodies from the ones used in Figure 12.

3.5 RNA levels of $\beta_{1,2}$-ARs in IH tissues

As described above, in the attempts to detect ARs in IH by IHC, inconsistent results were noted from one IH tissue to another and from one antibody to another. At the recommendation of dissertation advisory committee, it was decided to utilize qRT-PCR

to detect RNA levels of ARs in IH tissues. By doing so, the expectation was to avoid potential problems with quality of the antibodies and the difficulty of antibody-labeling adrenergic receptors. Hemangioma tissues from patients of various ages, from 3 months to 10 years of age, were chosen, and their RNA isolated as described in Methods. Receptors assayed include $\beta_{1\text{-}3}$- and α_{1b}-ARs (Figure 13). For each receptor, expression level was normalized to β-actin, a reference gene chosen because it was expressed in all hemangioma tissues tested. This was in contrast to other reference genes like glyceraldehyde 3-phosphate dehydrogenase (GAPDH) and hypoxanthine phosphoribosyltransferase 1 (HPRT1); some tissues did not even express GAPDH or HPRT1. β-actin might have been a good reference gene in this case because it is a structural gene, whereas GAPDH and HPRT1 are metabolic genes. Structural genes may be better than metabolic genes to serve as reference genes for surgically resected tissues, whereas it may be the other way around for cultured cells.

The level of expression of AR/β-actin was re-normalized to AR expression in a positive control tissue/cell type normalized to β-actin in the same control, set to 1. For example, β_1-AR/β-actin of tissues was normalized to β_1-AR/β-actin in cardiac tissue which was set to 1, whereas β_2-AR/β-actin of tissues was to β_2-AR/β-actin in bladder SMCs which was also set to 1. Expression levels of β_3- and α_{1b}-ARs among hemangioma tissues varied from patient-to-patient and were generally low compared to their positive controls (Figure 13C, D). However, $\beta_{1,\,2}$-ARs were consistently detected in most hemangioma specimens, except those from ages 15 and 21 months, and levels were more remarkable for β_2- than β_1-AR. (Figure 13A, B).

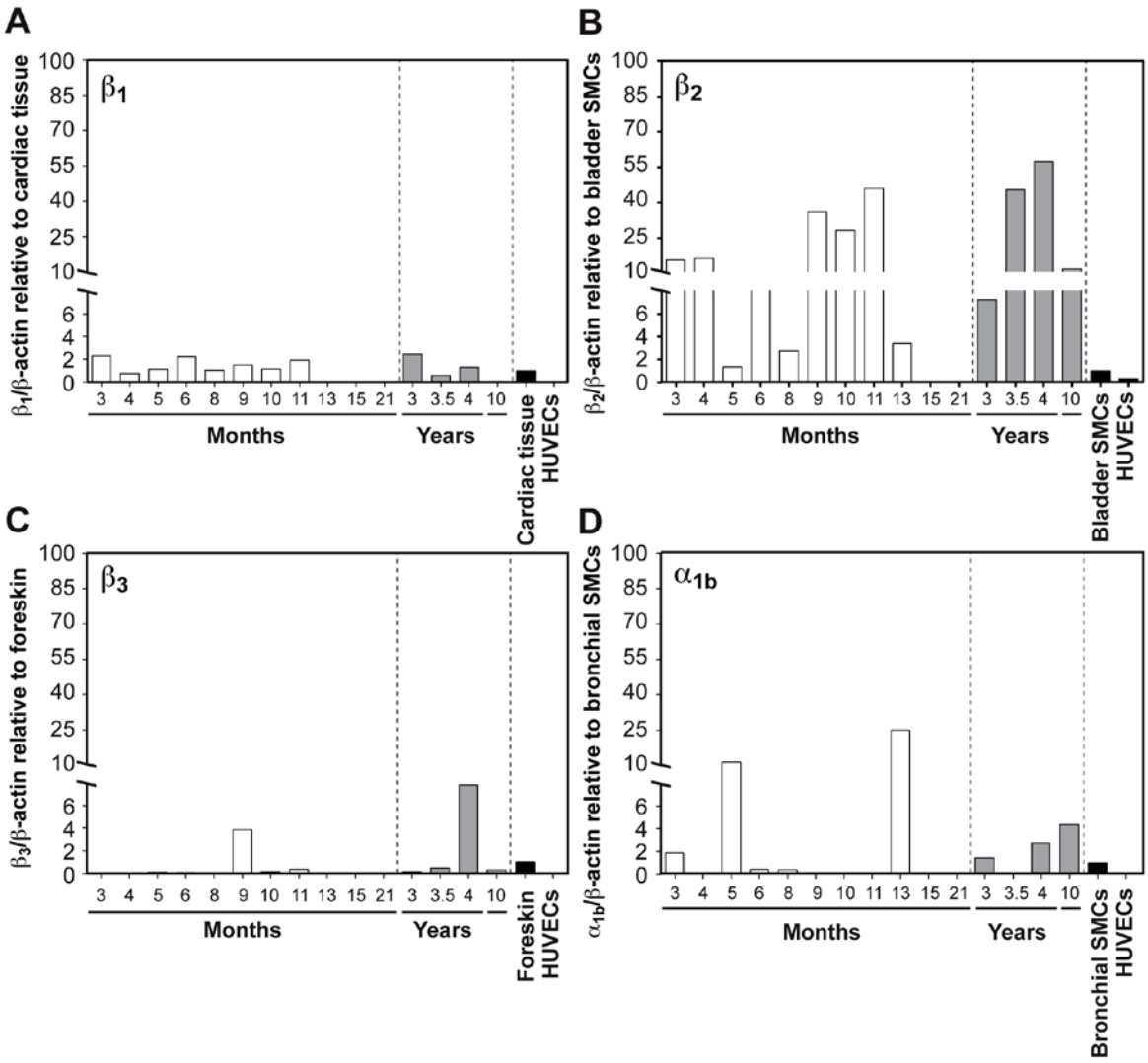

Figure 13. $\beta_{1,\ 2}$-adrenergic receptors are highly expressed across hemangioma tissues.

RNA was extracted from hemangioma tissues resected from patients of different ages, and qRT-PCR performed as described in Methods. Samples were run in triplicates, and the entire analysis was repeated once. Copy numbers for adrenergic receptors and β-actin were obtained by the standard curve method. Each qRT-PCR included HUVECs and a positive control tissue/cell type (cardiac tissue for β_1 in **A**, bladder SMCs for β_2 in **B**, foreskin for β_3 in **C** and bronchial SMCs for α_{1b} in **D**), to which values of adrenergic receptor/β-actin were normalized.

RNA levels of $\beta_{1,2}$-ARs in IH tissues: significance & caveats

Expression of $\beta_{1,2}$-ARs in IH tissues was easily appreciated in IH tissues. To date, RNA expression of β-ARs has been frequently reported in hemangioma-derived cells, but not in IH tissues (Wong, Hardy et al. 2012; Rössler, Haubold et al. 2013). In addition, IH tissues from different ages and patients are represented, providing a spectrum of information.

In order to examine RNA levels of β_2-AR in IH tissues more closely, RNA levels of β_2-AR to CD31 (Figure 14A) and to αSMA (Figure 14B) for each tissue were obtained. IH has abundances of endothelial cells and pericytes; therefore, RNA levels of β_2-AR were normalized to markers of endothelial, CD31, and pericytic, αSMA, cells. RNA levels of β_2-AR were more remarkable if they were normalized to CD31 compared to αSMA. In order to get an idea of endothelial cell contents of tissues, RNA levels of CD31 to β-actin were derived (Figure 14C). In contrast to what was done for IH tissues, these quotients from Figure 13 were not re-normalized to those of positive controls, which were HUVECs for β_2/CD31 (Figure 14A), bladder SMCs for β_2/αSMA (Figure 14B) and HUVECs again for CD31/β-actin (Figure 14C). Although the tissues varied widely in their relative endothelial cell contents to β-actin, it was affirming to see that all tissues had endothelial cells, especially ones that did not express ARs, from ages 15 and 21 months. Expression levels of ARs might be heterogeneous in a tissue, and parts low in receptors might have been used to isolate RNA, which could explain why samples from ages 15 and 21 months did not express ARs.

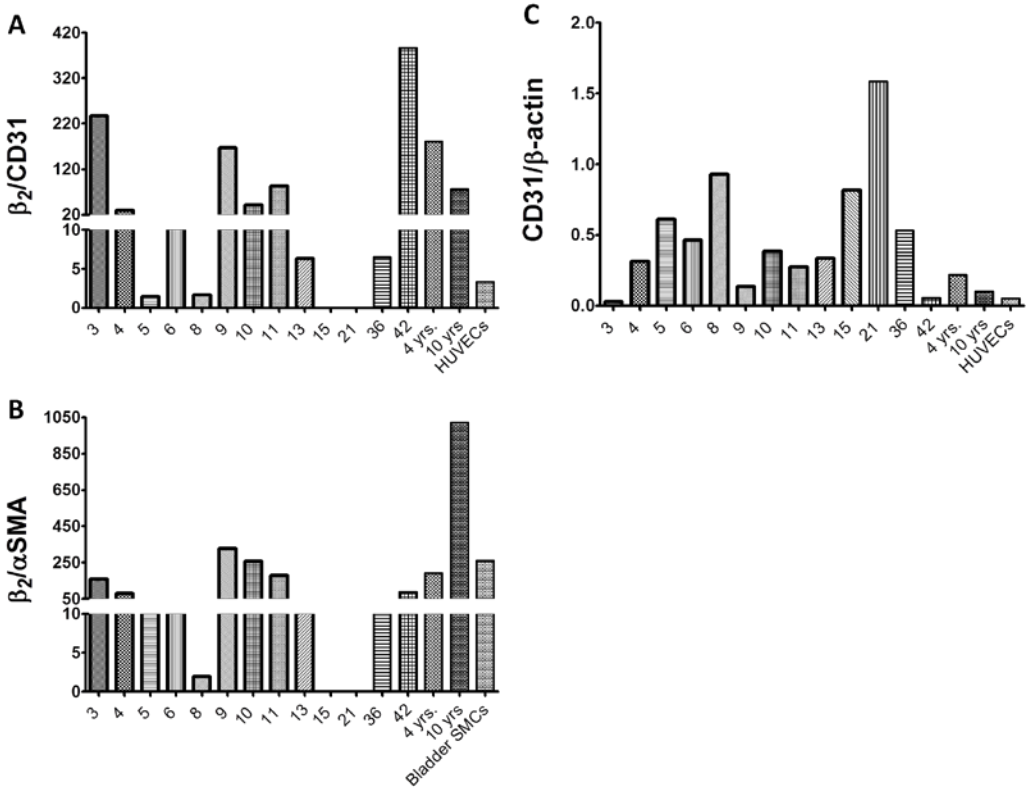

Figure 14. RNA levels of β_2-AR in IH tissues normalized to different genes and endothelial cell contents of IH tissues.
RNA levels of β_2-AR were normalized to CD31 in **A** and αSMA in **B**. CD31 levels of IH tissues were normalized to β-actin in **C**.

Different positive controls were used for each adrenergic receptor- cardiac tissue for β_1-AR, bladder SMCs for β_2-AR, foreskin for β_3-AR and bronchial SMCs for α_{1b}-AR. Such measures were necessary because, unfortunately, no one positive control expressed high levels of all 4 ARs assayed. In addition, each time point (e.g., 3 months) had tissue from one patient, so variability of AR expression among multiple patients at the same time point could not be assessed. Although cDNA samples of tissues were loaded into triplicate wells for qRT-PCR, these provided technical, not tissue, replicates; hence no error bars could be added to Figures 13 and 14.

Unfortunately, β_2-AR detection in bladder SMC, a positive control, by Western blot with the two β_2-AR antibodies from Figure 12 was not successful (not shown), so no attempts were made with IH tissues. Expression of β_1-AR in IH tissues was not assessed by Western blot or IHC. Micro RNAs could have reduced RNA levels of $\beta_{1,2}$-ARs, thereby resulting in lower protein levels of $\beta_{1,2}$-ARs than one might have expected from RNA levels. However, given that $\beta_{1,2}$-ARs were expressed across many IH tissues, this possibility was not likely to have occurred consistently in the samples.

3.6 RNA levels of $\beta_{1,2}$-ARs in hemangioma-derived cells

After finding that $\beta_{1,2}$-ARs were consistently expressed in most hemangioma tissues, their expression levels in specific populations of hemangioma-derived cells were assessed. Several reference genes, β-actin, GAPDH, HPRT1 and S9, were tested, and the standard curve method was utilized to generate copy numbers of the reference genes for samples.

Table 1. Copy numbers of β-actin among hemangioma-derived cells & controls.

ECs 17	ECs 20	ECs 21	ECs 125	ECs 133	ECs 150	ECs I-69	Peric-ytes 146	Peric-ytes 157	Peric-ytes I-69	SCs 97	SCs 120	SCs 125
37	91	65	22	50	40	68	67	28	16	81	46	66

SCs 128	SCs 129	SCs 133	SCs 140	SCs I-54	Bladder SMCs	Cardiac tissue
52	118	114	75	80	36	1

Table 2. Copy numbers of GAPDH among hemangioma-derived cells & controls.

ECs 17	ECs 20	ECs 21	ECs 125	ECs 133	ECs 150	ECs I-69	Peric -ytes 146	Peric -ytes 157	Peric -ytes I-69	SCs 97	SCs 120	SCs 125
21	51	54	36	71	45	94	72	19	21	55	56	67

SCs 128	SCs 129	SCs 133	SCs 140	SCs I-54	Bladder SMCs	Cardiac tissue
53	62	47	48	49	25	4

Table 3. Copy numbers of HPRT1 among hemangioma-derived cells & controls.

ECs 17	ECs 20	ECs 21	ECs 125	ECs 133	ECs 150	ECs I-69	Peric -ytes 146	Peric -ytes 157	Peric -ytes I-69	SCs 97	SCs 120	SCs 125
267	291	245	132	326	74	345	132	45	34	144	146	148

SCs 128	SCs 129	SCs 133	SCs 140	SCs I-54	Bladder SMCs	Cardiac tissue
98	247	276	122	123	39	39

Table 4. Copy numbers of S9 among hemangioma-derived cells & controls.

ECs 17	ECs 20	ECs 21	ECs 125	ECs 133	ECs 150	ECs I-69	Peric -ytes 146	Peric -ytes 157	Peric -ytes I-69	SCs 97	SCs 120	SCs 125
145	87	174	34	178	82	309	144	24	4	77	44	100

SCs 128	SCs 129	SCs 133	SCs 140	SCs I-54	Bladder SMCs	Cardiac tissue
41	52	88	70	59	77	12

All samples expressed the 4 reference genes, and GAPDH was chosen because its copy numbers varied the least among the cells. As noted above, a different reference gene, β-actin, was used for hemangioma tissues. Like what was done for hemangioma tissues, expression levels of $\beta_{1,2}$-AR/GAPDH were re-normalized to AR expression in a positive control tissue/cell type normalized to GAPDH in the same control, set to 1.

Expression of β_1-AR was noted in all HemECs, but not in most Hem-Pericytes and HemSCs (Figure 15A). Expression of β_2-AR was detected in all three cell types, but the highest and most consistent expression occurred in HemECs (Figure 15B).

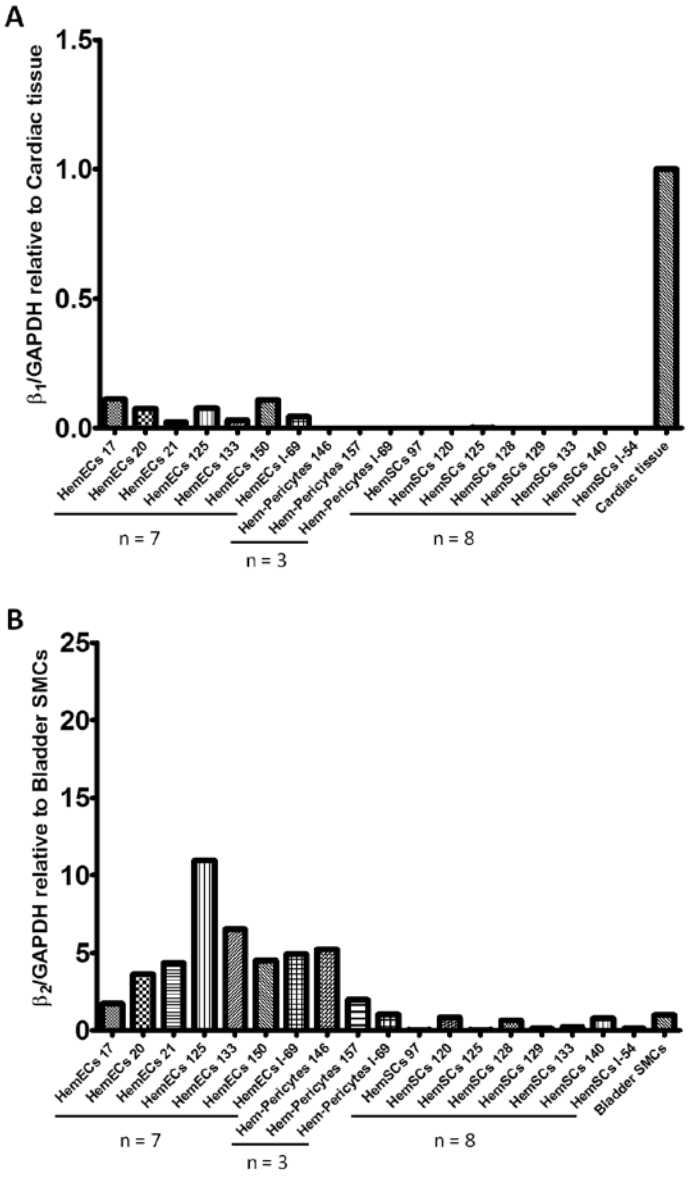

Figure 15. $\beta_{1,2}$-ARs levels in hemangioma-derived cells.
A. β_1-AR expression relative to GAPDH, normalized to cardiac tissue.
B. β_2-AR expression relative to GAPDH, normalized to bladder SMCs. Four reference genes, β-actin, GAPDH, HPRT1 and S9, were tested, and GAPDH was chosen because its expression varied the least among the samples. Please refer to Tables 1-4 for copy numbers.

RNA levels of $\beta_{1,2}$-ARs in hemangioma-derived cells: significance & caveats

RNA levels of $\beta_{1,2}$-ARs in hemangioma-derived cells have been reported in literature (Wong, Hardy et al. 2012; Rössler, Haubold et al. 2013). In Figure 15, hemangioma-derived cells from different patients are represented, providing a wide spectrum of information.

Different positive controls were used for each adrenergic receptor- cardiac tissue for β_1-AR and bladder SMCs for β_2-AR. This was necessary because neither expressed high levels of both $\beta_{1,2}$-ARs. Although $\beta_{1,2}$-ARs were expressed in both IH tissues and hemangioma-derived cells, expression levels were higher in tissues. This might be a result of change in levels of $\beta_{1,2}$-ARs brought on by cell culture. However, hemangioma-derived cells in culture have been noted to retain characteristics they show *in vivo.* For instance, endothelial cell markers such as angiopoietin-2, E-selectin and Jagged1 were expressed by IH tissues and HemECs in culture (Calicchio, Collins et al. 2009; Kräling, Razon et al. 1996; Yu, Varughese et al. 2001; Smadja, Mulliken et al. 2012; Boscolo, Stewart et al. 2011). Likewise, pericytic markers such as αSMA, calponin, NG2 and PDGFR were expressed by IH tissues and Hem-Pericytes in culture (Boscolo, Stewart et al. 2011; Boscolo, Mulliken et al. 2013).

As noted above, cDNA samples of cells were loaded into triplicate wells for qRT-PCR, and these provided technical replicates. Cells were grown and harvested from single plates, from which RNA extracted and cDNA reverse-transcribed. As they were not grown in multiple wells or plates, no error bars could be added to the graphs in Figure 15. Nevertheless, Figure 15 contained cells from multiple patients for each

hemangioma-derived cell type, so a statistical analysis of data was made feasible in Figure 16.

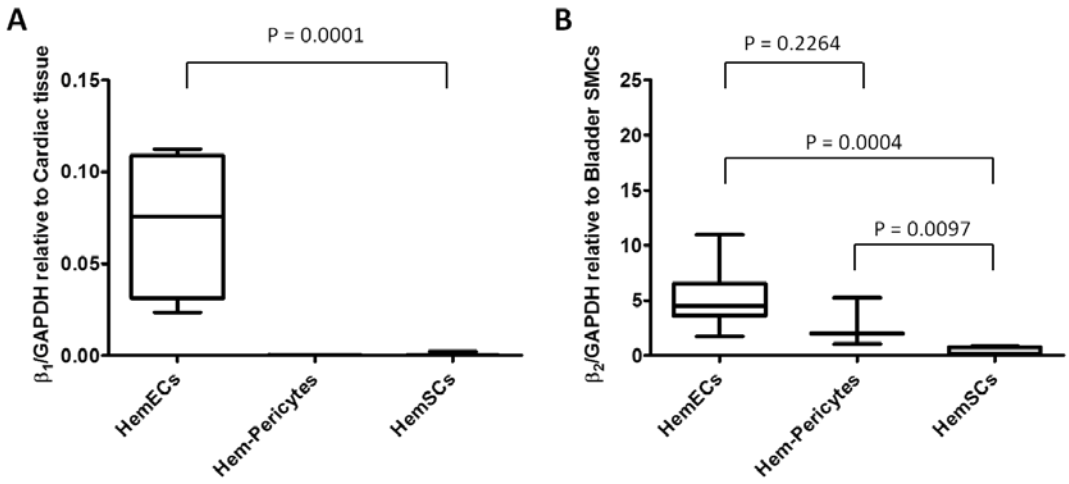

Figure 16. $\beta_{1,2}$-ARs levels by hemangioma-derived cell types.
A. β_1-AR expression relative to GAPDH, normalized to cardiac tissue, for each cell type. The differences in receptor levels were significant for HemECs-HemSCs. Only 1 out of 3 Hem-Pericytes expressed β_1-AR, so further statistical analysis was not done.
B. β_2-AR expression relative to GAPDH, normalized to bladder SMCs, for each cell type. The differences in receptor levels were significant for the following pairs: HemECs-HemSCs and Hem-Pericytes-HemSCs. The differences were not significant for HemECs-Hem-Pericytes.

Although the attempts to detect ARs in IH tissues by IHC and Western blot yielded inconsistent and unsuccessful results, ARs were consistently detected in hemangioma-derived cells by qRT-PCR. Given that β-ARs were expressed consistently across many hemangioma-derived cells, one can deduct the location of β-ARs in IH tissues, on endothelial cells for β_1-AR and on endothelial, pericytic and stem cells for β_2-AR.

Chapter IV

Hemangioma-derived cell types affected by propranolol

4.1 Effect of propranolol on hemangioma-derived cells

After much trial-and-error, the presence of known targets of propranolol, β-ARs, was confirmed in IH. From this point on, potential importance of β-ARs, in the efficacy of propranolol in IH, was studied. Experimental results from this section indicated that propranolol affects proliferation of HemECs and Hem-Pericytes and contractility of Hem-Pericytes.

4.2 Propranolol reduces proliferation of HemECs and pericytes

As described above, some researchers showed that propranolol inhibits proliferation of HemECs at 300 μM; while others noted that proliferation of HemECs and HemSCs was reduced by propranolol at 50 μM (Chim, Armijo et al. 2012; Wong, Hardy et al. 2012). The Bischoff Laboratory has an extensive set of hemangioma-derived cells, so effect of propranolol on proliferation of hemangioma-derived cells was assessed.

Proliferation of hemangioma-derived cells was tested after treating with either phosphate buffered saline (PBS) or propranolol twice daily over a 5-day period. Proliferation assays were performed on HemECs (n = 4), Hem-Pericytes (n = 3) and HemSCs (n = 3). Results for HemSCs 133, HemECs 158 and HDMECs are shown in Figure 17A, whereas Hem-Pericytes 154 and non-hemangioma pericytes are shown in Figure 17B. Each isolate was from a different IH from a different patient. Error bars are based on counts from 4 different wells.

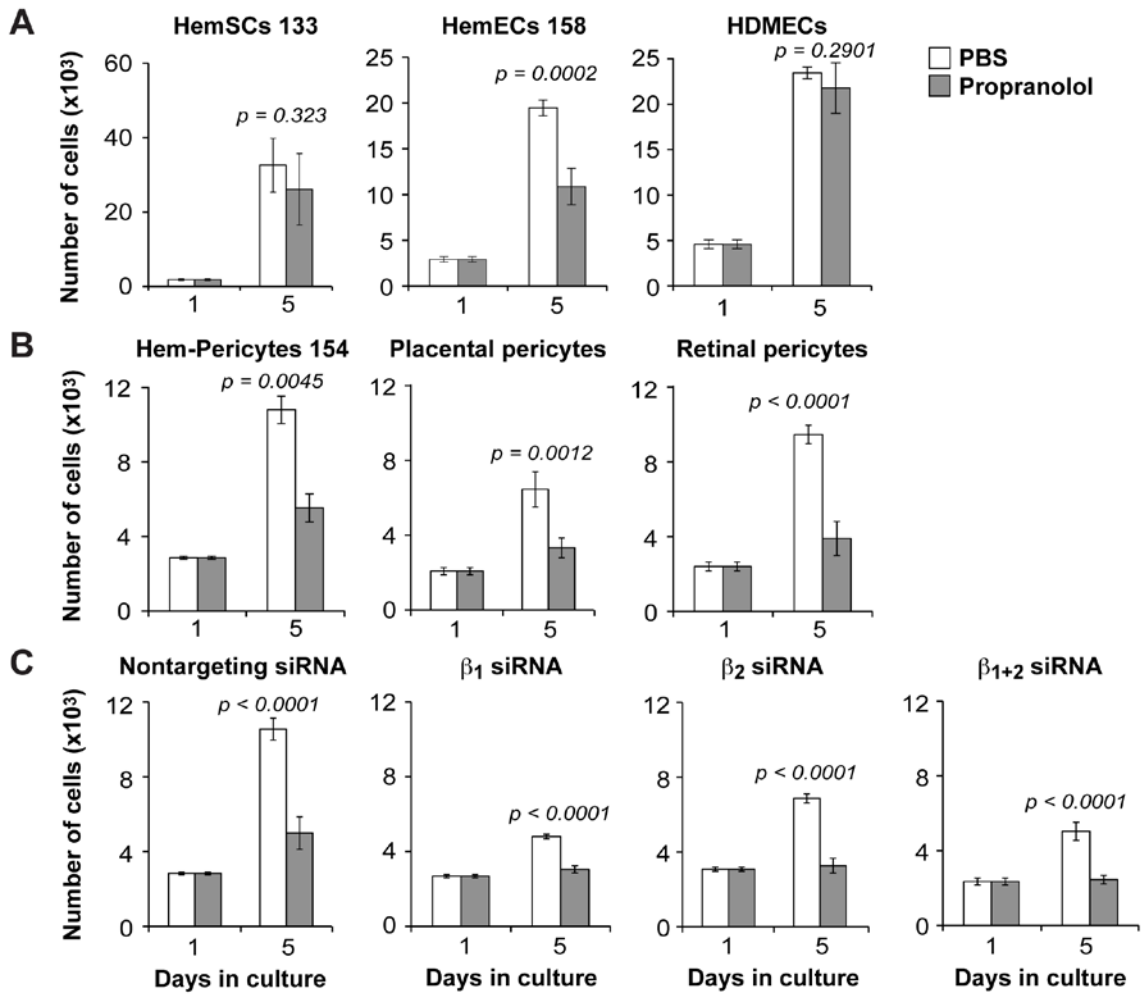

Figure 17. Proliferation of hemangioma-derived and non-hemangioma-derived cells in response to PBS or propranolol.
A. Propranolol did not reduce proliferation of HemSCs 133 and HDMECs but reduced proliferation of HemECs 158. **B.** Propranolol reduced proliferation of Hem-Pericytes 154 & human placental and retinal pericytes. **C.** Propranolol reduced proliferation of Hem-Pericytes 154 transfected with β-ARs siRNAs.

As described above, RNA expression of β-ARs in IH tissues and hemangioma-derived cells was noticeable, so it was assessed whether the receptors contributed towards cellular proliferation. Four separate plates of Hem-Pericytes 154 were transfected with non-targeting, β_1-, β_2- or β_{1+2}-ARs siRNAs, and their proliferation rates in response to PBS or propranolol treatment were determined. Non-targeting siRNA treatment had no effect on proliferation of Hem-Pericytes 154 treated with PBS over 5 days (white bars

for Day 5 in Figure 17B and 17C). On the other hand, β-ARs siRNAs transfection reduced proliferation compared to non-targeting siRNA among PBS-treated cells: β_1-AR by 54%, β_2-AR by 35% and β_{1+2}-ARs by 52% (white bars relative to non-targeting siRNA on Day 5 in Figure 17C). Propranolol further reduced proliferation in Hem-Pericytes 154 transfected with β_1-, β_2- and β_{1+2}-ARs siRNAs (gray bars in Figure 17C). siRNA knockdown efficiencies are shown in Figure 18. Off-target effects of non-targeting siRNA might have affected β-ARs levels, but unfortunately they were not assessed. Hem-Pericytes 154 should have been transfected with no siRNA, non-targeting siRNA, β_1-, β_2- and β_{1+2}-ARs siRNAs.

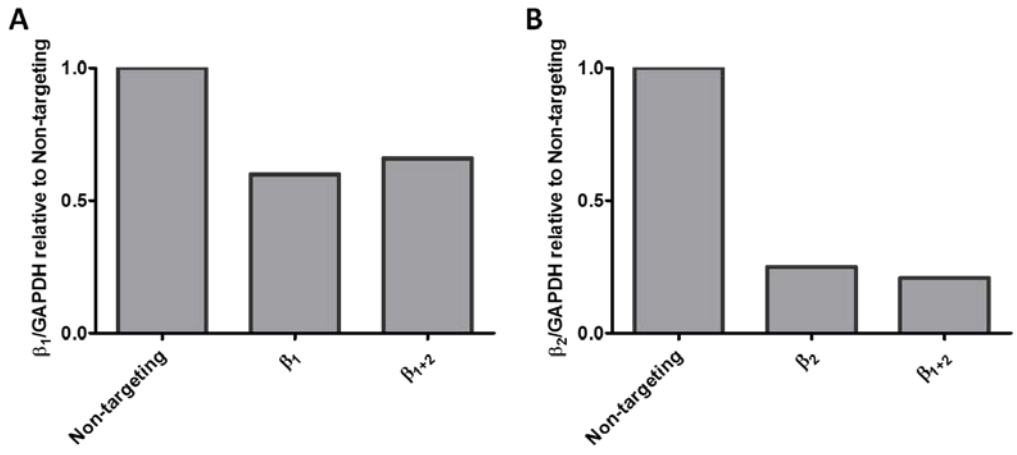

Figure 18. $\beta_{1,2}$-ARs knockdown efficiencies in Hem-Pericytes 154.
A. β_1-AR/GAPDH levels in pericytes transfected with β_1- and β_{1+2}-ARs siRNAs relative to non-targeting siRNA.
B. β_2-AR/GAPDH levels in pericytes transfected with β_2- and β_{1+2}-ARs siRNAs relative to non-targeting siRNA.

β-ARs siRNAs transfection was not performed in HemECs, so this should be done in the future.

Proliferation assays: significance & caveats

Propranolol has been reported to affect proliferation of HemECs at 300 µM (Chim, Armijo et al. 2012; Ji, Li et al. 2012). In Figure 17, propranolol reduced proliferation of HemECs and Hem-Pericytes at 10 µM, without significantly affecting HemSCs. Numbers from proliferation assays for each cell type are provided below to supplement Figure 17.

Table 5. Cell numbers on Day 5.

HemECs	Average cell # on Day 5- PBS	Average cell # on Day 5- propranolol	Percent reduction
133	57,100	56,600	0.9
150	6,465	4,350	32.7
158	19,465	10,865	44.2
I-69	37,850	25,100	33.7

Hem-Pericytes	Average cell # on Day 5- PBS	Average cell # on Day 5- propranolol	Percent reduction
146	16,100	10,220	36.5
154	10,800	5,533	48.8
156	9,580	5,925	38.2

HemSCs	Average cell # on Day 5- PBS	Average cell # on Day 5- propranolol	Percent reduction
94	15,490	12,907	16.7
97	112,200	112,400	-
133	32,590	26,130	19.8

	Average cell # on Day 5- PBS	Average cell # on Day 5- propranolol	Percent reduction
HDMECs	23,440	21,780	7.1
Placental pericytes	6,455	3,330	48.4
Retinal pericytes	9,465	3,905	58.7

Into each well of 48-well plates, 3750 cells were seeded (density of 5000 cells/cm^2), and Table 5 lists cells whose numbers at least doubled by Day 5. The different proliferation

rates within and among cell types can be easily appreciated. The differences in rates might have occurred because cells were derived from tissues, resected from different patients, at different ages and different points along the natural course of IH.

As noted above, proliferation of HemECs was reduced by propranolol, but not that of a non-pathologic endothelial cell type, HDMECs. On the other hand, proliferation of Hem-Pericytes and non-hemangioma pericytes, from human placenta and retina, was reduced by propranolol treatment, which indicates that the anti-proliferative effect of propranolol is not restricted to Hem-Pericytes. Another point of interest is reduction of proliferation in Hem-Pericytes transfected with β_1-, β_2- and $\beta_{1,2}$-ARs siRNAs. The striking decrease in proliferation strongly suggests that β-AR contributes to the proliferative capacity of Hem-Pericytes. In these transfected cells, propranolol treatment nearly abolished proliferation over the 5 days.

As described in Methods, HemECs were grown in media supplemented with 20% fetal bovine serum (FBS) and growth factors, whereas Hem-Pericytes were in media with 10% FBS without growth factors. Parameters such as percentage of serum and presence of growth factors could have been modified to assess proliferation more extensively. In addition, 10 μM of propranolol was used in proliferation assays, which was much greater than the binding affinities of propranolol at $\beta_{1,2}$-ARs.

Another caveat is that cells were treated either with PBS or propranolol designed for intravenous administration in patients. Ideally, a vehicle that closely resembled propranolol should have been used instead of PBS, but the vehicle, provided by Boston Children's Hospital Pharmacy, was not available when proliferation assays had been conducted. The dilution factor was 1 in 340 for PBS and propranolol.

Finally, no agonists, such as epinephrine, were used with propranolol. As an antagonist at β-ARs, propranolol by itself may not exert effects at the receptors. Nevertheless, proliferation of HemECs and Hem-Pericytes was reduced by propranolol alone. One possibility is that propranolol might have acted on targets other than β-ARs, but phosphorylation status of β-ARs and levels of downstream molecules such as cAMP were not assessed; whether propranolol bound β-ARs to decrease cellular proliferation or not could not be ascertained. Another possibility is that propranolol acted as an inverse agonist at β-ARs.

Propranolol reduced proliferation of HemECs and Hem-Pericytes over the 5 days, but no effects were noted on Day 2, even though proliferation rates varied widely among cells (not shown). As described above, patients often experienced changes in color and size of IH as early as 24 hours after initial treatment. Given this discrepancy, reduction of cellular proliferation may be a reason for long-term efficacy of propranolol in IH, but not for immediate efficacy within 24 hours of administration.

4.3 Cellular contractility assessment as a functional assay.

$\beta_{1,2}$-ARs were detected in hemangioma-derived cells, and it was of interest to find out whether these receptors served specific functions in IH. Patients treated with propranolol experienced decrease in lesion firmness and redness often within 24 hours, so vascular volume reduction was postulated to be a reason for the efficacy of drug. If propranolol is able to contract hemangioma-derived cells, vascular volume in hemangioma vessels may be reduced. Cellular contractility has been well-described in literature, especially that of bovine retinal pericytes (BRPs). Percentage of serum was

found to directly correlate with cellular contractility (Kelley, D'Amore et al. 1987). It was of interest to see if a similar set-up could be applied to hemangioma-derived cells.

After discussing this possibility with my supervisor Dr. Joyce Bischoff, she set up a meeting with Dr. Ira Herman from Tufts. After learning how to perform contractility assays, baseline contractility of hemangioma-derived and non-hemangioma-derived cells was assessed and compared among one another (Figure 19).

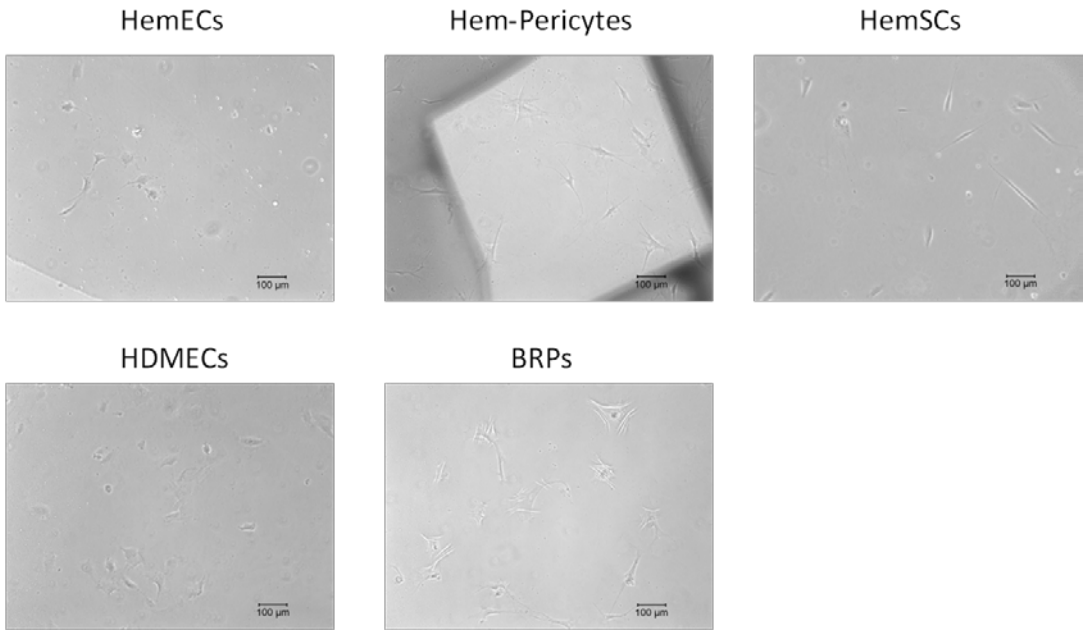

Figure 19. Hemangioma-derived cells, HDMECs and BRPs on polydimethyl-siloxane (PDMS).
Cells were seeded on PDMS as described in Methods. Two % serum was used for the 5 cell types in order to avoid excessive contractility. Pictures are representative of multiple wells. The picture of Hem-Pericytes was taken near a "mark," designed to facilitate cell-locating after treatment.

Among the 3 hemangioma-derived cell types, HemECs and HemSCs exhibited low contractility, with fewer than 5% of cells contracting on PDMS. Contractility of HDMECs and Hem-Pericytes was about even, with 10-50% of cells contracting at any given time. BRPs exhibited the highest amount of contractility, with 50-100% of cells contracting.

Therefore, Hem-Pericytes were the most contractile on PDMS among hemangioma-derived cells. This was intriguing because pericytes surround small vessels, contract or relax to change vessel diameters and therefore, regulate vascular volume (Peppiatt, Howarth et al. 2006; Yemisci, Gursoy-Ozdemir et al. 2009). After low contractility of HemECs 133, 150, 158 and I-69 and HemSCs 94 and 133 was noted, contractility assays were performed on Hem-Pericytes as described in 4.4.

4.4 Hem-Pericytes and contractility assay

As noted above, HemECs and HemSCs did not contract or "wrinkle" the PDMS as readily as Hem-Pericytes, so contractility assays were performed on Hem-Pericytes isolated from different IH tumor specimens (Figure 20B). Elisa Boscolo, a Bischoff Laboratory member, isolated Hem-Pericytes from proliferating and involuting phases. She assessed expression of β_2-AR among these cells and generously provided them, enabling contractility assays to proceed. In her studies, Hem-Pericytes 146 and 154 expressed β_2-AR at relatively high levels compared to other Hem-Pericytes (not shown).

Hem-Pericytes 146 and 154 exhibited relaxation of wrinkles upon treatment with the agonist, epinephrine (dark gray bar), but addition of propranolol (light gray bar) blocked this relaxation (Figure 20A, left column). The same phenomena were not observed in human placental and retinal pericytes, Hem-Pericytes 156, and Hem-Pericytes from involuting phase of IH, which are I-69, I-79 and I-82 (Figure 20A, left column). Among Hem-Pericytes from involuting phase, β_2-AR expression levels (not shown) did not correspond to whether cells exhibited relaxation or inhibition upon treatment with epinephrine and propranolol.

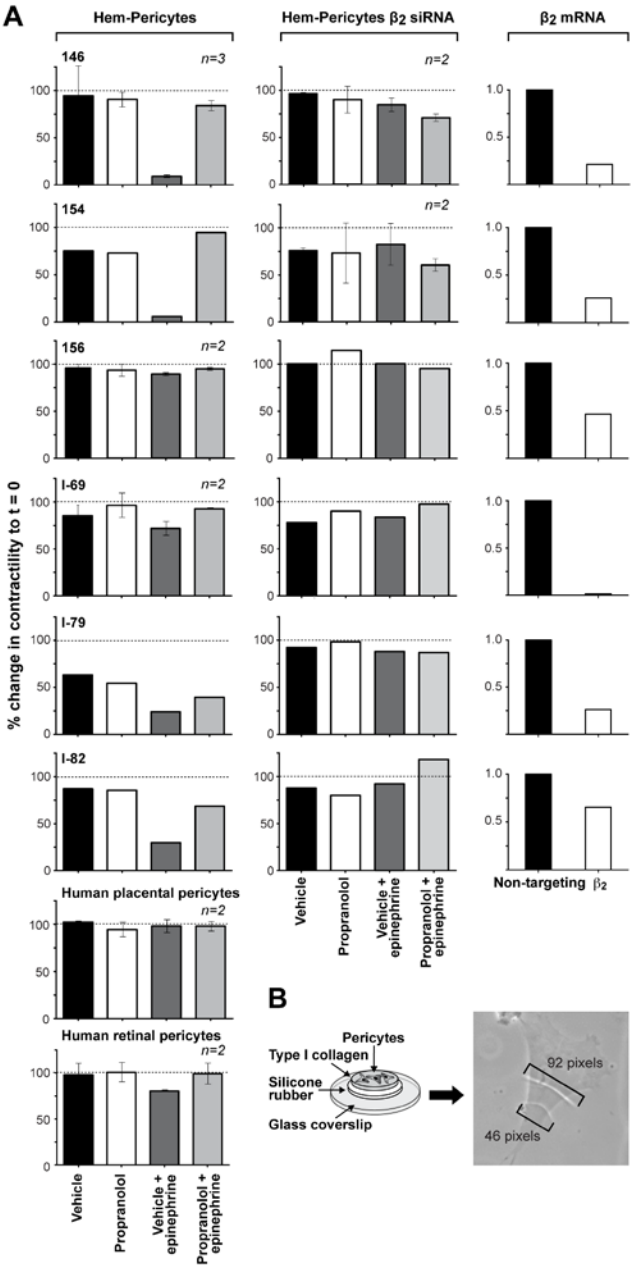

Figure 20. Contractility assays of Hem-Pericytes.
A. Quantification of data from 6 Hem-Pericytes, 3 each from proliferating and involuting phases, are shown. The 4 different colors represent the 4 different treatments. The height of each bar is percentage of contractility of cells to pre-treatment. Therefore, bar height correlates how close the after-treatment contractility scores are to the pre-treatment contractility scores. As denoted, some cells were assayed multiple times. The right column shows siRNA knockdown efficiency.
B. Assay set-up. Measurement of wrinkle lengths for quantification. Please refer to Methods for details.

In order to assess whether β_2-AR is required for contractility, siRNA was used to silence β_2-AR in Hem-Pericytes, followed by contractility assay (Figure 20A, middle column). β_2-AR was chosen instead of β_1-AR because of its relatively high expression in hemangioma tissues and hemangioma-derived cells compared to β_1-AR. After β_2-AR siRNA treatment, relaxation of wrinkles in response to epinephrine (dark gray bar) and inhibition of this relaxation in response to propranolol (light gray bar) were no longer observed, most prominently for Hem-Pericytes 146 and 154. No such effects of β_2-AR siRNA were observed in Hem-Pericytes 156 and Hem-Pericytes from involuting phase because these cells were not responsive to the epinephrine and propranolol treatments prior to β_2-AR knockdown (Figure 20A, middle column). β_2-AR knockdown efficiencies are shown, too (Figure 20A, right column).

Contractility assays: significance & caveats

Not only are $\beta_{1,\,2}$-ARs, targets of propranolol, abundant in IH, but they may serve specific functions in Hem-Pericytes. Indeed, contractility assays of Hem-Pericytes 146 and 154 showed that cells relaxed in response to epinephrine, and this relaxation was inhibited by propranolol. Silencing β_2-AR with siRNA blunted these phenomena. Hem-Pericytes have not been studied extensively in literature, and contractility assays delineated their potential role in reduction of IH by propranolol. Although contractility assays do not show whether whole hemangioma vessels contract in response to propranolol, they point to an effect of propranolol in Hem-Pericytes. This may be important in finding mechanism(s) of propranolol in IH because pericytes surround small vessels and regulate their diameters by relaxing and contracting (Peppiatt, Howarth et al. 2006; Yemisci, Gursoy-Ozdemir et al. 2009).

On the other hand, for Hem-Pericytes 156, I-69, I-79 and I-82, cells showed relatively little relaxation in response to epinephrine compared to Hem-Pericytes 146 and 154. In addition, the inhibition of relaxation by propranolol was relatively small compared to Hem-Pericytes 146 and 154. These responses were similar to those exhibited by human placental and retinal pericytes. After silencing β_2-ARs in Hem-Pericytes 156, I-69, I-79 and I-82 with siRNA, the cellular contractility of all 4 conditions changed relatively little compared to their contractility before treatment. This was also true for Hem-Pericytes 146 and 154. In summary, as shown by the different responses of Hem-Pericytes in contractility assays, multiple factors may contribute towards contractility, in which β_2-AR in Hem-Pericytes can be important. This variability in contractility may be related to variability in clinical responses among IH patients treated with propranolol- 3% of IH patients did not respond to propranolol in a study (Bagazgoitia, Torrelo et al. 2011). As noted in the figure, contractility assays were performed multiple times- 3 times for Hem-Pericytes 146 and twice for Hem-Pericytes 156, I-69, human placental and retinal pericytes. Combination of β_2-AR siRNA knockdown and contractility assay was done twice each for Hem-Pericytes 146 and 154. Such reproducibility ensured that results from Figure 20 were legitimate.

One caveat is that off-target effects of non-targeting siRNA were not assessed. Non-targeting siRNA did not affect proliferation of Hem-Pericytes 154, but it could have affected β_2-AR levels of Hem-Pericytes in contractility assays. Therefore, Hem-Pericytes should have been transfected with no siRNA, non-targeting siRNA and β_2-AR siRNA, and their β_2-AR levels compared.

Another caveat is that Hem-Pericytes were in a state of contraction prior to the addition of reagents. They were tested to detect loss of contraction or prevention of such loss of contraction in response to reagents. If Hem-Pericytes were in a state of relaxation prior to the addition of reagents, they could have been tested to detect appearance of contraction. Doing so may imitate contraction of Hem-Pericytes around hemangioma vessels, more so than the current set-up.

Epinephrine, an agonist of β-ARs, needed to be added to cells in order to appreciate changes in their contractility; propranolol by itself did not change contractility of Hem-Pericytes much. As noted above, this point raises the question of whether addition of an agonist, such as epinephrine, to cells in tube formation and proliferation assays would lead to different results. Propranolol is an antagonist at β-ARs, so its effects may not be detected in the absence of an agonist. An exception would be, however, if propranolol were an inverse agonist at β-ARs in IH. Among tube formation, proliferation and contractility assays, propranolol was used in conjunction with epinephrine only in contractility assays. Even though effects from combination of epinephrine and propranolol make β-ARs the likely targets of the drugs in contractility assays, phosphorylation status of the receptors and intracellular cAMP levels were not assessed, so this notion was not confirmed. In summary, proliferation and contractility assays showed potential effects of propranolol on hemangioma-derived cells; proliferation assays hinted that propranolol is an inverse agonist, while contractility assays hinted that propranolol is an antagonist of β-ARs in IH.

Finally, as described above, Hem-Pericytes were used in contractility assays because they contracted PDMS more readily than HemECs or HemSCs. PDMS was

thermally cross-linked by passing over low flame twice. If one were to decrease cross-linking of PDMS by passing over low flame once, HemECs or HemSCs might be able to contract PDMS more readily. However, this parameter was kept consistent for all cell types because changing it from one cell type to next might have given unfair advantage to certain cell types, thereby skewing results.

Chapter V

Reproduction of clinical effect *in vivo*

5.1 *In vivo* studies

So far, the presence of β-ARs in IH has been confirmed, and Hem-Pericytes were identified as targets of propranolol *in vitro*; a functional assay was utilized to find that contractility of Hem-Pericytes was affected by propranolol. In addition, propranolol reduced proliferation of HemECs and Hem-Pericytes over 5 days, which may be relevant in long-term efficacy in IH. With these results in hand, the effects of propranolol were assessed in an *in vivo* model of IH.

In vivo model of IH

An *in* vivo model of disease gives researchers an appropriate environment to perform experiments, so a murine model of IH was developed. All *in vivo* studies described here are covered under an animal protocol (10-11-1840R) approved by the Animal Care and Use Committee at Boston Children's Hospital. The Bischoff Laboratory showed that HemSCs, when suspended in Matrigel and subcutaneously implanted into nude/nude mice, formed hemangioma-like vessels within 7 days. In the Matrigel sections, researchers detected GLUT-1^{+} blood vessels, a diagnostic marker of IH. It was also noted that the number of vessels decreased by 28 days, whereas adipocytes became more noticeable during the same time period. These characteristics reproduced natural course of IH, providing researchers with an *in vivo* model (Khan, Boscolo et al. 2008).

GFP-labeled HemSCs were shown to differentiate into both endothelial cells lining the lumen of the vessels and pericytes surrounding the vessels and at later time points, adipocytes (Khan, Boscolo et al. 2008; Boscolo, Mulliken et al. 2011). HemECs do not form vessels in this model when implanted alone, without a partner cell

that can differentiate into pericyte or smooth muscle cell. Likewise, Hem-Pericytes do not form vessels in this model when implanted alone (Boscolo, Mulliken et al. 2013). However, HemECs co-implanted with Hem-Pericytes form vessels readily within 7 days. In summary, hemangioma-derived cells mixed with Matrigel form hemangioma-like vessels and adipocytes, thereby recapitulating key aspects of IH pathogenesis. Unfortunately, aspects such as tumor enlargement of proliferating phase and shrinkage of involuted phase are not observed in this model.

5.2 Selecting HemSCs for *in vivo* experiments

As described above, HemSCs express VEGF-A, which binds VEGFR-1 to differentiate HemSCs to HemECs in an autocrine manner (Boscolo, Mulliken et al. 2011). The newly-differentiated HemECs then promote neighboring HemSCs to become Hem-Pericytes by their expression of Jagged1, which was found critical for differentiation of HemSCs to Hem-Pericytes (Boscolo, Stewart et al. 2011). Therefore, HemSCs were utilized to study effects of propranolol on hemangioma vessels.

The Bischoff Laboratory members have isolated numerous HemSCs over the years, and it was important to choose appropriate candidates among them for *in vivo* experiments. With the help of Jill Wylie-Sears, a Bischoff Laboratory member, 11 HemSCs, previously isolated by the laboratory, were tested. She evaluated the 11 HemSCs via flow cytometry and assessed for absence of CD31, commonly found on endothelial cells, and CD45, a hematopoietic cell marker, but presence of CD29, integrin β_1 that is commonly expressed in many mammalian cells, and CD90, a mesenchymal marker (not shown). While she evaluated the HemSCs by flow

cytometry, HemSCs were assessed for their proliferative potential using the indicated set-up (Figure 21).

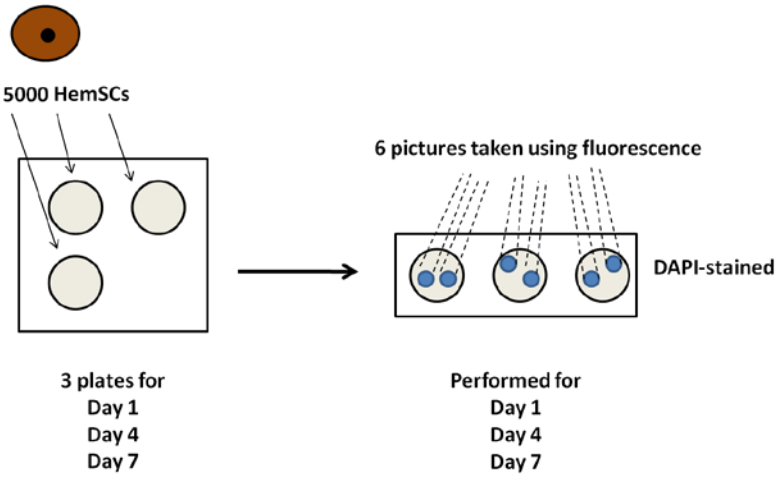

Figure 21. Proliferation assay set-up for HemSCs.
HemSCs were assessed for their proliferation using the above set-up. 4', 6-diamidino-2-phenylindole (DAPI) was used as an indicator of proliferation. Please refer to Methods for details.

Thus, using immunostaining with DAPI as a read-out, proliferation rates of HemSCs were determined (Figure 22).

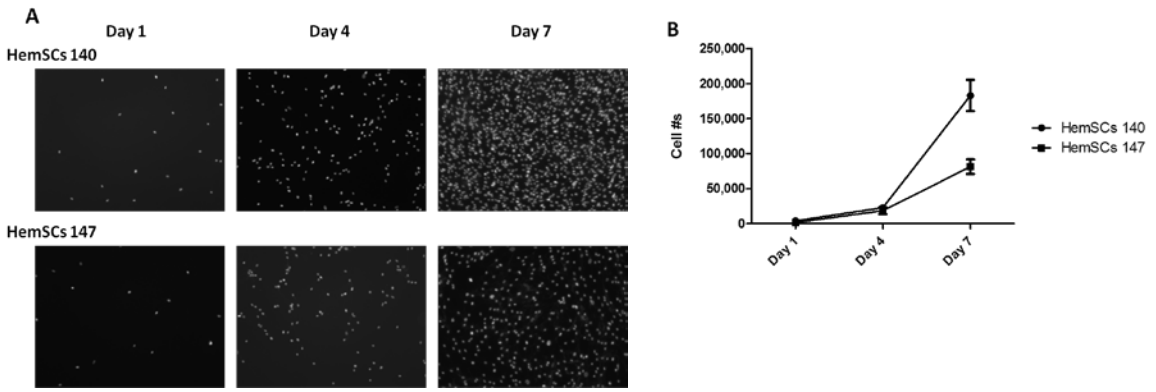

Figure 22. Quantification of proliferation in HemSCs.
A. Six pictures of DAPI-stained nuclei were taken on Days 1, 4 and 7. Shown are representative pictures from HemSCs 140 and 147 on each day.
B. Proliferation graphs of HemSCs 140 and 147.

Combining results from flow cytometry and proliferation, the 11 HemSCs were divided into 2 groups- one group with the right flow cytometry profile and fast proliferation, and another group that did not fit either/both traits (Table 6).

Table 6. HemSCs categorized for *in vivo* studies.

Candidates	Not candidates
120	122
127	135
128	147
129	148
140	
149	
I-54	

In order to assess the candidates even further, their RNA levels of VEGF-A were determined. As described above, VEGF was postulated to be a central molecule in the pathogenesis of IH. VEGF-A can bind VEGFR-1 on HemSCs, which is important for their differentiation to HemECs. HemSCs also express the highest levels of VEGF-A among the 3 hemangioma-derived cell types. Therefore, candidates with high levels of VEGF-A were desirable, in addition to having the right flow cytometry profile and fast proliferation rates. Cryovials of the 7 candidates from Table 6 were thawed, cells cultured, and their RNA levels of VEGF-A determined. Samples other than the 7 candidates were included for comparison (Figure 23). Although cDNA samples of cells were loaded into triplicate wells for qRT-PCR, these provided technical replicates; cells were grown and harvested from single plates, from which RNA extracted and cDNA reverse-transcribed. As they were not grown in multiple wells or plates, no error bars could be added to the graph.

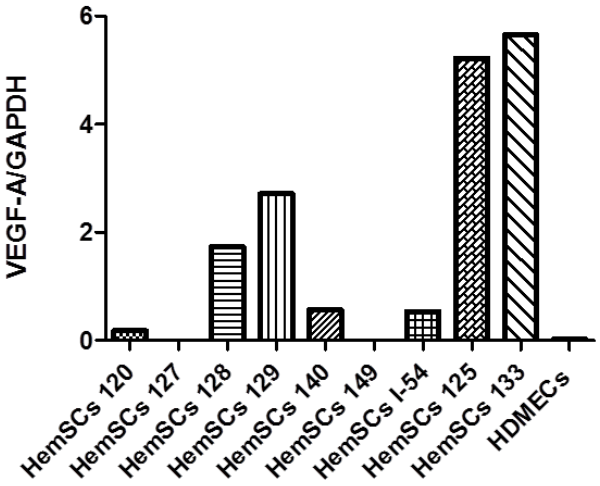

Figure 23. VEGF-A levels of the "candidate" HemSCs for *in vivo* studies. Ratios of VEGF-A to GAPDH are shown for the HemSCs & HDMECs. HemSCs 127 and 149 did not grow upon being thawed. HemSCs 125 & 133 and HDMECs are included for comparison.

According to Figure 23, HemSCs 128 and 129 seemed the most promising among the 7 candidates for *in vivo* studies. A comprehensive evaluation would have involved assessing levels of secreted VEGF-A by ELISA, as well as confirming endothelial and pericytic differentiation capabilities of the HemSCs *in vitro*. Although HemSCs 125 and 133 expressed higher levels of VEGF-A than the candidates in Figure 23, they were of limited availability.

In conclusion, HemSCs 128 and 129 were determined as candidates for *in vivo* studies based on flow cytometry characterization, proliferation rates and VEGF-A levels by qRT-PCR.

5.3 Rationale for using micro-ultrasonography for *in vivo* analyses

At the conclusion of *in vivo* experiments, researchers harvest the cell/Matrigels and prepare histological sections, from which additional analyses such as microvessel density (MVD) calculation and IHC can be performed. Recently, researchers have used micro-ultrasonography to quantify vascular volume in areas of interest in mice and obtained valuable information. Contrast agent is injected into animal circulation via cannulated tail vein and is confined within the vasculature, providing an indicator of vascular volume. This information from areas of interest is collected by micro-ultrasonography probe and quantified by Vevo2100 unit (VisualSonics; Kang, Allen et al. 2011).

A major advantage of this method is the ability to collect data at multiple time points in the same animal, which adds depth to traditional methods like MVD calculation and IHC, in which data are collected at only one time point. As noted above, patients treated with propranolol experience decrease in lesion firmness and redness within 24 hours, so vascular volume reduction might be a reason for the efficacy of propranolol in IH. Therefore, contrast-enhanced micro-ultrasonography provides a method to detect potential changes in vascular volume as a result of propranolol treatment.

After persistent practice, I became proficient at cannulating murine tail veins to be able to inject contrast agent into animal circulation. In addition, I received a formal training by VisualSonics staff and a personal training by Patrick Allen, a former Bischoff Laboratory member, to gain competency in using the Vevo2100 unit. Thus, preparations were under way for utilizing micro-ultrasonography in *in vivo* experiments.

No reduction of vascular volume in vessels formed by HemSCs

Initially, HemSCs were suspended in Matrigel and implanted into athymic nude/nude mice. After vascular volume measurement on Day 7, mice were treated with either vehicle or propranolol for 7 days. As noted above, HemSCs can differentiate to HemECs, which then promote neighboring HemSCs to differentiate to Hem-Pericytes.

However, propranolol treatment did not significantly reduce vascular volume by Day 14, and difficulty was noted in achieving similar mean contrast values at the start of treatment on Day 7 (Figure 24B). Explanted cell/Matrigels were analyzed for histological evaluation. Twenty pictures from mid-Matrigel hematoxylin & eosin (H & E) sections of all animals in vehicle and propranolol groups were taken randomly with a microscope. Luminal structures containing at least one red blood cell (RBC) were counted as a microvessel. MVD was determined for the two groups and found to be statistically equivalent (Figure 24C). *In vivo* experiments with HemSCs were performed a total of 6 times, with HemSCs 120, 128, 129 and 133, and Figure 24 shows data combined from 2 such experiments. Additional data from micro-ultrasonography analyses are shown in the supplementary figure.

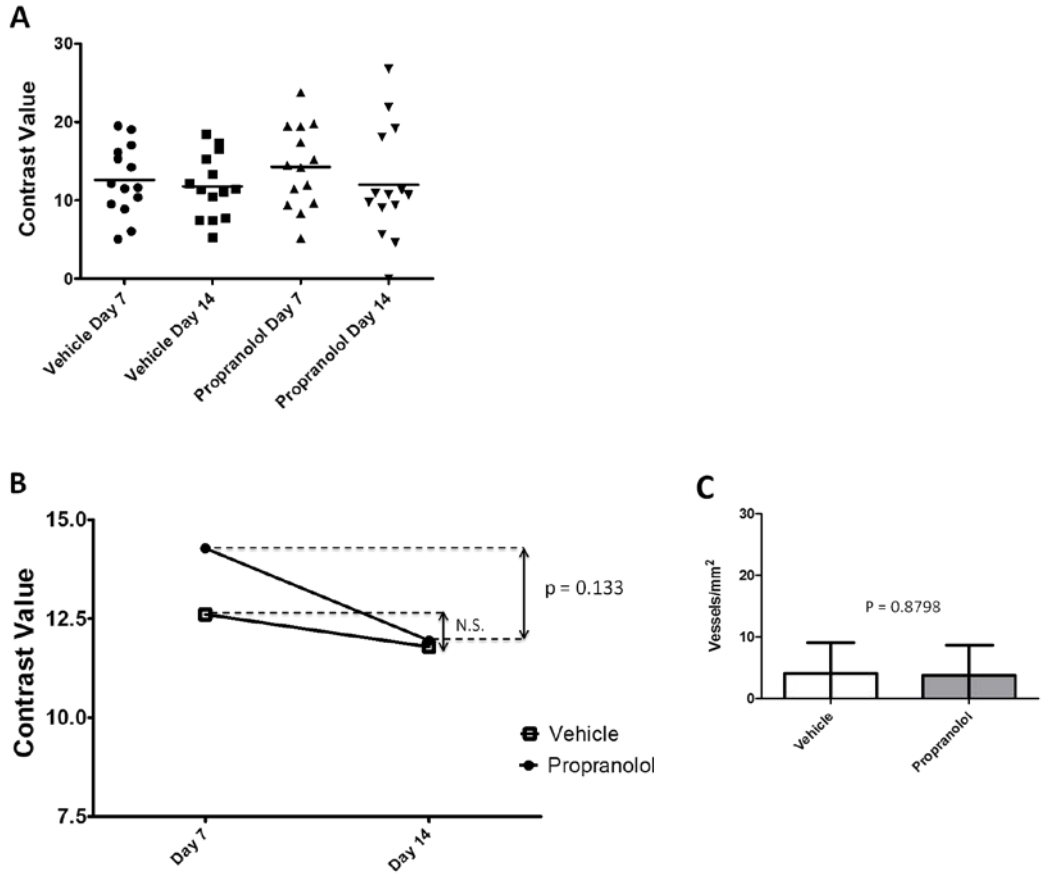

Figure 24. *In vivo* studies with HemSCs.
Mice were implanted with HemSCs and Matrigel on Day 0. Each group had 14 mice. After vascular volume measurement on Day 7, mice were treated with vehicle or propranolol for 7 days on Days 7-13.
A. Contrast values of individual mice on Days 7 and 14 are shown.
B. Line graphs represent changes in mean contrast values for each group.
C. MVD calculation. N = 14 for each group.

5.4 Propranolol reduced vascular volume in vessels formed by HemECs 158 and Hem-Pericytes 154

In vivo studies with HemSCs were performed 6 times, but the clinical observation of vascular volume reduction after propranolol treatment was not reproduced. Therefore, experimental set-up was re-evaluated, and it occurred that HemSCs needed to differentiate to HemECs and Hem-Pericytes and form hemangioma vessels *in vivo* in 7

days. Hem-Pericytes that differentiated from HemSCs *in vivo* might not have expressed β_2-AR as highly as fully differentiated Hem-Pericytes *in vitro*. Therefore, they might have been less contractile.

Therefore, HemECs and Hem-Pericytes, cell types more differentiated than HemSCs, were mixed in Matrigel and implanted into mice. Similar mean contrast values at the start of treatment on Day 7 were achieved (Figure 25B), and mean contrast values of both groups (n = 17 for each) decreased by Day 14, but the drop from the propranolol group was significant, whereas that of the vehicle group was not (Figure 25B). This is the combined result of two separate experiments performed at different times; significant reduction of contrast values in the propranolol-treated group was noted each time. On the other hand, MVD calculations from harvested Matrigels did not show significant differences between the two groups (Figure 25C).

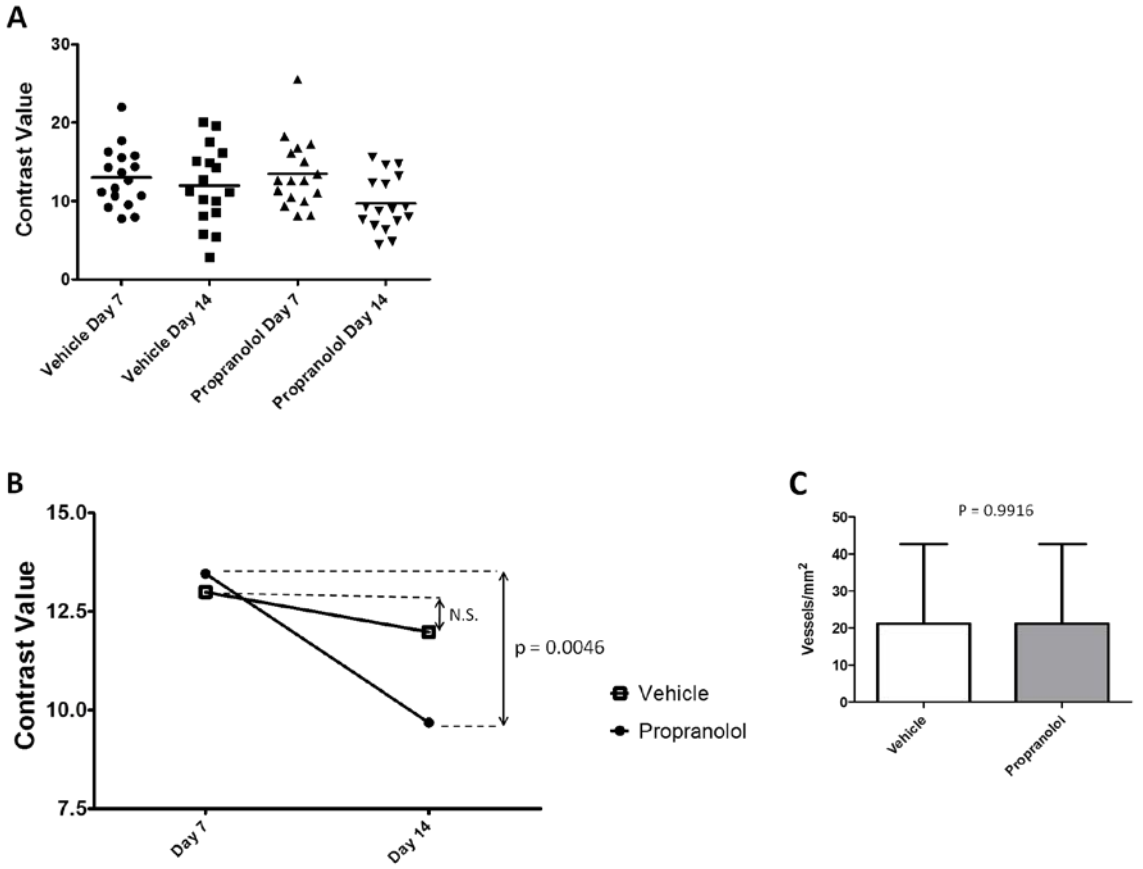

Figure 25. *In vivo* studies with HemECs 158 and Hem-Pericytes 154.
Mice were implanted with HemECs 158, Hem-Pericytes 154 and Matrigel on Day 0. Each group had 17 mice. After vascular volume measurement on Day 7, mice were treated with vehicle or propranolol for 7 days on Days 7-13.
A. Contrast values of individual mice on Days 7 and 14 are shown.
B. Line graphs represent changes in mean contrast values for each group.
C. MVD calculation. N = 17 for each group.

Micro-ultrasonography analyses of vascular volume: significance & caveats

As described above, IH patients treated with propranolol experience decrease in redness and firmness of lesion relatively quickly, as early as 24 hours after initial treatment (Léauté-Labrèze, Dumas de la Roque et al. 2008; Sans, de la Roque et al. 2009). This quick turnaround led many to attribute vascular volume reduction of the tumor as a main reason for improvement. Indeed, one group found that when lesions of

IH patients, treated with propranolol, were measured with Doppler ultrasound, significant reductions in lesion volume and vessel density were detected. In this study, patients received at least 4 weeks of propranolol treatment (Bingham, Saltzman et al. 2012). Vascular volume was reduced after 7 days of propranolol treatment in the *in vivo* experiments with HemECs 158 and Hem-Pericytes 154 in Figure 25. To date, vascular volume reduction in an *in vivo* model of IH has not been reported after propranolol treatment. MVD could only be calculated at one time point, on Day 14 in Figure 25, so even though MVD was equivalent for the 2 treatment groups, whether or not propranolol reduces vessel density over 7 days could not be determined.

Propranolol is a non-selective β-AR antagonist and often prescribed to reduce blood pressure. Even though vascular volume reduction was significant for the propranolol-treated group in the *in vivo* experiments with HemECs 158 and Hem-Pericytes 154, this phenomenon might be attributed to the expected effect of the drug. However, some factors make this argument less persuasive. First, vascular volume reduction was not significant for the *in vivo* experiments in which a different cell type, HemSCs only instead of HemECs and Hem-Pericytes, was used. Second, micro-ultrasonography analyses were performed one day after the last propranolol treatment, well past the half-life (3-5 hours) of the drug, so the noted vascular volume reduction was independent from the transient reduction of blood pressure by propranolol.

One solution to this dilemma could have been measuring vascular volume of a structure (e.g., kidney) near cell/Matrigels- vascular volume reduction should be noted for cell/Matrigels, but not for the nearby structure, after propranolol treatment.

Unfortunately, this would have meant that mice would be under sedation much longer, approximately 1 hour/mouse under the current set-up (see Methods).

As noted above, tumor enlargement of proliferating phase and shrinkage of involuted phase are not observed in the *in vivo* model. Therefore, tumor size changes in response to propranolol can not be appreciated in the model. In addition, IH patients are usually treated with 1-5 mg/kg of propranolol per day, whereas animals were treated twice daily with 5 mg/kg in Figures 24 and 25.

In summary, despite some differences in details regarding treatment of IH patients and *in vivo* experiments using a murine model of IH, vascular volume reduction after propranolol treatment was noted in both. This similarity gives further support to the notion that a reason behind efficacy of propranolol in IH patients is vascular volume reduction brought on by the contractile Hem-Pericytes.

5.5 Histological evaluation of explanted cell/Matrigels

Additional analyses were performed on the explanted cell/Matrigels. The explanted cell/Matrigels were immunostained with human-specific CD31 antibody. This was done because murine cells might have contributed to vessel formation in the *in vivo* studies. It was of interest to see whether the vascular volume reduction noted after propranolol treatment could be attributed to effects on the injected HemECs 158 and Hem-Pericytes 154, instead of murine cells. Brownish, luminal structures containing at least one RBC were counted as a human $CD31^+$ vessel. Significant differences in the number of human $CD31^+$ vessels were noted, in which the propranolol-treated group exhibited higher numbers of human vessels (Figure 26A).

Vessel areas were measured in the explanted cell/Matrigels and compared between the 2 treatment groups. This was performed because the differences in vascular volume after propranolol treatment might have resulted from differences in vessel areas; larger vascular volume from larger vessels and smaller vascular volume from smaller vessels. If Hem-Pericytes contracted around hemangioma vessels in Matrigels after propranolol treatment, the vessel areas might have been smaller compared to those of Matrigels from the vehicle-treated mice. However, no significant differences in vessel areas were noted between the two treatment groups (Figure 26B).

As noted above, propranolol decreased proliferation of Hem-Pericytes 154 *in vitro*. In order to assess whether the same phenomenon occurred *in vivo*, the explanted cell/Matrigels were immunostained with a marker of proliferation, Ki67, and a marker of pericytes, αSMA. However, no significant differences in the number of $Ki67^{+}/\alpha SMA^{+}$ cells were noted between the two treatment groups (Figures 26C, D).

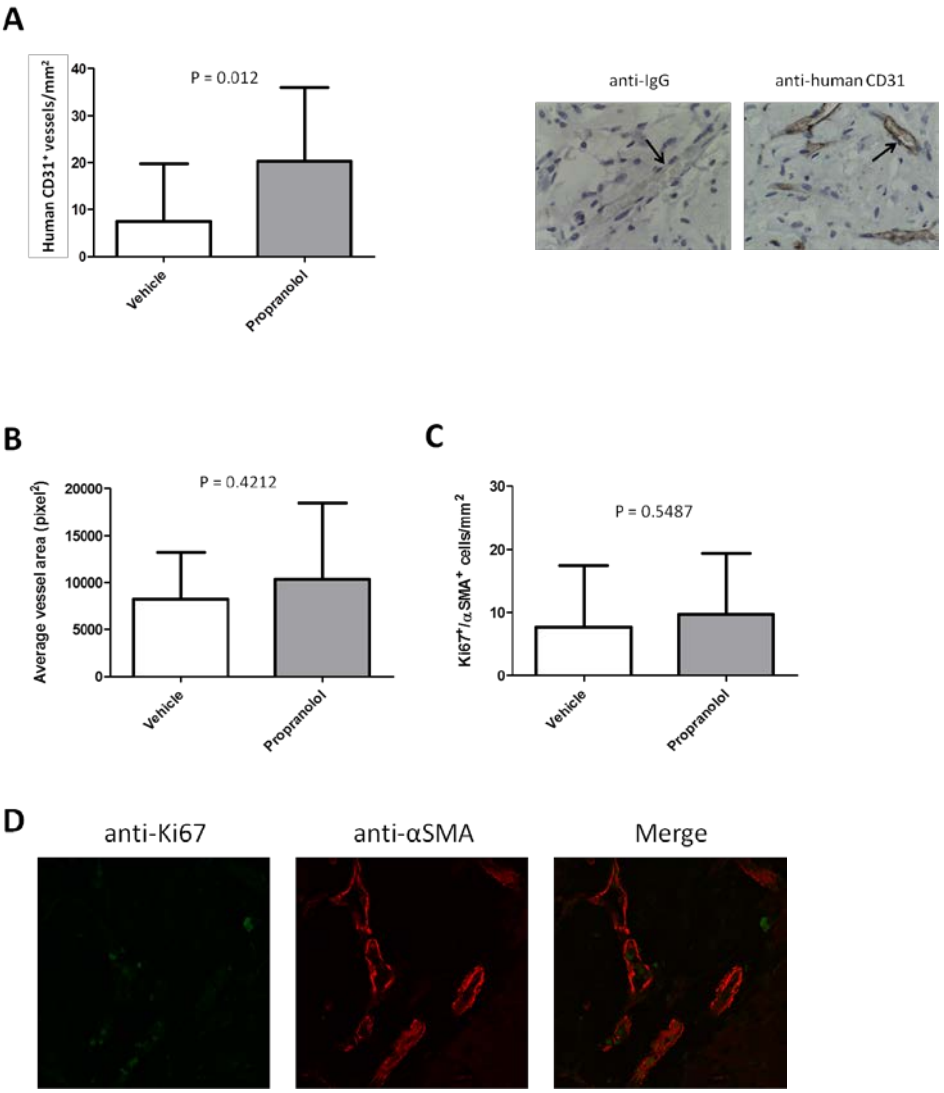

Figure 26. Additional histological data from *in vivo* experiments with HemECs 158 and Hem-Pericytes 154.
A. Human $CD31^+$ vessels in Matrigels. N = 17 for each group. **B.** Vessel areas in Matrigels. N = 17 for each group. **C.** $Ki67^+/\alpha SMA^+$ cells in Matrigels. N = 17 for each group. **D.** Example pictures.

Histological evaluation of explanted cell/Matrigels: significance & caveats

As described above, micro-ultrasonography analyses of the *in vivo* experiments with HemECs 158 and Hem-Pericytes 154 showed that vascular volume decreased in the group treated with propranolol. Vascular volume was quantified by scanning the entire

length of the Matrigels. The vessel numbers of explanted cell/Matrigels in both groups were statistically equivalent (Figure 25C). As noted above, vessels are human and murine luminal structures with at least one RBC on H & E sections of explanted cell/Matrigels. Therefore, extending the results from contractility assays, in which Hem-Pericytes remained contracted in response to propranolol, these results point to an effect of propranolol, in which pericytes contract vessels to reduce vascular volume. On the other hand, no differences in vessel numbers were detected after propranolol treatment, in contrast to reduced proliferation of HemECs and Hem-Pericytes *in vitro*. An important difference in experimental set-up is that vascular volume was quantified from the entire length of the Matrigels, approximating 3-dimensions, whereas histological evaluation of explanted cell/Matrigels was assessed from specific Matrigel sections, not as closely approximating 3-dimensions as vascular volume measurement. This difference might have influenced all results from histological evaluation of explanted cell/Matrigels.

More vessels formed with HemECs and Hem-Pericytes (Figure 25C) compared to HemSCs alone (Figure 24C). In terms of time, after implantation, HemECs and Hem-Pericytes had to find relative positions in Matrigel to form hemangioma vessels within 7 days, whereas HemSCs had to first differentiate to HemECs and Hem-Pericytes, which then had to find their relative positions to form vessels within the same duration, 7 days. This may explain the higher MVDs with HemECs and Hem-Pericytes compared with HemSCs alone.

On the other hand, MVD calculations might have yielded different numbers had different criteria been used. As listed in Methods, luminal structures containing at least

one RBC were counted as a microvessel, but absence of lumen or RBC may not necessarily rule out existence of vessel. Researchers have used various markers such as CD31, a marker of endothelial cells, and CD34, a marker of endothelial and hematopoietic cells, to calculate MVD (de la Taille, Katz et al. 2000). Others have used von Willebrand factor, a protein produced by endothelium and endothelial stroma that helps prevent excessive bleeding, to calculate MVD (Weidner, Carroll et al. 1993). For both examples, presence of neither lumen nor RBC was required to constitute a microvessel, and areas with the greatest density of positive endothelial cells were selected for counting. Therefore, MVD calculations might have given higher numbers had different criteria been used.

As noted above, numbers of human $CD31^+$ vessels were determined because it was of interest to find out whether vascular volume reduction from propranolol treatment could be attributed to drug effect on human, not murine, vessels. Given the statistically equivalent numbers of total vessels in both groups, the numbers of human $CD31^+$ vessels were expected to be statistically equivalent again. However, the number of human $CD31^+$ vessels was significantly higher in the propranolol-treated than in the vehicle-treated mice, which was unexpected (Figure 26A). In addition, the numbers of human $CD31^+$ vessels (Figure 26A) and total vessels in the propranolol-treated group (Figure 25C) were similar, which was surprising. A possible reason for this finding is experimental set-up, which should have been modified. Researchers from the Bischoff Laboratory used plant lectins specific for human or murine endothelium to demonstrate that 3 types of vessels are detected when human cells are implanted on mice: human vessels, murine vessels and chimeric vessels containing both human and murine

endothelium (Kang, Allen et al. 2011). All brownish, luminal structures containing at least one RBC were counted as a human $CD31^+$ vessel, and these included structures that appeared brown only in parts of the lumen. Therefore, a more extensive evaluation would have used such lectins specific for human or murine endothelium to categorize vessels into human, murine or chimeric vessels.

Although vessel areas of explanted cell/Matrigels in the *in vivo* experiments with HemECs 158 and Hem-Pericytes 154 were statistically equivalent or numerically larger for mice treated with propranolol than those treated with vehicle, the vessel areas of both groups prior to treatment were unknown; this is a limitation of histological evaluation. Therefore, whether vascular volume was reduced because of contraction of Hem-Pericytes *in vivo* could not be confirmed.

Propranolol reduced proliferation of Hem-Pericytes 154 *in vitro*. Whether this anti-proliferative effect contributed to the decrease in vascular volume was addressed by analyzing the proliferative status of αSMA^+ cells in the explanted cell/Matrigels from the *in vivo* experiments with HemECs 158 and Hem-Pericytes 154 (Figure 26C). Matrigel sections were immunostained with Ki67 and αSMA, and double-positive cells were counted. There was no significant difference between the two treatment groups. Thus, the anti-proliferative effect of propranolol on Hem-Pericytes was not evident 14 days after cell/Matrigel implantation. This might have been because of several differences in experimental designs between *in vitro* proliferation assays and *in vivo* assays using murine model of IH. For instance, PBS or propranolol was directly added to wells containing Hem-Pericytes in *in vitro* assays on Days 1-5 (Figure 17B). On the other hand, HemECs and Hem-Pericytes were mixed with Matrigel and subcutaneously

implanted on nude mice. After allowing 7 days to pass for hemangioma vessel formation in Matrigel, animals were treated with vehicle or propranolol, first metabolized by murine liver before distribution to rest of body, on Days 7-13. These may be contributing factors behind lack of difference between the groups in Figure 26C.

The anti-proliferative effect of propranolol on HemECs was not assessed *in vivo* by immunostaining with Ki67 and CD31, which should be performed in the future.

Chapter VI

METHODS

6.1 Isolation of hemangioma-derived cells and *in vitro* culture

Specimens of IH were obtained under a human subject protocol approved by the Committee on Clinical Investigation, Boston Children's Hospital (04-12-175R). The clinical diagnosis was confirmed by the Department of Pathology, and informed consent was obtained from parents of patients. HemECs, Hem-Pericytes and HemSCs were isolated as described below.

For all hemangioma-derived cells, freshly-resected hemangioma tissues were placed on ice, washed in PBS and minced into ~ 1 mm pieces. Tissues were digested in Dulbecco's Modified Eagle Medium (DMEM) supplemented with 2% FBS (HyClone SV30014.03), 1x Ca^{2+}, 1x Mg^{2+}, 1x PSF (100 U/ml penicillin, 100 µg/ml streptomycin, 0.25 µg/ml amphotericin; Invitrogen 15240-096) and 0.2% collagenase A (Roche 11088785103) for 30 minutes at 37 ˚C. Afterwards, tissues were homogenized with a pestle in a 50 mL conical tube, and the supernatant filtered with a 100 µm cell strainer (BD Falcon 352360). The filtered supernatant was centrifuged at 1500 rpm for 10 minutes, and the resulting pellet re-suspended in PBS/0.6% ACD-A/0.5% BSA, which is composed of 22.3 g of glucose, 22 g of sodium citrate, 8 g of citric acid in 1 L of dH_2O. From here, steps diverged for HemECs, Hem-Pericytes and HemSCs isolations.

For HemECs, endothelial cells were selected using anti-CD31-coated magnetic beads (Dynal 111.55). The CD31+ cells were cultured on fibronectin-coated (1 µg/cm^2, Chemicon FC-010) plates with endothelial basal medium (EBM-2, Lonza CC-3156). EBM-2 was supplemented with 20% FBS, endothelial growth media-2 SingleQuots (EGM-2 SingleQuots, Lonza CC-4176) without hydrocortisone and 1x GPS (Cellgro 30-

009-CI). HemECs were tested for endothelial markers like CD31, CD146 and VE-cadherin (Boye, Yu et al. 2001).

For Hem-Pericytes, cells were seeded on non-coated tissue culture plates in DMEM 10% FBS, 1x GPS (Cellgro 30-009-CI), which provided a selective growth advantage. The resulting cell populations were tested for markers of pericytes like αSMA, calponin, NG2, PDGFR-β and smMHC (Boscolo, Mulliken et al. 2013).

For HemSCs, cells were selected with anti-CD133-coated magnetic beads (Miltenyi Biotec 130-050-80). As described above for HemECs, the CD133+ cells were cultured on fibronectin-coated (1 μg/cm^2) plates with EBM-2, supplemented with 20% FBS, EGM-2 SingleQuots without hydrocortisone and 1x GPS (Cellgro 30-009-CI). HemSCs were tested for positivity of markers like CD90 and Oct-4, negativity of CD31 and hematopoietic cell marker CD45 and their ability to differentiate to HemECs and Hem-Pericytes (Khan, Boscolo et al. 2008).

6.2 Non-hemangioma cell and tissue culture

Human umbilical vein endothelial cells (HUVECs) were kindly provided by the Vascular Research Division at the Brigham & Women's Hospital (Chavakis, Kanse et al. 1998). Human dermal microvascular endothelial cells (HDMECs) were isolated from neonatal foreskin obtained by human subject protocol, approved by the Partners Human Research Committee, Brigham & Women's Hospital (1999-P-002486/14; Kräling and Bischoff 1998). HUVECs and HDMECs were cultured on fibronectin-coated (1 μg/cm^2) plates with EBM-2, supplemented with 20% FBS, EGM-2 SingleQuots without hydrocortisone and 1x GPS (Cellgro 30-009-CI). bmMPCs were cultured on fibronectin-

coated (1 μg/cm^2) plates with EBM-2, supplemented with 20% FBS, EGM-2 SingleQuots (without heparin, hFGF-B, hydrocortisone and VEGF) and 1x GPS (Cellgro 30-009-CI). Human placental and retinal pericytes were purchased from Promocell (C-12981) and Cell Systems (ACBRI 183), respectively and grown in DMEM 10% FBS, 1x GPS (Cellgro 30-009-CI). Smooth muscle cells (SMCs) from bladder, bronchus and colon were purchased from ScienCell (HBdSMC, HBSM and HCoSMC, respectively), generously provided by Rosalyn Adam and cultured in smooth muscle cell media from ScienCell (Cat. 1101). Human cardiac tissue was generously provided by Bernhard Kühn (protocol Z06-10-0489). Bovine retinal pericytes were generously provided by Jennifer Durham. They were cultured in DMEM supplemented with 10% bovine calf serum (Atlanta Biologicals S11450), 1x antibiotic-antimycotic (Gibco 15240) and 1x L-glutamine (Gibco 25030).

6.3 Tube formation assay

Into each well of a 24-well plate (Costar 3526), 300 μL of thawed, growth factor-reduced Matrigel (BD Biosciences 354230) were dispensed. The Matrigel was allowed to solidify in a 37 ˚C incubator for 20 minutes. Sixty thousand cells in 500 μl of EBM-2, supplemented with 0.1% BSA , were seeded onto each well of solidified Matrigel at 3.0 x 10^4 cells/cm^2. The media, in which cells were suspended, contained vehicle or 10 μM of propranolol. Vehicle, closely resembling an injectable solution of propranolol (Sandoz NDC 0781-3777-95, 1 mg/mL), was prepared by Boston Children's Hospital Pharmacy. After 18 hours, pictures of cells were taken under bright field at 10X (Nikon Eclipse TS100).

6.4 5-HT_{1B} immunostaining (IF)

Formalin-fixed, paraffin-embedded IH tissues and brain tissues (obtained from Department of Pathology, Boston Children's Hospital) were deparaffinized in xylene and hydrated through sequential ethanol gradient. Antigen was retrieved by heating the sections in 1x antigen unmasking solution (Vector H-3300) at 90-95 ˚C for 23 minutes. The sections were blocked with 5% goat serum (Vector S-1000) for 30 minutes and incubated with rabbit anti-5-HT_{1B} receptor (1:100, abcam ab85937) or rabbit IgG (1:100, Vector I-1000) for 1 hour and followed by Alexa Fluor 488-conjugated anti-rabbit IgG (1:200, Invitrogen A11034) for 1 hour. The sections were washed in PBS and mounted with medium containing DAPI (Vector H-1200). Pictures were taken at 40X using Leica TCS SP2 Acousto-Optical Beam Splitter confocal system with DMIRE2 inverted microscope- diode 405 nm, argon 488 nm and HeNe 594 nm.

6.5 α_{1b}- and β_2-ARs immunostaining (DAB)

Formalin-fixed, paraffin-embedded IH tissues and brain tissues (obtained from Department of Pathology, Boston Children's Hospital) were deparaffinized in xylene and hydrated through sequential ethanol gradient. Antigen was retrieved by heating the sections in 1x antigen unmasking solution (Vector H-3300) at 90-95 ˚C for 23 minutes. The sections were blocked with 5% goat serum (Vector S-1000) for 30 minutes and incubated with rabbit anti-α_{1b}-AR (1:200, abcam ab84405), rabbit anti-β_2-AR (1:200, Novus NBP1-19449), rabbit anti-β_2-AR (1:200, abcam ab61778) or rabbit IgG (1:200, Vector I-1000) for 1 hour. Peroxidase was quenched by incubating in 3% H_2O_2 for 5 minutes. This was followed by incubation with peroxidase labeled anti-rabbit IgG

(1:200, Vector PI-1000) for 1 hour. DAB enhancing solution (ImmPACT DAB Cat# SK-4105) was applied, which was followed by Hematoxylin QS (Vector H-3404). Sections were dehydrated through sequential ethanol gradient. They were then washed in xylene and mounted with Permount (Fisher SP15-100). Pictures were taken at 20X with a microscope (Zeiss Axiophot II, equipped with AxioCam MRc5 and supplemented with AxioVision Rel. 4.8 software).

6.6 quantitative real time polymerase chain reaction (qRT-PCR)

RNAs from cells and tissues were extracted using RNeasy Micro kit (Qiagen 74004) and TRIzol (Invitrogen 15596-026), respectively. Concentrations and ratios of 260/230 and 260/280 were measured with Nanodrop 8000 Spectrophotometer (Thermo). Samples with 260/230 and 260/280 ratios greater than 1.7 were chosen, and their cDNAs synthesized with Quanta qScript cDNA Synthesis kit (VWR Scientific 10414-098). Primers for qRT-PCR are listed in Table 1. Reactions were prepared with SYBR Green master mix (Roche 04913850001) and performed on Applied Biosystems' StepOnePlus Real-Time PCR system for primers of ARs and β-actin according to the following: initial denaturation at 95 °C for 10 minutes, followed by 40 cycles of denaturation at 95 °C for 15 seconds and annealing at 53 °C for 1 minute. Afterwards, temperature was raised to 95 °C before it was lowered for melting curve detection from 48 to 95 °C, by 0.3 °C increment.

These steps were modified for primers of 5-HT_{1B} receptor, GAPDH, HPRT1, S9 and VEGF-A because of higher melting temperatures, according to the following: initial denaturation at 95 °C for 10 minutes, followed by 40 cycles of denaturation at 95 °C for

15 seconds and annealing at 60 °C for 1 minute. Afterwards, temperature was raised to 95 °C before it was lowered for melting curve detection from 55 to 95 °C, by 0.3 °C increment.

Table 7. Sequences of primers for qRT-PCR.

Gene	Forward	Reverse
5-HT_{1B} receptor	5'-CTGTGTATGTGAACCAAGTC-3'	5'-TAGGGAGATGATGAAGAAGGG-3'
α_{1b}-AR	5'-GATCCATTCCAAGAACTTTCAC-3'	5'-CAGAACACCACCTTGAACAC-3'
β_1-AR	5'-TCTTTTGTGTGTGCGTGTGA-3'	5'-ATGCTTCTCCCTTCCCCTAA-3'
β_2-AR	5'-CACCAACTACTTCATCACTTCAC-3'	5'-GACACAATCCACACCATCAG-3'
β_3-AR	5'-TGAAATCCAGTTGCCATTGA-3'	5'-CACCATGTAAGGCACCACTG-3'
β-actin	5'-TGAAGTGTGACGTGGACATC-3'	5'-GGAGGAGCAATGATCTTGAT-3'
GAPDH	5'-TGCACCACCAACTGCTTAG-3'	5'-GATGCAGGGATGATGTTC-3'
HPRT1	5'-TGGACAGGACTGAACGTCTTG-3'	5'-CCAGCAGGTCAGCAAAGAATTTA-3'
S9	5'-GATTACATCCTGGGCCTGAA-3'	5'-ATGAAGGACGGGATGTTCAC-3'
VEGF-A	5'-AGCCTTGCCGCCTTGCTGCTCTA-3'	5'- GTGCTGGCCTTGGTGAGG-3'

6.7 Cellular proliferation in response to propranolol

Three thousand, seven hundred fifty HemECs, HemSCs and HDMECs in 150 µL of EBM-2, supplemented with 20% FBS, EGM-2 SingleQuots without hydrocortisone and 1x GPS (Cellgro 30-009-CI) were plated into each well of a 48-well plate (BD Falcon 353078), at a density of 5000 cells/cm^2. Likewise, 3750 pericytes in 150 µL of DMEM 10% FBS, 1x GPS (Cellgro 30-009-CI) were plated into each well of a 48-well plate, at a density of 5000 cells/cm^2. For each cell type, two additional wells were plated at a density of 5000 cells/cm^2 to determine the number of attached cells, 24 hours after plating (Day 1). Cells were treated twice daily with PBS or 10 µM of propranolol (Sandoz NDC 0781-3777-95, 1 mg/mL at pH 4) from Day 1 to 5. Cells were counted in quadruplicate wells using an automated cell counter (Millipore Scepter 2.0, Cat # PHCC20060). All particles whose diameters ranged 10-25 µM were counted.

6.8 siRNA transfection

Non-targeting #3, β_1- and β_2-AR siRNAs were designed by and purchased from Dharmacon (D-001810-03-05, L-005425-00-0005 and L-005426-01-0005, respectively). Non-targeting siRNA #3 has no homology to any known human gene, and its off-target effects have been minimized. β_1- and β_2-AR siRNAs were each a pool of 5 siRNAs, designed to maximize knockdown. Hem-Pericytes 154 grew in DMEM 10% without antibiotics until they reached 60-90% confluence on 12-well plates (Costar 3512). Cells were then transfected with 10 nM of siRNA of interest using Lipofectamine RNAiMAX (Life Technologies, 13778-075), prepared in reduced-serum media (Gibco OPTI-MEM I 31985). The cells were trypsinized 24 hours after transfection and prepared for

contractility, proliferation assays or re-plated on 12-well plates to assess extent of knockdown by qRT-PCR. Contractility assay and assessment of knockdown by qRT-PCR were performed 48 hours after transfection. Proliferation assay was performed for 5 days following transfection.

6.9 Contractility assay

Six-and-a-half microliters of polydimethylsiloxane (PDMS) from Sigma-Aldrich (DMPS12M-100G, viscosity 12,500 cST) were pipetted onto marked, round glass coverslips (Fisher Scientific 12-545-81) with a positive displacement pipette (Gilson F148502) and spread for one hour at 40 °C. PDMS were thermally cross-linked by passing over low flame twice, and then coated with electrical charge for 13 seconds using a plasma etcher (SPI Plasma-Prep II 11005). They were then covered with 0.1 mg/mL of type I collagen from rat (BD Biosciences 354236) suspended in PBS. Each coverslip was placed into a well of a 24-well plate (Costar 3526). The 24-well plate was UV-irradiated for five minutes, and 4000 cells in DMEM 2% FBS, 1x GPS (Cellgro 30-009-CI) were pipetted into each well. After 48 hours, pictures of wrinkled cells, in relation to marks on coverslips, were taken under bright field at 10X (Nikon Eclipse TS100).

After pictures were taken, cells were treated with 10 μM of one of the following four conditions by a Bischoff Laboratory member: vehicle (n = 6 wells), propranolol (n = 6), vehicle & epinephrine (n = 6) or propranolol & epinephrine (n = 6). As noted above, vehicle that closely resembled the solution in which intravenous propranolol is suspended (Sandoz NDC 0781-3777-95, 1 mg/mL at pH 4) was prepared by Boston

Children's Hospital Pharmacy. Epinephrine 1:1000 was also purchased from the same pharmacy (Hospira NDC 0409-7241-01, 1 mg/mL). Within an hour after addition of reagents, pictures of the same cells were taken again. I was blinded to the treatments until after the pictures were taken. Contractility for each cell and all four conditions were quantified using the following formula: C = N x L, N = # wrinkles and L = length in pixels from ImageJ (Markhotina, Liu et al. 2007).

6.10 Proliferation assay of HemSCs

HemSCs were cultured in EBM-2, supplemented with 20% FBS, EGM-2 SingleQuots without hydrocortisone and 1x GPS (Cellgro 30-009-CI). Autoclaved, round glass coverslips (Fisher Scientific 12-545-81) were placed in 3 wells of 4-well plates (Nunc 176740). For each HemSCs, 3, 4-well plates were prepared for counting on Days 1, 4 and 7. Coverslips were then coated with 1% gelatin in ddH_2O (pH adjusted to 7.5 and sterile-filtered). Five thousand HemSCs were seeded onto each well (1.9 cm^2) at a density of 2632 cells/cm^2. On Days 1, 4 and 7, cells were fixed with 4% paraformaldehyde for 5 minutes and washed with PBS. A needle and forceps were used to flip coverslips with cells on them, onto a microscope glass slide (Fisher 12-550-15) with drops of medium containing DAPI (Vector H-1200). Fluorescent pictures of nuclei were taken at 10X (Nikon Eclipse TS100). Two pictures were taken for each coverslip, for a total of six pictures each on Days 1, 4 and 7. The numbers of nuclei were calculated using ImageJ, and the 6 counts averaged for cell numbers on Days 1, 4 and 7.

6.11 *In vivo* model of infantile hemangioma

Initially, 2.5 million HemSCs were suspended in 250 µl of Matrigel (BD Biosciences 356237) and injected subcutaneously on the backs of 20, 6-week old male athymic nude/nude mice (Massachusetts General Hospital, Boston, MA). This experimental set-up was performed a total of 6 times, with HemSCs 120, 128, 129 and 133, but no significant changes in vascular volume were detected after propranolol treatment for 7 days.

Therefore, hemangioma vessels were formed using HemECs and Hem-Pericytes, based on the rationale that the more differentiated cells might form vessels that resemble the vessels in a well-established IH. A mixture of HemECs 158 and Hem-Pericytes 154, 1.25 million cells from each cell type, was suspended in 250 µl of Matrigel and injected subcutaneously on the backs of 20, 6-week old male athymic nude/nude mice.

For experiments involving HemSCs alone & HemECs 158 and Hem-Pericytes 154, two mice were set aside from the rest of group and injected with 250 µl of Matrigel without any cells, to serve as negative controls. Mice whose Matrigels had contrast values at day 7 above those of negative controls were continued further in experiment, whereas those that did not were sacrificed. The surviving mice were then paired by their contrast values and divided into either the vehicle or propranolol treatment group; this was to ensure that each group had a similar distribution of contrast values at the start of treatment. Then, either the vehicle or propranolol at 5 mg/kg, twice a day for 7 days, was injected into their peritoneum.

6.12 Micro-ultrasonography analysis of vascular volume

Seven days after implanting cells and Matrigel or Matrigel alone, the Matrigel implants were subjected to contrast-enhanced micro-ultrasonography using VisualSonics' Vevo 2100 unit.

Mice were sedated using isoflurane, targeting respiratory rate of 50 per minute. Tail veins of mice were cannulated using modified, winged infusion set (Allegro Medical 549230), through which nontargeted contrast agent (VisualSonics VS-11913) was injected to quantify vascular volume in Matrigels. A micro-ultrasonography probe, mounted on a motor, scanned the length of the Matrigels in 0.1 mm segments, and the amount of contrast agent was quantified by the Vevo 2100 unit. Twenty minutes passed for contrast agent to be cleared from murine circulation, and the above steps were repeated. The two measurements were averaged to determine contrast values of mice. The above steps took approximately an hour per mouse.

After 7 days of treatment, contrast values of cell/Matrigel implants were determined as above.

6.13 Microvessel density (MVD)

Twenty pictures from mid-Matrigel H & E sections of all animals in vehicle and propranolol groups were taken randomly at 40X with a microscope (Zeiss Axiophot II, equipped with AxioCam MRc5 and supplemented with AxioVision Rel. 4.8 software). Luminal structures containing at least one RBC were counted as a microvessel. The average MVD counted in 20 pictures was expressed as vessels/mm^2.

6.14 Human $CD31^+$ vessel calculation

Formalin-fixed, paraffin-embedded mid-Matrigel sections, from *in vivo* experiments with HemECs 158 and Hem-Pericytes 154, were deparaffinized in xylene and hydrated through sequential ethanol gradient. Antigen was retrieved by heating the sections in 1x antigen unmasking solution (Vector H-3300) at 90-95 ˚C for 23 minutes. The sections were blocked with 5% horse serum (Vector S-2000) for 30 minutes and incubated with mouse anti-human CD31 (1:40, Dako M0823) or mouse IgG (1:40, Dako X0931) for 1 hour. Peroxidase was quenched by incubating in 3% H_2O_2 for 5 minutes. This was followed by incubation with peroxidase labeled anti-mouse IgG (1:200, Vector PI-2000) for 1 hour. DAB enhancing solution (ImmPACT DAB Cat# SK-4105) was applied, which was followed by Hematoxylin QS (Vector H-3404). Sections were dehydrated through sequential ethanol gradient. They were then washed in xylene and mounted with Permount (Fisher SP15-100). Twenty pictures were taken randomly at 40X with a microscope (Zeiss Axiophot II, equipped with AxioCam MRc5 and supplemented with AxioVision Rel. 4.8 software). Brownish, luminal structures containing at least one RBC were counted as a human $CD31^+$ vessel. The average of the 20 pictures was expressed as human $CD31^+$ vessels/mm^2.

6.15 Vessel area calculation

The areas of microvessels used in MVD calculations, from *in vivo* experiments with HemECs 158 and Hem-Pericytes 154, were measured using ImageJ and expressed as $pixel^2$.

6.16 Ki67 & αSMA immunostaining

Formalin-fixed, paraffin-embedded mid-Matrigel sections, from *in vivo* experiments with HemECs 158 and Hem-Pericytes 154, were deparaffinized in xylene and hydrated through sequential ethanol gradient. Antigen was retrieved by heating the sections in 1x antigen unmasking solution (Vector H-3300) at 90-95 ˚C for 23 minutes. The sections were blocked with 5% goat serum (Vector S-1000) for 30 minutes and incubated with rabbit anti-Ki67 (1:100, abcam ab66155) or rabbit IgG (1:100, Vector I-1000) for 1 hour and followed by FITC-conjugated anti-rabbit IgG (1:200, Vector FI-1000) for 1 hour. The sections were washed in PBS and then blocked again with 5% horse serum (Vector S-2000) for 30 minutes and incubated with mouse anti-αSMA (1:750, Sigma A2547) or mouse IgG (1:750, Vector I-2000) for 1 hour and followed by Texas Red-conjugated anti-mouse IgG (1:200, Vector TI-2000) for 1 hour. The sections were washed in PBS and mounted with medium containing DAPI (Vector H-1200). Ten pictures were taken at 63X using Leica TCS SP2 Acousto-Optical Beam Splitter confocal system with DMIRE2 inverted microscope- diode 405 nm, argon 488 nm and HeNe 594 nm. Cells with both green and red colors were counted, averaged and expressed as $Ki67^+$ & αSMA^+ cells/mm^2.

6.17 Statistical analysis

Proliferation data of hemangioma-derived cells and IHC data from *in vivo* experiments (MVDs, human $CD31^+$ vessels, vessel areas and $Ki67^+$ and αSMA^+ cells) were analyzed by two-tailed, unpaired t-tests.

Contrast values of mice injected with HemSCs and HemECs 158 and Hem-Pericytes 154 were analyzed by two-tailed, paired t-tests. All data analyses were performed using GraphPad Prism Version 5.04, and differences were considered significant when $p < 0.05$. Dr. David Zurakowski, a biostatistician at Boston Children's Hospital, was consulted regarding statistical analyses of data from micro-ultrasonography experiments.

Chapter VII

Conclusions

Summary

$\beta_{1,2}$-ARs are known receptors of the drug and confirmed to be abundant in IH by qRT-PCR. Proliferation of HemECs and pericytes, including Hem-Pericytes, was reduced by propranolol. An *in vitro* contractility assay detected that propranolol affected contractility of Hem-Pericytes. The importance of β_2-AR in contractility of Hem-Pericytes was verified by siRNA knockdown. IH patients treated with propranolol experienced decrease in vascular volume that was reproduced *in vivo* in a murine model of IH. Thus, HemECs and Hem-Pericytes are potential cellular targets of propranolol in IH.

Possibility of additional cell types affected by propranolol

In vivo experiments using a murine model of IH showed that propranolol reduced vascular volume. Although quantification of human $CD31^+$ vessels in explanted cell/Matrigels showed that the implanted HemECs formed vessels, vascular volume reduction might not have been solely accomplished through effect of propranolol on hemangioma-derived cells. This notion is plausible because the implanted cells in Matrigel form vascular networks that are perfused as a result of connection to murine circulation. Therefore, various types of murine cells have access to the vascular networks within Matrigels.

One example of such cell type is mast cells. A group of researchers quantified and compared numbers of mast cells in tissue sections from IH, other vascular anomalies such as port wine stain, arteriovenous malformation and normal skin. They found high numbers of mast cells in proliferating and involuting phases of IH, with the number in proliferating phase higher than that in involuting phase. The number of mast

cells decreased over the course of IH, so that in late involuting phase its number was similar to those found in other vascular anomalies and normal skin. The researchers postulated that mast cells might play a role in the involution of IH (Pasyk, Cherry et al. 1984). Although mast cells were not quantified in the *in vivo* experiments described above, they are an example of a murine cell type that could have contributed to vascular volume reduction after propranolol treatment.

Endothelial cells synthesize molecules, such as von Willebrand factor, P-selectin and angiopoietin-2, and store them in Weibel-Palade bodies. Upon binding of IgE, mast cells release their contents, which include cytokines, heparin and histamine. In response to histamine, contents of the Weibel-Palade bodies are released from endothelial cells, and angiopoietin-2 contributes to vessel destabilization and angiogenesis. This sequence of events may be relevant in IH pathogenesis, and mast cells express β_2-AR, whose agonism may decrease the release of histamine (Johnson 2002). Paradoxically, a β-AR antagonist such as propranolol had no effect on release of histamine by mast cells (Ind, Barnes et al. 1985); nevertheless, effects of propranolol on mast cells in IH present an intriguing area of study.

Propranolol treatment reduced vascular volume in hemangioma vessels that formed as a combination of HemECs and Hem-Pericytes. As described above, the Bischoff Laboratory isolated HemECs, Hem-Pericytes and HemSCs from IH. Although these 3 cell types have allowed researchers to study many questions and provided valuable knowledge, efficacy of propranolol in IH may also occur through a cell type yet to be isolated from IH.

Possibility of propranolol affecting natural course of IH

Clinicians noted that oral propranolol, 2 mg/kg per day, is an effective, safe treatment for IH in 97% of patients. However, 17% of patients experienced rebound in size and color after cessation of treatment (Zaher, Rasheed et al. 2011). The occasional rebound in IH after cessation of propranolol treatment was also reported by different clinicians at various locations (Awadein and Fakhry 2011; Missoi, Lueder et al. 2011), so many clinicians choose to maintain patients on the drug for several months until they believe IH had started involuting. This observation brought up an interesting point of discussion at a dissertation advisory committee meeting; it would be of interest to find out whether propranolol alters the natural course of IH. In other words, propranolol might be able to expedite the natural course of IH, making tumors involute earlier than had the patient not been treated, or it might not change the natural course, but simply hold the tumor at bay and prevent growth until it starts to involute on its own.

Proliferating phase is characterized by dense, disorganized vessels, whereas involuting phase is characterized by enlarged, well-organized vessels. In other words, vessels decrease in number but enlarge in area as IH switches from proliferating to involuting phase. Histological analyses of *in vivo* experiments with HemECs 158 and Hem-Pericytes 154 showed that total vessel numbers were equivalent in the two groups (Figure 25C), while human $CD31^+$ vessels were statistically more numerous in the propranolol-treated group (Figure 26A). Vessel areas were statistically equivalent for the groups, but numerically larger for the propranolol-treated group (Figure 26B). In summary, histological analyses of *in vivo* experiments were inconclusive on whether or not propranolol could change the natural course of IH.

The Bischoff Laboratory obtained IH tissues from a patient treated with propranolol. Along with this tissue, other IH tissues from patients of similar age were selected, and their H & E slides reviewed with Dr. Harry Kozakewich, a pathologist at Boston Children's Hospital. Although the goal was to find if propranolol treatment could have changed tissue architecture compared to non-treated, pathology review was inconclusive; variabilities among individuals could have contributed to different tissue architecture even though ages at time of resection were similar. In summary, it was not determined whether propranolol made IH involute earlier than had the patient not been treated, or it simply held the tumor at bay and prevented growth until it started to involute on its own.

A case for cellular effect of propranolol in IH

Propranolol has often been administered in oral and intravenous forms to IH patients, so its effects have been systemic. Although there have been numerous reports in literature confirming the efficacy of propranolol in IH, some have doubted whether propranolol has any effect on IH itself at all. Proponents of this hypothesis argue that the systemically-distributed propranolol may simply constrict vessels feeding IH, cutting off blood supply and eventually leading to clinical improvement. This idea is plausible, but unlikely. Researchers noted that 85-90% of IH patients experienced improvement after application of propranolol ointment to their lesions two or three times daily for 5 months (Kunzi-Rapp 2012; Xu, Lv et al. 2012). The fact that topical application of propranolol improved IH suggested that its efficacy was brought on by local, not systemic, effect of the drug; in other words, propranolol has a cellular effect on IH. Therefore, it is unlikely

that propranolol is effective in IH simply because vessels feeding IH are constricted without propranolol having effect(s) on IH itself.

Other β-AR antagonists for IH

Clinicians have attempted β-AR antagonists other than propranolol to treat IH. One such drug is timolol, a nonselective β-AR antagonist often prescribed to decrease intraocular pressure in glaucoma patients. Topical timolol treatment improved IH in 92% of patients (Chambers, Katowitz et al. 2012). Another example is atenolol, a selective β_1-AR antagonist often prescribed for cardiovascular diseases. Unlike propranolol, which is lipophilic, atenolol is hydrophilic, so it appears at relatively low concentrations in brain and is less likely to produce side effects such as nightmares and hallucinations. Clinicians noted improvement of nose tip and sacral hemangiomas with oral atenolol treatment. Although atenolol is a selective β_1-AR antagonist, it may not be entirely specific for β_1-AR, so it may also be able to bind β_2-AR to reduce IH (Raphaël, de Graaf et al. 2011).

Although neither timolol nor atenolol has been utilized as extensively as propranolol for treating IH, their efficacy expands the choices clinicians have in treating IH. For instance, topical timolol may be prescribed for patients whose parents may be uneasy about systemic side effects of propranolol. Atenolol may be prescribed for IH patients who also carry diagnoses of lung conditions such as asthma, in which β_2-AR blockade is detrimental.

Identifying potential targets of IH: a work in progress

Many experiments described above revolved around β-ARs in IH, especially β_2-AR. Although *in vitro* contractility assays underscored the importance of β_2-AR for contractility of Hem-Pericytes, β-ARs may not be the only receptor for propranolol in IH. 5-HT_{1B} receptors have been well-characterized to function in brain, which was one of the reasons why β-ARs, more prevalent in rest of the body, were more extensively studied. Presence of 5-HT_{1B} receptors in IH was assessed by IHC and qRT-PCR, but a comprehensive evaluation to assess for their presence or absence in a spectrum of IH samples has not been done.

In addition to the possible existence of additional receptors for propranolol in IH, target molecules downstream of the receptors may be more numerous than those that are traditionally associated with β-AR. As described above, β-AR stimulation activates adenylyl cyclase to increase cAMP, which activates PKA and subsequently eNOS. While levels of these substrates may be affected by propranolol treatment, other substrates may be affected, too.

For instance, PLC cleaves phosphatidylinositol 4,5-bisphosphate (PIP_2) to diacylglycerol (DAG) and inositol 1, 4, 5-trisphosphate (IP_3), which initiates intracellular calcium release and activates protein kinase C (PKC). Phosphorylation of cytosolic proteins in human neutrophils by PKC was reduced upon treatment with 500 μM of propranolol. PKC is not directly downstream of β-AR, so these findings suggested that propranolol might inhibit PKC because of its amphipathic nature rather than its antagonism at β-AR (Sozzani, Agwu et al. 1992). Although concentration of propranolol used in these experiments was high, they hinted at existence of multiple

targets affected by the drug. As noted above, proliferation of HemECs and Hem-Pericytes was reduced by propranolol only, without epinephrine (Figure 17 A, B; Table 5), which indicated that propranolol might be acting as an inverse agonist at β-ARs or at targets other than β-ARs. PKC is an example of such a target.

Future directions

In order to clarify mechanism of propranolol in reducing IH, one needs to start by studying downstream molecules of β-AR and assessing whether they are affected by propranolol treatment. For instance, one can assess whether changes in levels of cAMP can be correlated with changes in contractility of Hem-Pericytes. If so, activation of PKA can be correlated with changes in levels of cAMP and eNOS.

As noted above, contractility assays do not show whether whole vessels contract in response to propranolol. Confirmatory results from experiments on whole hemangioma vessels can help link cellular action of propranolol on Hem-Pericytes (contraction around vessels) with vascular volume reduction of hemangioma vessels as shown by micro-ultrasonography analyses. Assays described in literature utilized optical fibers, a laser apparatus and fluorescence imaging to calculate changes in vessel diameters. (Nakatani, Iwasaki et al. 2007; Bergh, Ekman, et al. 2005). Although vessels whose diameters (1-4 mm) might be larger than hemangioma vessels were used in these studies, such methods may be modified to measure hemangioma vessel diameter changes in response to propranolol. One may also need to add epinephrine to the hemangioma vessel explant set-up to reproduce results from *in vitro* contractility assays and to emulate physiological environment.

Many clinicians choose to maintain patients on the drug for several months until they believe IH had started involuting because lesions on some patients had been reported to rebound after cessation of therapy. A future experiment along the lines of this observation would be testing whether vascular volume, as measured by micro-ultrasonography, increases back up after propranolol cessation. Another future experiment is to assess the effect of silenced β_2-AR *in vivo*, whether the vascular volume reduction from propranolol treatment would be negated or not.

As noted above, a group of researchers hypothesized that propranolol reduces IH through 3 pathways- vasoconstriction, anti-angiogenesis and apoptosis (Storch and Hoeger 2010). *In vitro* contractility assays and *in vivo* assays with micro-ultrasonography pointed to vasoconstriction as a likely reason behind efficacy of propranolol in IH.

On the other hand, propranolol may reduce IH via more than just vasoconstriction, but by a combination of effects. To assess the possibility of anti-angiogenesis, Shoshana Greenberger and I focused on HemSCs because they express the highest levels of VEGF-A among the hemangioma-derived cells. However, possible anti-angiogenic activity of propranolol, with or without epinephrine, on HemECs and Hem-Pericytes needs to be assessed, too. In addition, while vasoconstriction brought on by Hem-Pericytes may explain the immediate efficacy of propranolol within 24 hours of administration, decreased proliferation of HemECs and Hem-Pericytes over several days may be responsible for the long-term efficacy of propranolol.

In vitro contractility assays and *in vivo* studies underlined the likely role of Hem-Pericytes in the efficacy of propranolol. Another future experiment to confirm the role of

Hem-Pericytes is to perform an *in vivo* experiment with HemECs and non-hemangioma pericytes such as human placental and retinal pericytes. They did not respond to epinephrine and propranolol in contractility assays, so they might behave differently from Hem-Pericytes *in vivo*. If vascular volume reduction is not noted with non-hemangioma pericytes, then the role of Hem-Pericytes in vascular volume reduction by propranolol is more firmly established.

Contribution to the field

These experiments identified HemECs and Hem-Pericytes as potential cellular targets of propranolol in IH, which is novel because Hem-Pericytes have not been studied extensively, yet. $\beta_{1,2}$-ARs are known receptors of the drug and confirmed to be abundant in IH. Proliferation of HemECs and pericytes, including Hem-Pericytes, was reduced by propranolol, likely through its inverse agonism at β-ARs. Contractility of Hem-Pericytes was affected by propranolol, likely through its antagonism at β-ARs. The importance of β_2-AR in contractility of Hem-Pericytes was verified by a combination of β_2-AR siRNA knockdown and contractility assay. IH patients treated with propranolol experienced decrease in redness and firmness of lesion, which likely resulted from vascular volume reduction that was reproduced *in vivo* and verified by micro-ultrasonography analyses. Although mechanism of propranolol in reducing IH has not been clarified yet, the aforementioned findings indicate a focus on Hem-Pericytes is warranted and pave the way for upcoming experiments.

The findings described in this work are closely tied to adrenergic receptors and their potential relevance in IH. As noted above, β-ARs are highly expressed in IH, both

in tissues and cells. The noted reduction of proliferation of Hem-Pericytes and HemECs may be a result of reduction of β-AR signaling through MAPK pathway. Although propranolol stimulated phosphorylation of MAPK in Chinese Hamster Ovary cells (Baker, Hall et al. 2003), it may do the opposite in hemangioma-derived cells. Results from contractility assays also point to the likely key role of β-ARs in the actions accomplished by propranolol in IH. A likely sequence of events is that epinephrine leads to activation of β-AR, resulting in cAMP increase and subsequent PKA activation in Hem-Pericytes. PKA phosphorylates and inactivates myosin light chain kinase, which leads to relaxation of Hem-Pericytes on silicone. This sequence of events is opposed by propranolol, so Hem-Pericytes remain contracted upon treatment with propranolol and epinephrine. Therefore, these results indicated that contractility of Hem-Pericytes are likely influenced by signaling through β-ARs, and the key role of Hem-Pericytes in vascular volume reduction of hemangioma vessels was established by micro-ultrasonography in *in vivo* experiments.

Chapter VIII

ACKNOWLEDGMENTS

This work was supported by NIH P01 AR48564. Dr. John Mulliken surgically resected and provided hemangioma tissue specimens. Hem-Pericytes were isolated and provided by Dr. Elisa Boscolo, while HemECs and HemSCs were isolated and provided by Dr. Lan Huang. Dr. Shoshana Greenberger performed initial experiments on the effects of propranolol on HemECs and HemSCs. Smooth muscle cells from bladder, bronchus and colon were generously provided by Dr. Rosalyn Adam, as was cardiac tissue by Dr. Bernhard Kühn. Drs. Jennifer Durham and Ira Herman provided expertise for performing and interpreting contractility assays. Use of the plasma etcher for contractility assays was kindly approved by Dr. Ali Khademhosseini. Dr. Harry Kozakewich offered opinions on immunostaining of β_2-AR in IH and tissue architecture of different IH specimens. Jill Wylie-Sears performed characterization of 11 HemSCs by flow cytometry. Proficiency with Vevo 2100 was achieved with help from Dr. Patrick Allen. Dr. David Zurakowski was consulted regarding statistical analysis of data from micro-ultrasonography. Figures 13, 17 & 20 were prepared by Kristin Johnson. Drs. Zoltan Arany, Laurie Jackson-Grusby and Bruce Zetter provided valuable advice and guidance as the dissertation advisory committee. Drs. Pat D'Amore, Marsha Moses, Bruce Zetter and Len Zon reviewed this dissertation. Dr. Joyce Bischoff encouraged, guided and supported in countless ways through the years.

SUPPLEMENT

Vascular volume changes in each mouse implanted with HemSCs only

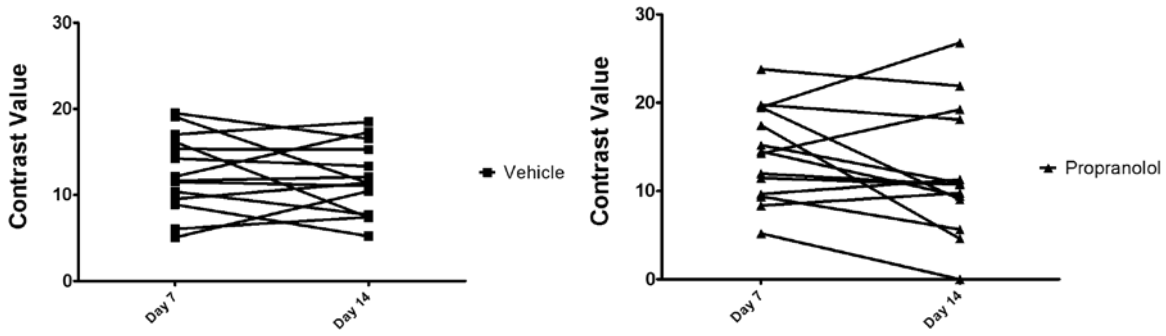

Vascular volume changes in each mouse implanted with HemECs 158 and Hem-Pericytes 154

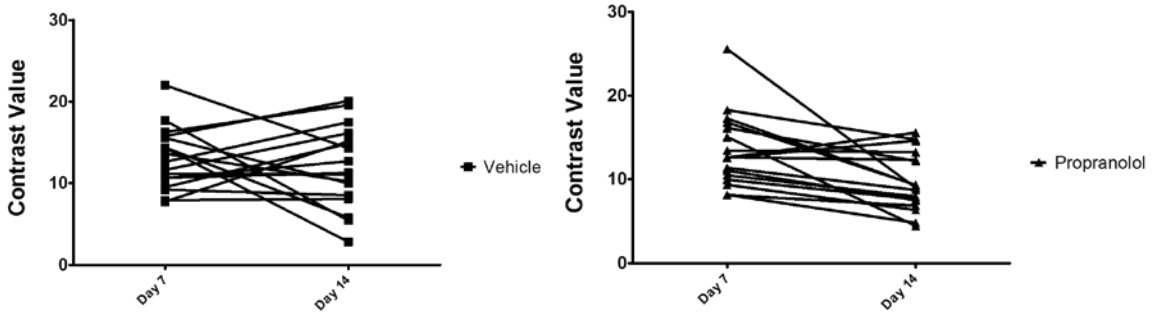

Supplementary Figure. Vascular volume changes for each mouse on Days 7 and 14.

General trend for the vehicle-treated group is similar for mice implanted with HemSCs only or with HemECs 158 and Hem-Pericytes 154: vascular volume stayed the same or increased, with the exception of some mice.

For the propranolol-treated group in mice implanted with HemSCs only, vascular volume decreased for many mice, but it stayed the same or increased for several others.

For the propranolol-treated group in mice implanted with HemECs 158 and Hem-Pericytes 154, a downward trend for most mice is easily noted.

REFERENCES

Adepoju, O., Wong, A., et al. (2011). "Expression of HES and HEY genes in infantile hemangiomas." Vasc Cell. **3**: 19.

Annabi, B., Lachambre, M.P., et al. (2009). "Propranolol adrenergic blockade inhibits human brain endothelial cells tubulogenesis and matrix metalloproteinase-9 secretion.**"** Pharmacol Res. **60**(5): 438-45.

Awadein, A., Fakhry, M.A. (2011). "Evaluation of intralesional propranolol for periocular capillary hemangioma." Clin Ophthalmol. **5**: 1135-40.

Azzi, M., Charest, P.G., et al. (2003). "Beta-arrestin-mediated activation of MAPK by inverse agonists reveals distinct active conformations for G protein-coupled receptors." Proc Natl Acad Sci USA. **100**(20): 11406-11.

Bagazgoitia, L., Torrelo, A., et al. (2011). "Propranolol for infantile hemangiomas." Pediatr Dermatol. **28**(2): 108-14.

Baker, J.G., Hall, I.P., et al. (2003). "Agonist and inverse agonist actions of beta-blockers at the human beta 2-adrenoceptor provide evidence for agonist-directed signaling." Mol Pharmacol. **64**(6): 1357-69.

Barlow, C.F., Priebe, C.J., et al. (1998). "Spastic diplegia as a complication of interferon Alfa-2a treatment of hemangiomas of infancy." J Pediatr. **132**(3 Pt 1): 527-30.

Bautch, V.L. (2012). "VEGF-directed blood vessel patterning: from cells to organism." Cold Spring Harb Perspect Med. **2**(9): a006452.

Benedito, R., Roca, C., et al. (2009). "The notch ligands Dll4 and Jagged1 have opposing effects on angiogenesis." Cell **137**(6): 1124-35.

Berard, M., Sordello, S., et al. (1997). "Vascular endothelial growth factor confers a growth advantage in vitro and in vivo to stromal cells cultured from neonatal hemangiomas." Am J Pathol. **150**(4): 1315-26.

Bergh, N., Ekman, M., et al. (2005). "A new biomechanical perfusion system for ex vivo study of small biological intact vessels." Ann Biomed Eng. **33**(12): 1808-18.

Bielenberg, D.R., Bucana, C.D., et al. (1999). "Progressive growth of infantile cutaneous hemangomas is directly correlated with hyperplasia and angiogenesis of adjacent epidermis and inversely correlated with expression of the endogenous angiogenesis inhibitor, IFN-beta." Int J Oncol. **14**(3): 401-8.

Bingham, M.M., Saltzman, B., et al. (2012). "Propranolol reduces infantile hemangioma volume and vessel density." Otolaryngol Head Neck Surg. **147**(2): 338-44.

Black, J.W., Crowther, A.F., et al. (1964). "A new adrenergic betareceptor antagonist." The Lancet **283**(7342): 1080–1081.

Boscolo, E., Mulliken, J.B., et al. (2011). "VEGFR-1 mediates endothelial differentiation and formation of blood vessels in a murine model of infantile hemangioma." Am J Pathol. **179**(5): 2266-77.

Boscolo, E., Mulliken, J.B., et al. (2013). "Pericytes from Infantile Hemangioma Display Pro-angiogenic Properties and Dysregulated Angiopoietin-1." Arterioscler Thromb Vasc Biol. **33**(3): 501-9.

Boscolo, E., Stewart, C.L., et al. (2011). "JAGGED1 signaling regulates hemangioma stem cell-to-pericyte/vascular smooth muscle cell differentiation." Arterioscler Thromb Vasc Biol. **31**(10): 2181-92.

Boye, E., Yu, Y., et al. (2001). "Clonality and altered behavior of endothelial cells from hemangiomas." J Clin Invest. **107**(6): 745-52.

Bray, S.J. (2006). "Notch signaling: a simple pathway becomes complex." Nat Rev Mol Cell Biol. **7**(9): 678-89.

Burton, B.K., Schulz, C.J., et al. (1995). "An increased incidence of haemangiomas in infants born following chorionic villus sampling (CVS)." Prenat Diagn. **15**(3): 209-14.

Calicchio, M.L., Collins, T., et al. (2009). "Identification of signaling systems in proliferating and involuting phase infantile hemangiomas by genome-wide transcriptional profiling." Am J Pathol. **174**(5): 1638-49.

Chambers, C.B., Katowitz, W.R., et al. (2012). "A controlled study of topical 0.25% timolol maleate gel for the treatment of cutaneous infantile capillary hemangiomas." Ophthal Plast Reconstr Surg. **28**(2): 103-6.

Chavakis, T., Kanse, S.M., et al. (1998). "Vitronectin concentrates proteolytic activity on the cell surface and extracellular matrix by trapping soluble urokinase receptor-urokinase complexes." Blood. **91**(7): 2305-12.

Chim, H., Armijo, B.S., et al. (2012). "Propranolol induces regression of hemangioma cells through HIF-1α-mediated inhibition of VEGF-A." Ann Surg. **256**(1): 146-56.

Chisholm, K.M., Chang, K.W., et al. (2012). "β-Adrenergic receptor expression in vascular tumors." Mod Pathol. **25**(11): 1446-51.

Daaka, Y., Luttrell, L.M., et al. (1997). "Switching of the coupling of the beta2-adrenergic receptor to different G proteins by protein kinase A." Nature **390**(6655): 88-91.

Dai, Y., Hou, F., et al. (2012). "Decreased eNOS protein expression in involuting and propranolol-treated hemangiomas." Arch Otolaryngol Head Neck Surg. **138**(2): 177-82.

de la Taille, A., Katz, A.E., et al. (2000). "Microvessel density as a predictor of PSA recurrence after radical prostatectomy." Am J Clin Pathol. **113**(4): 555-62.

Diener, H.C., Kaube, H., et al. (1998). "A practical guide to the management and prevention of migraine." Drugs. **56**(5): 811-24.

Downward, J. (2004). "PI 3-kinase, Akt and cell survival." Semin Cell Dev Biol. **15**(2): 177-82.

Eklund, L., and Saharinen, P. (2013). "Angiopoietin signaling in the vasculature." Exp Cell Res. **319**(9): 1271-80.

Feng, Y., vom Hagen, F., et al. (2007). "Impaired pericyte recruitment and abnormal retinal angiogenesis as a result of angiopoietin-2 overexpression." Thromb Haemost. **97**(1): 99-108.

Fiedler, U., and Augustin, H.G. (2006). "Angiopoietins: a link between angiogenesis and inflammation." Trends Immunol. **27**(12): 552-8.

Gaengel, K., Genové, G., et al. (2009). "Endothelial-mural cell signaling in vascular development and angiogenesis." Arterioscler Thromb Vasc Biol. **29**(5): 630-8.

Gerhardt, H., Golding, M., et al. (2003). "VEGF guides angiogenic sprouting utilizing endothelial tip cell filopodia." J Cell Biol. **161**(6): 1163-77.

Greenberger, S., Adini, I., et al. (2010). "Targeting NF-kB in infantile hemangioma-derived stem cells reduces VEGF-A expression." Angiogenesis. **13**(4): 327-35.

Greenberger, S., Boscolo, E., et al. (2010). "Corticosteroid suppression of VEGF-A in infantile hemangioma-derived stem cells." N Engl J Med. **362**(11): 1005-13.

Greenberger, S., Yuan, S., et al. (2011). "Rapamycin suppresses self-renewal and vasculogenic potential of stem cells isolated from infantile hemangioma." J Invest Dermatol. **131**(12): 2467-76.

Guo, K., Ma, Q., et al. (2009). "Norepinephrine-induced invasion by pancreatic cancer cells is inhibited by propranolol." Oncol Rep. **22**(4): 825-30.

Haggstrom, A.N., Drolet, B.A., et al. (2007). "Prospective study of infantile hemangiomas: demographic, prenatal, and perinatal characteristics." J Pediatr. **150**(3): 291-4.

Hammes, H.P., Lin, J., et al. (2004). "Angiopoietin-2 causes pericyte dropout in the normal retina: evidence for involvement in diabetic retinopathy." Diabetes. **53**(4): 1104-10.

Hammill, A.M., Wentzel, M., et al. (2011). "Sirolimus for the treatment of complicated vascular anomalies in children." Pediatr Blood Cancer. **57**(6): 1018-24.

Hastings, M.M., Milot, J., et al. (1997). "Recombinant interferon alfa-2b in the treatment of vision-threatening capillary hemangiomas in childhood." J AAPOS. **1**(4): 226-30.

Hausdorff, W.P., Caron, M.G., et al. (1990). "Turning off the signal: desensitization of beta-adrenergic receptor function." FASEB J. **4**(11): 2881-9.

Hellström, M., Phng, L.K., et al. (2007). "Dll4 signalling through Notch1 regulates formation of tip cells during angiogenesis." Nature. **445**(7129): 776-80.

Hellström, M., Phng, L.K., et al. (2007). "VEGF and Notch signaling: the yin and yang of angiogenic sprouting." Cell Adh Migr. **1**(3): 133-6.

Hicklin, D.J., and Ellis, L.M. (2005). "Role of the vascular endothelial growth factor pathway in tumor growth and angiogenesis." J Clin Oncol. **23**(5): 1011-27.

Huang, H., Bhat, A., et al. (2010). "Targeting the ANGPT-TIE2 pathway in malignancy." Nat Rev Cancer. **10**(8): 575-85.

Ind, P.W., Barnes, P.J., et al. (1985). "Plasma histamine concentration during propranolol induced bronchoconstriction." Thorax **40**(12): 903-9.

Ji, Y., Li, K ., et al. (2012). "Effects of propranolol on the proliferation and apoptosis of hemangioma-derived endothelial cells." J Pediatr Surg. **47**(12): 2216-23.

Jinnin, M., Medici, D., et al. (2008). "Suppressed NFAT-dependent VEGFR1 expression and constitutive VEGFR2 signaling in infantile hemangioma." Nat Med. **14**(11): 1236-46.

Johnson, M. (2002). "Effects of beta2-agonists on resident and infiltrating inflammatory cells." J Allergy Clin Immunol. **110**(6 Suppl): S282-90.

Kang, K-T., Allen, P., et al. (2011). "Bioengineered human vascular networks transplanted into secondary mice reconnect with the host vasculature and re-establish perfusion." Blood. **118**(25): 6718-21.

Kaplan, P., Normandin, J, Jr., et al. (1990). "Malformations and minor anomalies in children whose mothers had prenatal diagnosis: comparison between CVS and amniocentesis." Am J Med Genet. **37**(3): 366-70.

Kelley, C., D'Amore, P., et al. (1987). "Microvascular pericyte contractility in vitro: comparison with other cells of the vascular wall." J Cell Biol. **104**(3): 483-90.

Khan, Z.A., Boscolo, E., et al. (2008). "Multipotential stem cells recapitulate human infantile hemangioma in immunodeficient mice." J Clin Invest. **118**(7): 2592-9.

Kleinman, M.E., Greives, M.R., et al. (2007). "Hypoxia-induced mediators of stem/progenitor cell trafficking are increased in children with hemangioma." Arterioscler Thromb Vasc Biol. **27**(12): 2664-70.

Koh, G.Y. (2013). "Orchestral actions of angiopoietin-1 in vascular regeneration." Trends Mol Med. **19**(1): 31-9.

Kräling, B.M., and Bischoff, J. (1998). "A simplified method for growth of human microvascular endothelial cells results in decreased senescence and continued responsiveness to cytokines and growth factors." In Vitro Cell. Dev. Biol. Anim. **34**: 308–315.

Kräling, B.M., and Razon, M.J., et al. (1996) "E-selectin is present in proliferating endothelial cells in human hemangiomas." Am J Pathol. **148**(4): 1181-91.

Kunzi-Rapp, K. (2012). "Topical propranolol therapy for infantile hemangiomas." Pediatr Dermatol. **29**(2): 154-9.

Lamy. S., Lachambre, M.P., et al. (2010). "Propranolol suppresses angiogenesis in vitro: inhibition of proliferation, migration, and differentiation of endothelial cells." Vascul Pharmacol. **53**(5-6): 200-8.

Léauté-Labrèze, C., Dumas de la Roque, E., et al. (2008). "Propranolol for severe hemangiomas of infancy." N Engl J Med. **358**(24): 2649-51.

Lv, M.M., Fan, X.D., et al. (2012). "Propranolol for problematic head and neck hemangiomas: an analysis of 37 consecutive patients." Int J Pediatr Otorhinolaryngol. **76**(4): 574-8.

Markhotina, N., Liu, G.J., et al. (2007). "Contractility of retinal pericytes grown on silicone elastomer substrates is through a protein kinase A-mediated intracellular pathway in response to vasoactive peptides." IET Nanobiotechnol. **1**(3): 44-51.

Maisonpierre, P.C., Suri, C., et al. (1997). "Angiopoietin-2, a natural antagonist for Tie2 that disrupts in vivo angiogenesis." Science. **277**(5322): 55-60.

Mersmann, H.J. (1998). "Overview of the effects of beta-adrenergic receptor agonists on animal growth including mechanisms of action." J Anim Sci. **76**(1): 160-72.

Missoi, T.G., Lueder, G.T., et al. (2011). "Oral propranolol for treatment of periocular infantile hemangiomas." Arch Ophthalmol. **129**(7): 899-903.

Mulliken, J.B., Fishman, S.J., et al. (2000). "Vascular anomalies." Curr. Probl. Surg. **37**: 517–584.

Musse, A.A., Meloty-Kapella, L., et al. (2012). "Notch ligand endocytosis: mechanistic basis of signaling activity." Semin Cell Dev Biol. **23**(4): 429-36.

Nakatani, E., Iwasaki, T., et al. (2007). "Ho:YAG laser irradiation in blood vessel as a vasodilator: ex vivo study." Proc. of SPIE **6424** 642420-3.

North, P.E., Waner, M., et al. (2000). "GLUT1: a newly discovered immunohistochemical marker for juvenile hemangiomas." Hum Pathol. **31**(1): 11-22.

North, P.E., Waner, M., et al. (2002). "Are infantile hemangiomas of placental origin?" Ophthalmology **109**(4): 633-4.

Olsson, A-K., Dimberg, A., et al. (2006). "VEGF receptor signalling - in control of vascular function." Nat Rev Mol Cell Biol. **7**(5): 359-71.

Pasyk, K.A., Cherry, G.W., et al. (1984). "Quantitative evaluation of mast cells in cellularly dynamic and adynamic vascular malformations." Plast Reconstr Surg. **73**(1): 69-77.

Patel, P.A., Tilley, D.G., et al. (2009). "Physiologic and cardiac roles of beta-arrestins." J Mol Cell Cardiol. **46**(3): 300-8.

Pauwels, P.J., Gommeren, W., et al. (1988). "The receptor binding profile of the new antihypertensive agent nebivolol and its stereoisomers compared with various beta-adrenergic blockers." Mol Pharmacol. **34**(6): 843-51.

Peppiatt, C.M., Howarth, C., et al. (2006). "Bidirectional control of CNS capillary diameter by pericytes." Nature **443**(7112): 700-4.

Picard, A., Boscolo, E., et al. (2008). "IGF-2 and FLT-1/VEGF-R1 mRNA levels reveal distinctions and similarities between congenital and common infantile hemangioma." Pediatr Res. **63**(3): 263-7.

Pippig, S., Andexinger, S., et al. (1993). "Overexpression of beta-arrestin and beta-adrenergic receptor kinase augment desensitization of beta 2-adrenergic receptors." J Biol Chem. **268**(5): 3201-8.

Raphaël, M.F., de Graaf, M., et al. (2011). "Atenolol: a promising alternative to propranolol for the treatment of hemangiomas." J Am Acad Dermatol. **65**(2): 420-1.

Rössler, J., Haubold, M., et al. (2013). "β1-Adrenoceptor mRNA level reveals distinctions between infantile hemangioma and vascular malformations." Pediatr Res. Jan 31.

Sans, V., de la Roque, E.D., et al. (2009). "Propranolol for severe infantile hemangiomas: follow-up report." Pediatrics. **124**(3): e423-31.

Smadja, D.M., Mulliken, J.B., et al. (2012). "E-selectin mediates stem cell adhesion and formation of blood vessels in a murine model of infantile hemangioma." Am J Pathol. **181**(6): 2239-47.

Sozzani, S., Agwu, D.E., et al. (1992). "Propranolol, a phosphatidate phosphohydrolase inhibitor, also inhibits protein kinase C." J Biol Chem. **267**(28): 20481-8.

Storch, C.H. and Hoeger, P.H. (2010). "Propranolol for infantile haemangiomas: insights into the molecular mechanisms of action." Br J Dermatol. **163**(2): 269-74.

van Es, J.H. and Clevers, H. (2005). "Notch and Wnt inhibitors as potential new drugs for intestinal neoplastic disease." Trends Mol Med. **11**(11): 496-502.

Varma, D.R., Shen, H., et al. (1999). "Inverse agonist activities of beta-adrenoceptor antagonists in rat myocardium." Br J Pharmacol. **127**(4):895-902.

Wallukat, G. (2002). "The beta-adrenergic receptors." Herz **27**(7): 683-90.

Walter, J.W., North, P.E., et al. (2002). "Somatic mutation of vascular endothelial growth factor receptors in juvenile hemangioma." Genes Chromosomes Cancer. **33**(3): 295-303.

Weidner, N., Carroll, P.R., et al. (1993). "Tumor angiogenesis correlates with metastasis in invasive prostate carcinoma." Am J Pathol. **143**(2): 401-9.

Wong, A., Hardy, K.L., et al. (2012). "Propranolol accelerates adipogenesis in hemangioma stem cells and causes apoptosis of hemangioma endothelial cells." Plast Reconstr Surg. **130**(5): 1012-21.

Wu, J.K., Adepoju, O., et al. (2010). "A switch in Notch gene expression parallels stem cell to endothelial transition in infantile hemangioma." Angiogenesis. **13**(1): 15-23.

Xiao, X., Hong, L., et al. (1999). "Promoting effect of estrogen on the proliferation of hemangioma vascular endothelial cells in vitro." J Pediatr Surg. **34**(11): 1603-5.

Xiao, X., Liu, J., et al. (2004). "Synergistic effect of estrogen and VEGF on the proliferation of hemangioma vascular endothelial cells." J Pediatr Surg. **39**(7): 1107-10.

Xu, G., Lv, R., et al. (2012). "Topical propranolol for treatment of superficial infantile hemangiomas." J Am Acad Dermatol. **67**(6): 1210-3.

Yemisci, M., Gursoy-Ozdemir, Y., et al. (2009). "Pericyte contraction induced by oxidative-nitrative stress impairs capillary reflow despite successful opening of an occluded cerebral artery." Nat Med. **15**(9): 1031-7.

Yu, Y., Varughese, J., et al. (2001). "Increased Tie2 expression, enhanced response to angiopoietin-1, and dysregulated angiopoietin-2 expression in hemangioma-derived endothelial cells." Am J Pathol. **159**(6): 2271-80.

Zaher, H., Rasheed, H., et al. (2011). "Oral propranolol: an effective, safe treatment for infantile hemangiomas." Eur J Dermatol. **21**(4): 558-63.

Zhang, L., Lin, X., et al. (2005). "Circulating level of vascular endothelial growth factor in differentiating hemangioma from vascular malformation patients." Plast Reconstr Surg. **116**(1): 200-4.

Zhang, L., Mai, H.M., et al. (2013). "Preliminary study on plasma RPN concentration of patients with infantile hemangioma treated with propranolol." Int J Clin Exp Med. **6**(5): 342-5.

Zhelyazkova-Savova, M.D. and Zhelyazkov, D.K. (2003). "Behavioural evidence of agonist-like effect of isoteoline at 5-HT1B serotonergic receptors in mice. J Pharm Pharmacol. **55**(1): 125-9.

Zhou, D., Wang, Z., et al. (1991). "The study of estradiol levels in patients with hemangiomas." Chinese Journal of Pediatric Surg. **12**: 71.